Purine and Pyrazolopyrimidine Derivatives

Design and Synthesis of Chemical Tools for Biological Applications

David Bliman

UNIVERSITY OF GOTHENBURG

Department of Chemistry and Molecular Biology

University of Gothenburg

2015

DOCTORAL THESIS

Submitted for fulfillment of the requirements for the degree of
Doctor of Philosophy in Chemistry

Purine and Pyrazolopyrimidine Derivatives: Design and Synthesis of Chemical Tools for Biological Applications

David Bliman

Cover picture: The purine core surrounded by protein crystal structures relevant to this thesis.

ISBN: 978-91-628-9239-5

http://hdl.handle.net/2077/37278

Department of Chemistry and Molecular Biology
University of Gothenburg
SE-412-96 Göteborg
Sweden

Printed by Ineko AB

Kållered, 2014

Abstract

Purines can be found in a multitude of naturally occurring compounds with a range of functions. This thesis describes the design and synthesis of purines and structurally related pyrazolopyrimidine derivatives intended for biological applications.

Pyrazolopyrimidines are structurally related to purines and are used as scaffolds for ATP-competitive protein kinase inhibitors. A pyrazolopyrimidine based selective inhibitor of receptor tyrosine kinase REarranged during Transfection (RET), a protein kinase involved in cell development, was modified with a photolabile protecting group. The modification allowed for photocontrolled release of the inhibitor. Photodependent inhibition of RET was demonstrated in both a biochemical assay and in a cell based RET-assay. The utility of the caged inhibitor was demonstrated in transgenic zebrafish embryos by demonstrating the effect of photocontrolled RET-inhibition on motoneuron development. In addition, it was shown that the timing of irradiation was critical for motoneuron development.

The purine structure is a key constituent of aminoacyl-adenosine monophosphate (aa-AMP), an intermediate in protein biosynthesis. Stable mimics of aa-AMP could have potential as inhibitors of protein biosynthesis, a mechanism identified as a target for antiinfectives. A series of 8-(triazolyl)purines was synthesized as aa-AMP mimics. In addition, their photophysical properties were studied to evaluate their potential as fluorescent probes. Unexpectedly, these compounds displayed very low quantum yields in contrast to previous data for similar structures.

Protein-protein interactions (PPIs) are ubiquitously present in cells, have a central role in cell signaling and have been identified as interesting drug targets. The α-helix secondary structure has been identified as a central element in many PPIs. In this project, 2,6,9-substituted 8-(triazolyl)purines were evaluated as α-helix mimetics and inhibitors of the p53/MDM2 PPI. A series of compounds were synthesized and two of the compounds exhibited micromolar activity against MDM2. In addition, a bromination procedure for 8-bromination of purines was developed. Bromination with pyridinium tribromide at room temperature resulted in high yields for electron rich 2,6,9-substituted purines. The procedure is a convenient alternative to elemental bromine for this transformation. The fluorescent properties of the compounds were also measured. One of the compounds showed a high quantum yield of 51% and several compounds had quantum yields between 5-10%. The fluorescent properties could be useful for example to study intracellular localization of bioactive compounds.

Keywords: Purine, Pyrazolopyrimidine, Photoactivation, Caged compounds, Protein kinases, Protein-protein interactions, Inhibitors, Fluorescence.

List of Publications

This thesis is based on the following papers, which are referred to in the text by their Roman numerals.

I. **A Caged Ret Kinase Inhibitor and its Effect on Motoneuron Development in Zebrafish Embryos**
D. Bliman, J.R. Nilsson, P. Kettunen, J. Andréasson and M. Grøtli
Submitted Manuscript

II. **Synthesis and photophysical characterization of 1- and 4-(purinyl)triazoles**
I. N. Redwan*, D. Bliman*, M. Tokugawa, C. Lawson, M. Grøtli
Tetrahedron, **2013**, *69*, 8857-8864.

III. **8-Bromination of 2,6,9-trisubstituted purines with pyridinium tribromide**
D. Bliman*, M. Pettersson*, M. Bood, M. Grøtli
Tetrahedron Lett., **2014**, *55*, 2929-2931.

IV. **Fluorescent 8-triazolylpurines as α-helix mimetics**
M. Pettersson*, D. Bliman*, J. Jacobsson, J.R. Nilsson, J Andréasson, M. Grøtli
Manuscript

Publication related to, but not discussed in this thesis:

Towards the development of chromone-based MEK1/2 modulators

I. N. Redwan, C. Dyrager, C. Solano, G. Fernández de Trocóniz, L. Voisin, D. Bliman, S. Meloche, M. Grøtli
Eur. J. Med. Chem., **2014**, *85*, 127-138.

*Equally contributing authors.

Contribution to Papers I-IV

I. Contributed to the formulation of the research problem; performed or supervised the synthesis; participated in the biological and photophysical evaluation; contributed to the interpretation of the results and to writing the manuscript.

II. Formulated the research problem, performed the synthesis, interpreted the results and wrote the manuscript together with INR.

III. Formulated the research problem, performed or supervised the synthesis, interpreted the results and wrote the manuscript together with MP.

IV. Formulated the research problem, performed or supervised the synthesis and the molecular modelling, interpreted the results, wrote the manuscript together with MP, and contributed to the photophysical characterization.

Abbreviations

aa-AMP	Aminoacyl-Adenosine monophosphate
aa-tRNA	Aminoacyl-transfer RNA
Ac	Acetyl
ADDP	Azodicarbonyl dipiperidine
ATP	Adenosine triphosphate
BODIPY	Boron dipyrromethene
Bu	Butyl
Cbz	Benzyloxycarbonyl
CDI	Carbonyldiimidazole
Cp*	pentamethylcyclopentadienyl
CuAAC	Copper catalyzed azide-alkyne cyclization
DCC	Dicyclohexylcarbodiimide
DCM	Dichloromethane
DFG	Aspartic acid-phenylalanine-glycine
DIAD	Diisopropyl azodicarboxylate
DMEDA	Dimethylethylenediamine
DMF	Dimethylformamide
DMSO	Dimethylsulfoxide
DNA	Deoxyribonucleic acid
E_{ArS}	Electrophilic aromatic substitution
EDC	1-Ethyl-3-(3-dimethylaminopropyl)carbodiimide
Equiv.	Equivalents
Et	Ethyl
FAD	Flavin adenine dinucleotide
FP	Fluorescence polarization
h	Hours
HATU	1-[Bis(dimethylamino)methylene]-1H-1,2,3-triazolo[4,5-b]pyridinium-3-oxide hexafluorophosphate
HMBC	Heteronuclear multiple bond correlation
HOBt	1-Hydroxybenzotriazole
hpf	Hours post fertilization
HPLC	High performance liquid chromatography
HRMS	High resolution mass spectrometry
iPr	*iso*-Propyl
LCMS	Liquid chromatography mass spectrometry
MDM2	Murine double minute 2
Me	Methyl
min	Minutes

MW	Microwave
NAD	Nicotinamide adenine dinucleotide
NBS	*N*-Bromosuccinimide
NIS	*N*-Iodosuccinimide
NOE	Nuclear Overhauser effect
NVOC	Nitroveratryloxycarbonyl
ONp	4-Nitrophenyl
PG	Protecting group
Ph	Phenyl
PL	Photolabile
PPI	Protein-protein interaction
PS	Polymer supported
Pyr	Pyridinium
RET	Rearranged during transfection
RNA	Ribonucleic acid
r.t.	Room temperature
RTK	Receptor tyrosine kinase
S_NAr	Nucleophilic aromatic substitution
SPR	Surface plasmon resonance
TBA	Tetrabutylammonium
TBDMS	*tert*-Butyldimethylsilyl
*t*Boc	*tert*-butoxycarbonyl
TFA	Trifluoroacetic acid
THF	Tetrahydrofuran
TIPS	Triisopropylsilyl
TMS	Trimethylsilyl

Contents

1. Aim of the Study

The overall aim of this thesis was to design and synthesize bioactive compounds based on the purine and pyrazolopyrimidine scaffolds. The wide occurrence of purines in nature and their key role in many biological processes make them interesting starting points for the synthesis of new bioactive compounds.

The specific objectives of the thesis were:

- To equip a pyrazolopyrimidine based protein kinase inhibitor with a photolabile protecting group in order to gain *in situ* control of inhibitor activity. Such compounds can be used to study time and space dependent biological processes.

- To design and synthesize 8-(triazolyl)purine based aminoacyl-AMP mimics as potential aminoacyl adenylate inhibitors. In addition, the possibility of using these compounds as probes were to be evaluated by measuring their photophysical properties.

- To evaluate the 8-(triazolyl)purine structure as a scaffold for nonpeptidic α-helix mimetics and inhibitors of protein-protein interactions by a combination of computational tools, synthesis and biochemical testing of the compounds against the p53/MDM2 complex.

2. Introduction

The quest to obtain a deeper understanding of the cellular mechanisms essential for all living organisms is driven by a curiosity in how complex systems such as human beings function on a molecular level. It is also driven by the need for medical cures. Despite successes in medicine and medicinal chemistry, there remain a number of diseases with little or insufficient treatment. One prerequisite if we are to move forward with new treatments is to gain further understanding of how biological systems function. The field of chemical biology aims at doing this. An important part of chemical biology involves the use of small molecules as tools to solve biological problems. There are several notable examples of this in the past 15 years. For example, bioorthogonal chemical reactions have been developed, enabling ligation of molecular entities to cell surfaces[1] and enzyme catalyzed inhibitor selection[2]. In another interesting example, Shokat and coworkers used a combination of designed small molecule inhibitors and genetics for studies of kinases in yeast[3]. Knowledge of organic chemistry is key in designing and synthesizing these compounds and the development of target-specific small molecules necessitates the synthesis of structurally diverse compounds. There are a number of chemical core structures that are often present in compounds with biological activity. Such chemical core structures, or chemical scaffolds, are known as privileged scaffolds[4] due to their utility in constructing biologically active molecules. This thesis is centered on one such privileged structure, the bicyclic purine scaffold.

2.1 Purines

Purine is the generic name of imidazo[4,5-*d*]pyrimidine (Scheme 1). It is a bicyclic heterocycle consisting of a 6-membered pyrimidine ring and a 5-membered imidazole ring. The fused ring system fulfills Hückels rule (4n+2 π electrons where n=0 or any integer) and is therefore aromatic giving it a flat geometry. Of the four theoretical tautomers of purine, *9H* and *7H* are favored in solution[5-7].

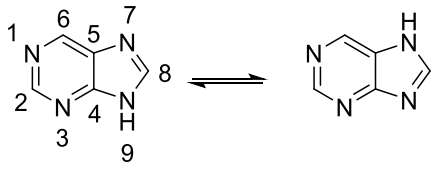

Scheme 1. The favored tautomers, *9H* (left) and *7H* (right), of purine.

The first synthesis of purine was performed by Emil Fischer in the late 1800s and was part of the early endeavors in organic synthesis[8]. Purine was synthesized by reacting uric acid with PCl_5 to form 2,6,8-trichloropurine which was reduced to purine via 2,6-iodopurine (Scheme 2)[9,10].

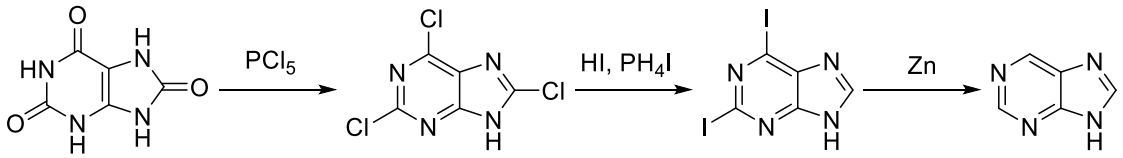

Scheme 2. The first synthesis of purine[9,10].

The purine core can be found in many compounds with important functions in biological systems. Purine constitutes a key structural element of deoxyribonucleic acid (DNA) and ribonucleic acid (RNA) as two of the four bases, adenine and guanine, has a purine core. Adenine can also be found in adenosine triphosphate (ATP), known to most as the main energy source of living organisms but which also plays a key role in cellular signaling. Other important examples are nicotinamide adenine dinucleotide (NAD) and flavin adenine dinucleotide (FAD), compounds involved in several important metabolic reactions. In addition to these ubiquitous examples there is a number of natural products that has been isolated from various plants and animals that contain the purine structure[11]. Structurally diverse examples include asmarines[12,13] and aphrocallistin[14] isolated from sea sponges *Raspailia sp.*, *Aphrocalliste Beatrix*, respectively (Figure 1).

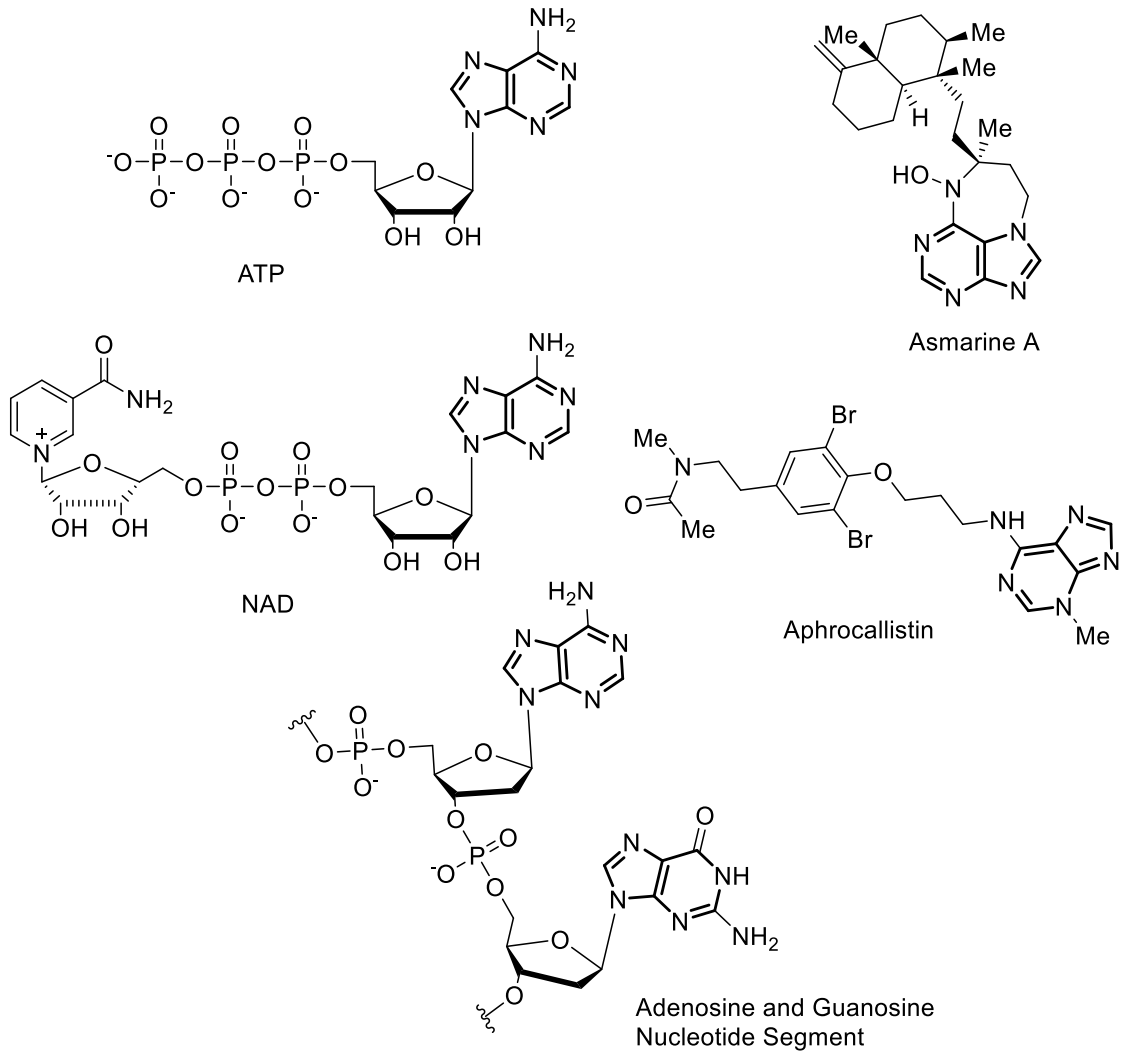

Figure 1. Examples of naturally occurring purine containing compounds. From top left to bottom right; ATP, asmarine A, NAD, aphrocallistin and a nucleotide segment.

The natural occurrence and importance of purine derivatives in nature has led to an interest in the development of methods to produce both naturally occurring and synthetic purine containing compounds. The literature on purine synthesis spanning from the late 1800s to today is extensive and methodologies have been developed to synthesize both the ring system as well as for substituting the core structure[15].

2.1.1 Purines from pyrimidines and imidazoles-building the core

The bicyclic system can be synthesized from pyrimidines (Scheme 3). This approach is suitable for obtaining *N*7-substituted purines[16], compounds difficult to obtain selectively by substitution of the bicyclic scaffold.

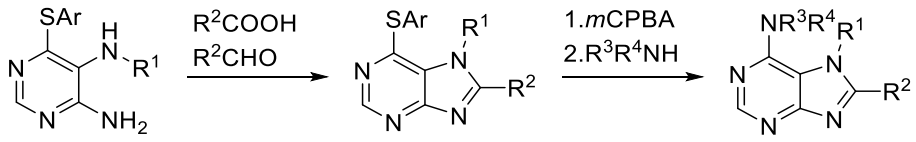

Scheme 3. Example of synthesis of purines from a pyrimidine precursor[16].

Oxopurines such as hypoxanthine and guanine can be obtained by ring closure of suitably substituted imidazoles[17]. This approach can be used to obtain acyclovir, a guanosine analog used as an antiviral drug (Scheme 4)[18]. Furthermore, ring closure of formamidinoimidazoles provide a route to 3,9-alkylated adenines[19].

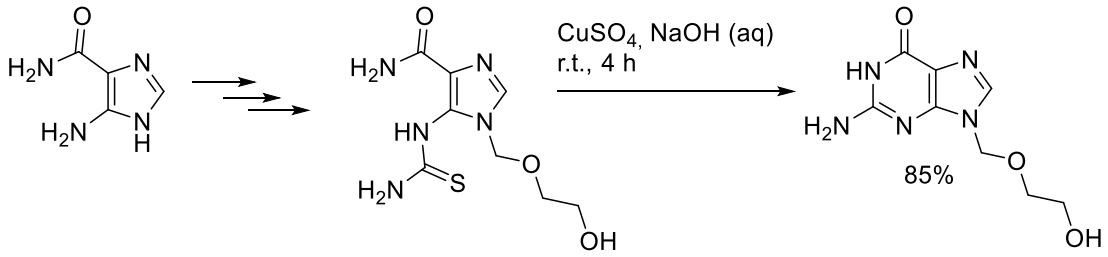

Scheme 4. Synthesis of acyclovir from an imidazole precursor[18].

2.1.2 Substitution reactions of purines-decorating the core

Commercially available purine derivatives such as adenine, 6-chloro-purine and 2-amino-6-chloropurine provide an attractive alternative starting point to highly substituted purines and methods for substitutions in the 2, *N*3, 6, *N*7, 8 and *N*9 positions have been reported (Scheme 5). This approach was used in this project to synthesize 6, 8, *N*9 and 2, *N*6, 8, *N*9-substituted purines and will be the focus of this thesis.

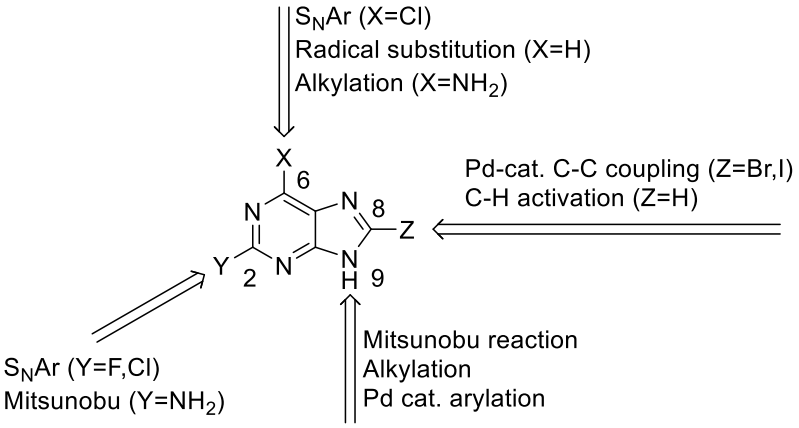

Scheme 5. Examples of reactions available to functionalize purines.

Substituents in the *N*9-position can be introduced by alkylation with alkyl halides under basic conditions. Even though *N*9 is generally more nucleophilic than *N*1, *N*3 and *N*7, this approach will give mixtures of regioismers in different ratios depending on reaction conditions[17] and substitution pattern of the purine[20]. Alkylation of adenine with alkyl halides using Cs_2CO_3 or K_2CO_3 as base gives 9-alkylation as the major isomer with the *N*7 [21, 22] or the *N*3-alkyl[17] as the minor isomer. Presence of a 8-bromo substituent shifts the regioselectivity towards the *N*3-alkylated isomer and both 2:1[23] and 6:4[24] ratios have been reported, although still in favor of the *N*9-isomer. The use of biphasic reaction systems with quaternary ammonium salts as phase transfer catalysts have also been reported to provide high *N*9-regioselectivity[25,26]. *N*7-Substitution can be achieved by protecting the *N*9-position followed by alkylation of *N*7 [27,28]. Another widely used method for introduction of substituents in the *N*9-postion is the Mitsunobu reaction[29]. This reaction generally has high selectivity for the 9-position and can be performed under mild conditions[30-32]. Aryl groups can be introduced by copper catalyzed C-N bond forming reactions with aryl boronic acids[33] or aryl halides[34]. Since purines with both halogens and amines in positions 2 and 6 are commercially available, these are practical starting points when substituents are desired in those positions. The difference in electrophilicity between 6-chloro and 2-fluoro in 6-chloro-2-fluoropurine can be exploited to regioselectively introduce amines in two consecutive nucleophilic aromatic substitution (S_NAr) reactions[30]. Alternatively, 6-chloro-2-iodo-purines can be used enabling regioselective functionalization by S_NAr in the 6-chloro position followed by palladium catalyzed coupling in the 2-iodo

position[35]. Recently, an example of a Minisci type reaction between a carboxylic acid and the 6-position of purine nucleosides without prior activation to provide 6-alkyl purines was published[36]. The 8-position generally needs to be activated before further functionalization. This can be achieved by lithiation[37, 38] and more frequently by bromination[21,39,40] or iodination[41] which opens up for palladium catalyzed C-C bond forming reactions[42] such as the Stille coupling to introduce alkenyls[43], Suzuki coupling for aryls and alkenyls[24, 44] and the Sonogashira coupling for alkynes[45]. In this study, most of the synthetic transformations in the 8-position was based on Sonogashira couplings and this reaction will be discussed in more detail in section 2.1.3. Recently, reports have been published on methods for C-H activation to introduce indole and pyrrole[46], and phenylacetylene[47,48] in the 8-position of purine derivatives. These methods are advantageous in that they do not require an additional activation step. Nevertheless, they often require high temperature and/or pressure to work and still have a rather limited substrate scope.

2.1.3 Sonogashira type Pd-coupling

Since their first appearance in the late sixties and seventies[49], the palladium catalyzed C-C bond forming reactions have arguably developed into one of the most utilized reaction types in organic synthesis[50,51]. Their importance was further acknowledged in 2010 when three of the pioneers in the field shared the Nobel Prize in chemistry for Pd-catalyzed C-C coupling[52]. One subclass that is central in this thesis is the coupling of a terminal alkyne and an aryl halide or aryl triflate. In 1975, Heck and coworker reported the coupling of aryl halides with acetylenes catalyzed by $Pd(OAc)_2(PPh_3)_2$ in amine base at elevated temperatures (100 °C)[53]. The same year Sonogashira and coworkers published a similar coupling reaction with $PdCl_2(PPh_3)_2$ and CuI as co-catalyst[54]. The addition of CuI allowed the reaction to take place at room temperature and the Sonogashira protocol has become the standard protocol for aryl-alkyne coupling reactions. The mechanism is suggested to proceed as outlined in Scheme 6[55,56], and comprises two catalytic cycles. In the palladium cycle, R-X adds to the Pd(0)-catalyst by oxidative addition. When a Pd(II)-precatalyst (such as $PdCl_2(PPh_3)_2$) is used, it needs to be reduced prior to the oxidative addition step. This can occur either by homocoupling of acetylenes or by amines or ethers present as reagents and/or solvents.[55] Cu(I) most likely coordinates to the alkyne, lowering its pKa and thereby facilitating the deprotonation of the terminal alkyne resulting in

a copper acetylide[57]. Transmetallation, *trans*/*cis* isomerization and reductive elimination results in the coupled product and regenerates the Pd(0) catalyst.

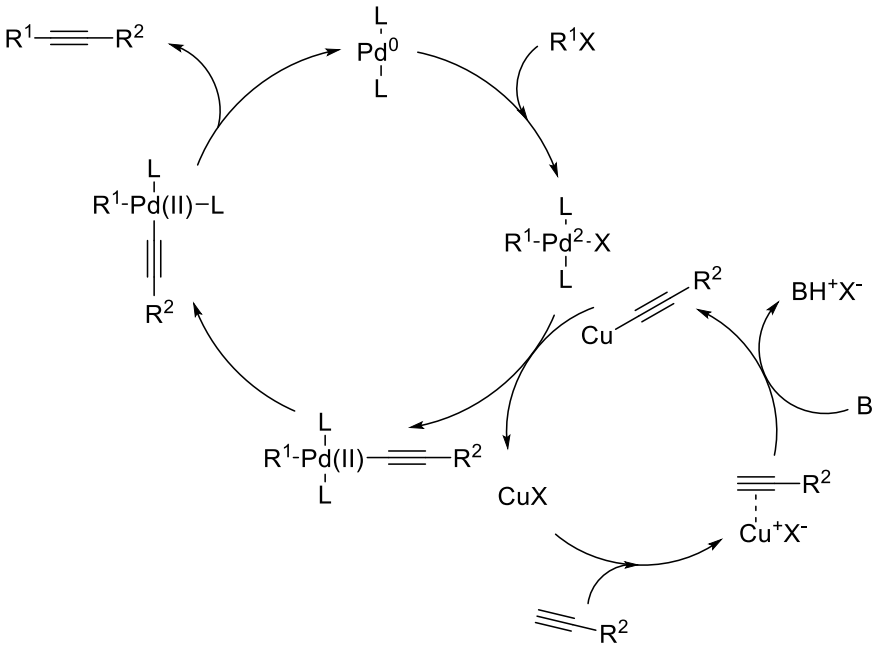

Scheme 6. Suggested mechanism for the Sonogashira type coupling of R-X and a terminal alkyne.

In the context of purines, the Sonogashira reaction has been used to introduce alkyne substituents in the 2-[41], 6-[58,59] and 8-[60,61]positions of purines and has also been used to alkynylate purine analogs[62,63].

2.1.4 1,2,3-triazoles

Another reaction type with relevance for this thesis is the Huisgen cycloaddition of a terminal alkyne and an azide. The thermal version of this reaction gives a mixture of the 1,4- and 1,5-triazole (Scheme 7). However, catalytic reactions with high regioselectivity have been developed, making this reaction useful.

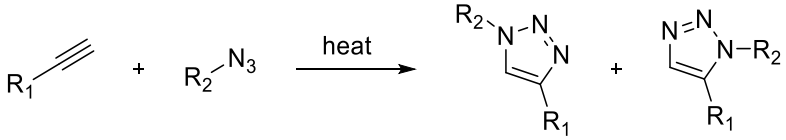

Scheme 7. Thermal azide-alkyne cycloaddition.

The reaction of a terminal alkyne and an azide in the presence of a Cu(I)-catalyst results in the 1,4-triazole with high regioselectivity and is often referred to as coppercatalyzed azide-alkyne cycloaddition (CuAAC). This reaction can be performed under mild conditions in a range of solvents including aqueous mixtures[64]. Since its first introduction[65,66], it has been widely utilized for chemical biology applications[67]. Mechanistic studies have revealed that the reaction rate is second order with respect to copper[68] and a mechanism based on these experiments in combination with computational studies[69] have been proposed (Scheme 8). The reaction is believed to proceed by coordination of copper to the alkyne followed by deprotonation. Coordination of the azide forms a metallacycle with the internal nitrogen coordinated to the copper. Ring contraction gives a metallated triazole and protonation releases the triazole and regenerates the copper complex.

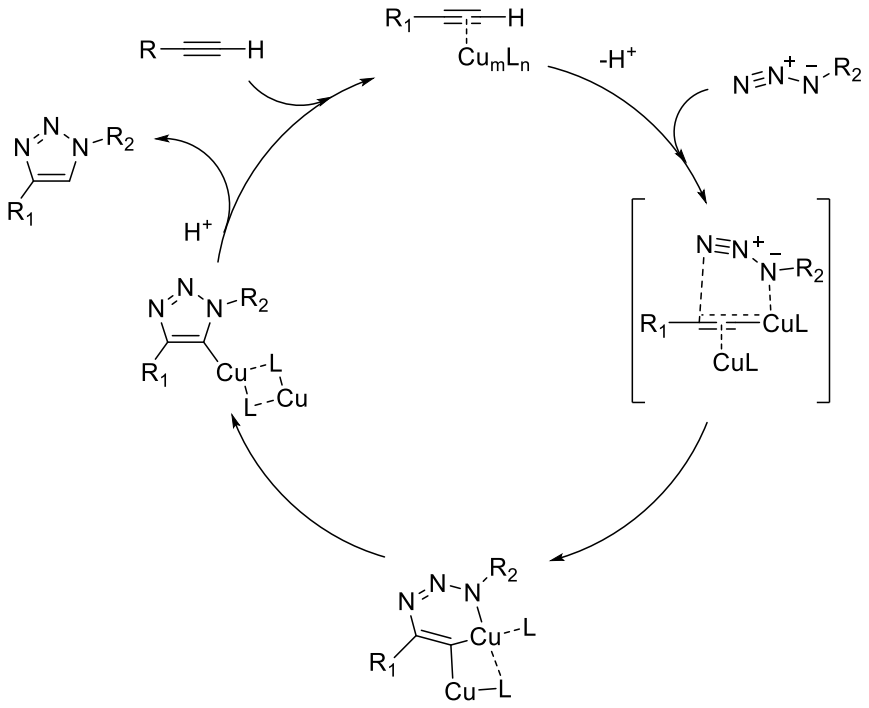

Scheme 8. Mechanistic proposal for the CuAAC.

The 1,5-triazole can be obtained with high regioselectivity by Cp*Ru(II)-catalyzed cyclization[70,71]. More recently, a metal-free base catalyzed reaction in DMSO has been reported to give the 1,5-triazole, also with high regioselectivity[72].

An example of the utility of this regiocontrol is the synthesis of stable triazole analogues of 1- and 3-phosphohistidine by Kee et al.[73] (Scheme 9).

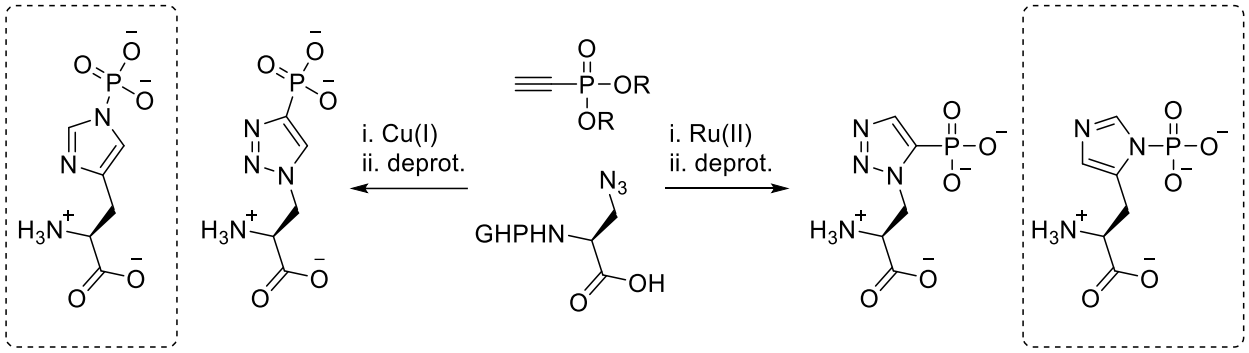

Scheme 9. 1-and 3-Phosphohistidine (in frames) and synthesis of stable analogues by complementing Cu(I)- and Ru(II)-catalysis[73].

2.1.5 Examples of existing purines and their use

Needless to say, these synthetic methodologies have been developed for and resulted in a number of compounds with interesting biologic activity. 2,6,9-Trisubstituted purines were the first purines to be developed as kinase inhibitors[74,75]. One example from this class is purvalanol A (Figure 2) which is a cyclin dependent kinase (CDK) inhibitor[30,76]. Several purine analogs are being developed or have been approved for clinical use[77]. Notably, all food and drug administration (FDA) approved drugs containing a purine substructure are either treatments for cancer or antivirals[78]. Early examples of purine based drugs include the antiviral acyclovir[79] mentioned in section 2.1, and 6-mercaptopurine[80], used to treat acute lymphotic leukemia. Abacavir is an example of a reverse transcriptase inhibitor used to treat HIV[81].

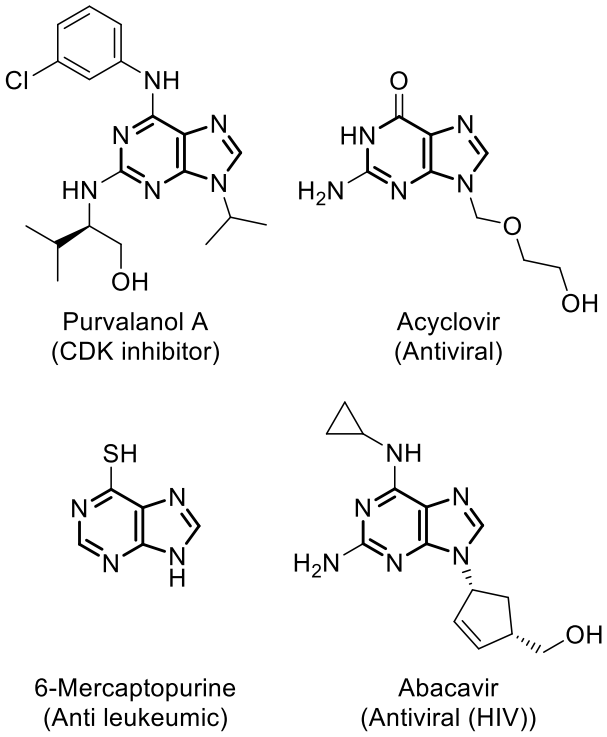

Figure 2. Examples of bioactive synthetic purines. Biological activity or commercial use in parenthesis.

2.2 Pyrazolo[3,4-*d*]pyrimidines

The frequent occurrence and importance of purine containing compounds in nature have spurred the interest, not only of purines but also of structurally related scaffolds. One of these are the pyrazolo[3,4-*d*]pyrimidines (Figure 3).

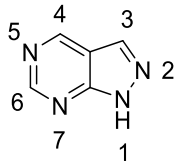

Figure 3. Pyrazolo[3,4-*d*]pyrimidine with IUPAC numbering.

Pyrazolo[3,4-*d*]pyrimidines can be synthesized by first forming the pyrazolo ring by reacting ethoxymethylenemalonitrile (accessible from malonitrile and triethyl ortoformate) with

hydrazine (monohydrate for N^1-H or substituted hydrazine for N^1-R). Condensation with formamide results in 4-amino substituted pyrazolopyrimidine (Scheme 10)[82].

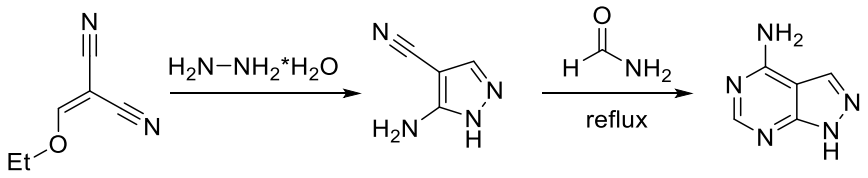

Scheme 10. Synthesis of 4-amino-pyrazolo[3,4-*d*]pyrimidine[82].

The substituent pattern in the 4- and 6- positions can be controlled by condensation with other substrates such as urea (4-amino-6-hydroxy) or thiourea (4-amino-6-thiol)[82]. Substitution in the 3-position can be introduced in the imidazolyl forming step[83] or by modification of the bicyclic system by activation using halogenation and subsequent palladium catalyzed C-C coupling[84]. Substitution in N^1 can be obtained by alkylation with alkyl halides[85,86].

The pyrazolopyrimidine scaffold has been used in the synthesis of nucleoside base analogs[62,87] and biologically active compounds towards several different targets[88], probably most notably as a scaffold for kinase inhibitors[89] due to its structural analogy to adenine and possibility of substitution in the 3-position. Pyrazolopyrimidines as kinase inhibitors will be discussed further in Chapter 3.

Besides being interesting from a bioactivity point of view, the conjugation of both purines and pyrazolopyrimidines make them suitable for modifications to provide them with interesting luminescent properties. The basis of this property and its applications in chemical biology will be discussed in section 2.3.

2.3 Use of light to manipulate biologically active compounds

Light is a useful tool in chemical biology. It can be used to change the physical and/or chemical properties of molecules *in situ* enabling both visualization and manipulation of activity. The tunable properties of light (e.g. wavelength, intensity, irradiation time) make it a potentially noninvasive and selective method for controlling chemical properties.

2.3.1 Fluorescent probes

Luminescence is defined as the emission of light that occurs when a system makes a transition from an electronically excited state to a lower energy state (the ground state). There are two types of luminescence, fluorescence and phosphorescence. This process is commonly visualized by a Jablonski diagram[90] (Figure 4), invented by Alexander Jablonski.

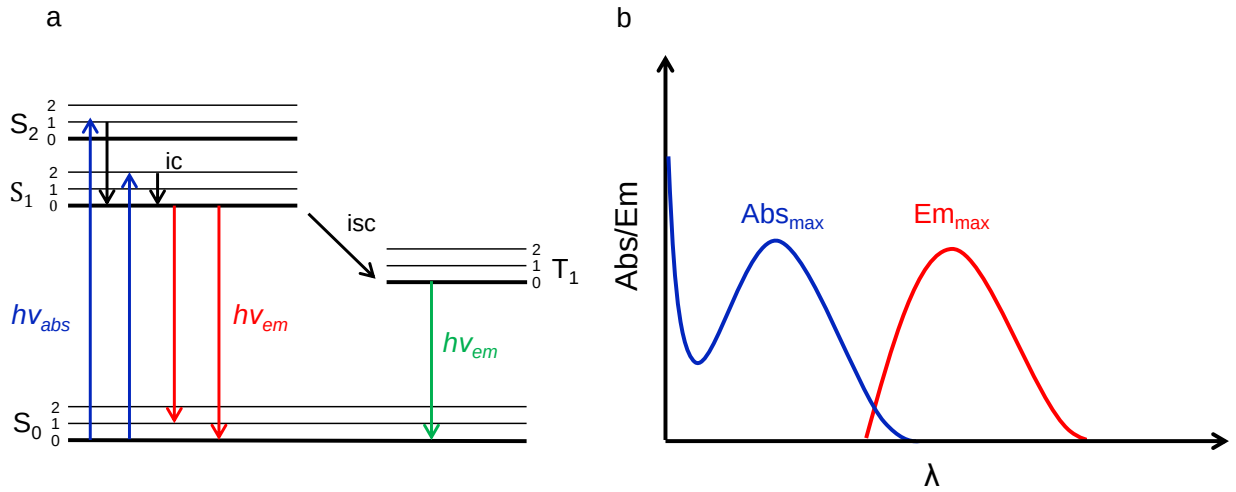

Figure 4. a) Simplified Jablonski diagram[91] illustrating energy transitions associated with absorption (blue arrows), internal conversion between vibrational states (ic, black vertical arrows), fluorescent emission (red arrows), inter system crossing between excited singlet and triplet state (isc, black diagonal arrow) and phosphorescent emission (green arrow). b) Schematic representation of absorption (blue) and emission (red) spectra.

If a compound is irradiated with light of a specific wavelength, it can absorb a photon. The compound will be excited from its ground state (S_0) to one of the vibrational energy levels of the first excited singlet state (S_1). The vibrational energy level transitions (internal conversions)

are very fast and all emission occurs from the $S_{1,0}$ level. From here, the compound can return to the ground state and in the process emit a photon. This process gives rise to fluorescence. As an effect of the internal conversion between vibrational levels, the emitted light is lower in energy (longer wavelength) than the absorbed light. The difference is known as the Stokesshift. From the first excited singlet state (S_1), relaxation can also occur to the excited triplet state (T_1) by intersystem crossing (ISC). T_1 to S_0 transition results in phosphorescence. Since this transition is forbidden, it is considerably slower than fluorescence. Phosphorescence is outside the scope of this thesis and will not be discussed further. The quantum yield (Φ_F) is a property generally used to describe the efficiency of a fluorescent compound and is defined as the ratio between emitted and absorbed photons.[91]

Compounds with the ability to emit fluorescence are often referred to as fluorophores. The first fluorophore that was discovered was quinine (Figure 5). Since then, the field has developed immensely. Both quantum dots[92,93] which are small nanocrystal semiconductors, and fluorescent proteins[94] as well as small molecule entities[95,96] (such as quinine) have been used for bioimaging. The two former constitute two separate scientific fields and are as such outside the scope of this thesis. Small molecular fluorescent probes have numerous applications in chemical biology[97]. Examples of small molecule fluorophores include fluoresceins, cyanines and boron dipyrromethene (BODIPY)-type compounds (Figure 5)[95,98]. Fluorescent analogs have been developed for both amino acids[99], phospholipids and nucleosides[100]. Fluorescent purines and purine analogs can be converted into fluorescent nucleic acids that can be introduced into DNA and RNA in order to study these systems[100,101]. These compounds mimic the Watson-Crick base pairing of the substituted base and are positioned within the studied structure, in contrast to external dyes mentioned above. Examples of fluorescent nucleotide base analogs include 2-aminopurine (2AP)[102] and quadracyclic adenine (qA)[103] (Figure 5).

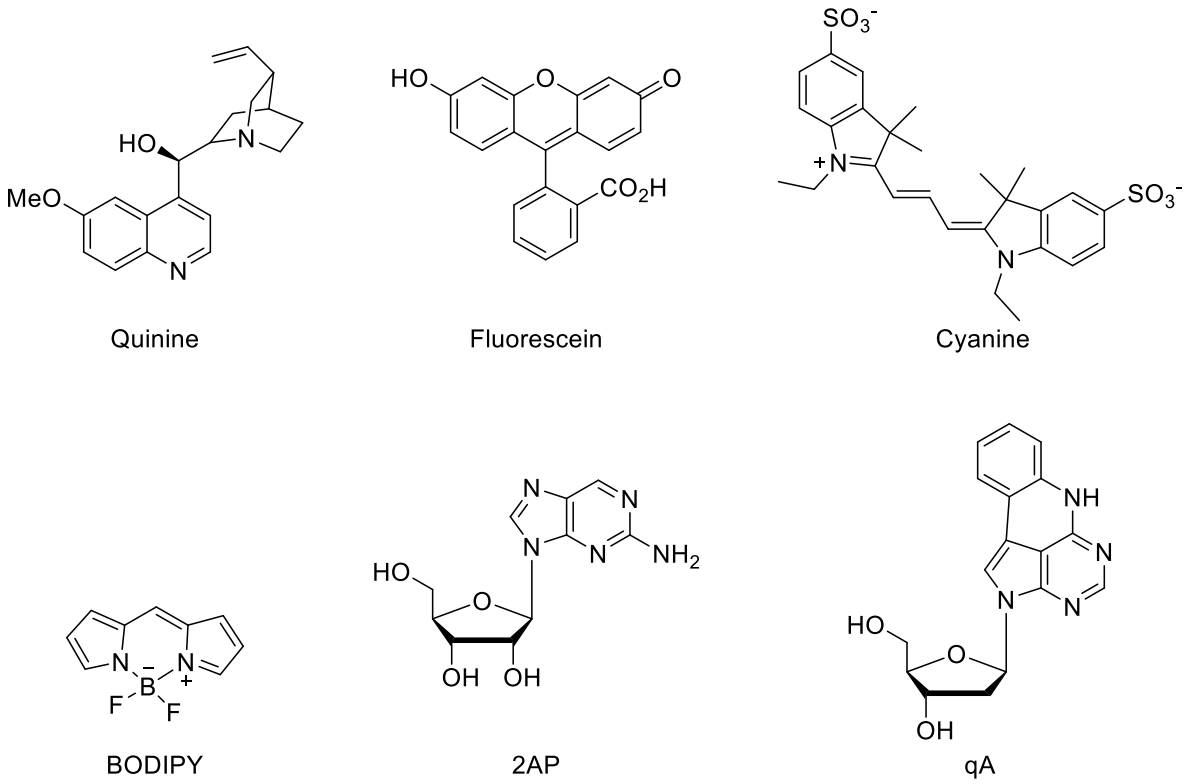

Figure 5. Examples of small molecule fluorescent probes.

In contrast to the small molecule dyes discussed above, only a few examples of inherently fluorescent enzyme inhibitors exist including fluorescent inhibitors of glutathione S-transferase[104], protein kinases[105] and a fluorescent tubulin inhibitor[106].

2.3.2 Photolabile protecting groups

As useful as small molecules are as biological probes, one disadvantage is that once the molecule is taken up by the system of interest (a cell or organism), the researcher lose control over it. When studying time and space dependent processes as for example organ or organism development, it is advantageous to be able to control the activation of a compound, both temporally (when) and spatially (where). One way of gaining such control is through the use of a photolabile protecting group (Scheme 11). The principle entails attaching a photolabile protecting group to a compound in a manner that masks its biological activity. The masked (inactive) compound, also referred to as caged, can then be administered to the system under

investigation and activation can be achieved by irradiation of light at a given time or at a specific place.

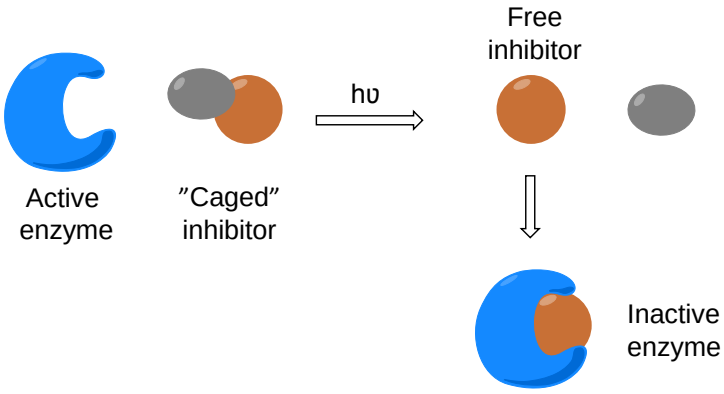

Scheme 11. Schematic illustration of decaging methodology for enzyme inhibitors.

This methodology has been used successfully to study neuronal signaling by caging signal substances such as glutamate[107] and cyclic adenosine monophosphate (cAMP)[108], study calcium uptake by using caged ion channel agonists[109] and to develop photoreleasable phospholipids[110]. Several classes of photolabile protecting groups have been developed and examples from some common groups are shown in Figure 9[111].

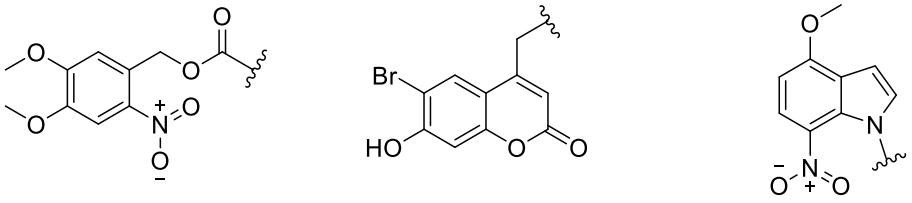

Figure 9. Examples of available photolabile protecting groups.

There are a number of factors to consider when choosing a photolabile protecting group for use in a biological system; the wavelength used for deprotection should not cause extensive cell damage and the light needs to penetrate into cells. In practice, this means that the

wavelength should be longer than 300 nm. Also the protected compound needs to be soluble in a solvent mixture suitable for the test system, typically a water buffer system and should ideally not generate any toxic or biologically active byproducts upon irradiation. The first and most commonly used photolabile protecting groups are the *o*-nitrobenzyl alcohols. These compounds were first used to protect ATP[112] at the terminal phosphate and have since been modified into a subgroup of photolabile protecting groups. One notable modification is the introduction of 4,5-dimethoxy substituents on the aromatic ring (NVOC, Figure 9). This serves to redshift the wavelength of the light needed for deprotection which facilitates the use of these photolabile protecting groups in biological systems. The mechanism of photoinduced deprotection for the unsubstituted *o*-nitro benzyl alcohols[113] and the modified substrates[114,115] have been studied. The deprotection has been proposed to proceed by absorption of a photon by **A** leading to excitation (Scheme 12).

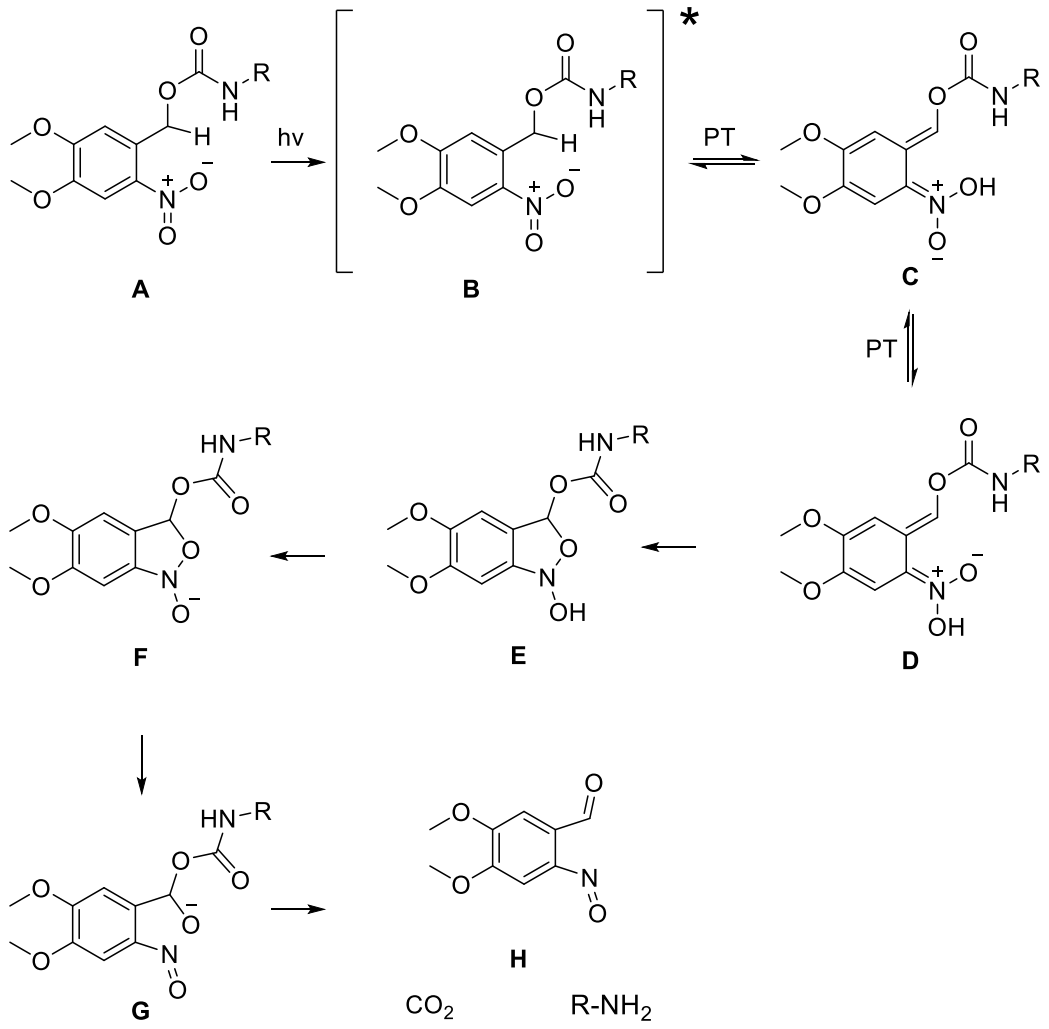

Scheme 12. Proposed mechanism for the photoinduced deprotection of NVOC-type protecting groups[115, 116]. hυ = light, * = excited state, PT = proton transfer.

The excited form (**B**) undergoes a proton transfer (PT) from the benzylic position to one of the oxygens of the nitro group to form an aci-nitro compound (**C**). After solvent mediated proton transfer or alternatively rotation of the nitro group, a ring closure occurs followed by rapid decomposition (**E**-**H**) to a nitrosoaldehyde, carbon dioxide and released compound. A recent study propose the rate limiting step to be the ring closing step (**D** to **E**) and that **E** to **H** is a concerted reaction not passing through **F** and **G**[116].

3. A caged pyrazolopyrimidine protein kinase inhibitor (Paper I)

3.1 Introduction

One type of enzymes that binds to purine containing substrates are protein kinases. In this chapter, the development, evaluation and utilization of a photoactivatable, or caged, inhibitor of the receptor tyrosine kinase (RTK) Rearranged during transfection (RET) is discussed.

3.1.1 Protein kinases

The Protein kinases, which are a subclass of transferases, are enzymes that transfer the γ-phosphate of ATP† to the –OH functionality of a serine, threonine or tyrosine of a substrate (Scheme 13). The reverse reaction is catalyzed by phosphatases.

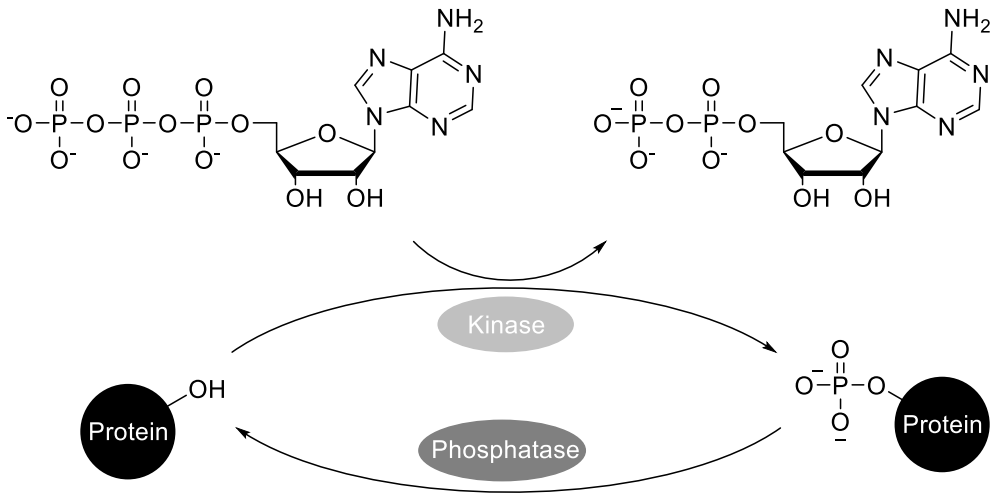

Scheme 13. Kinase mediated phosphorylation and phosphatase mediated dephosphorylation.

† Protein kinase CK2 can use GTP in place of ATP.
M. E. Gerritsen, D. J. Matthews, *Targeting Protein Kinases for Cancer Therapy*, John Wiley & Sons, Hoboken, NJ, USA, **2010**, page 84.

This deceptively simple chemical modification infers functional changes in the phosphorylated protein, affecting a diverse set of processes such as metabolism, neurotransmitter biosynthesis, DNA replication and transcription, apoptosis and cell differentiation[117,118]. The main part of intracellular signal transduction is relayed by phosphorylation cascades mediated by protein kinases[118]. The human kinome, the part of the genome coding for protein kinases, consists of more than 500 protein kinase genes[118, 119]. The catalytic site of protein kinases is highly conserved, not only within the human kinome but also across widely different species[120]. The high conservation implies that the role of protein kinases was established at an early stage of evolution and that it was vital for survival.

3.1.2 Anatomy and function of the catalytic domain

The conserved catalytic domain of protein kinases consists of two lobes, the larger *C*-terminal lobe consisting mainly of α-helices and the smaller *N*-terminal lobe easily recognized by the antiparallel β-sheet structure (Figure 10)[121]. The catalytic cleft where ATP bind lies between these two lobes. The segment connecting the two lobes is referred to as the hinge region. When ATP binds, two hydrogen bonds are formed between the backbone of the hinge region and N^2 and 6N of the adenine moiety of ATP. Ionic interactions between the α- and β-phosphates and amino acid residues at the catalytic site are mediated by two Mg^{2+} ions. The peptide substrate binds "in front" of the ATP binding site close to the γ-phosphate. Substrate binding and kinase activity are highly dependent on the conformation of the activation loop, situated at the substrate binding site[122]. In one end of the activation loop there is a highly conserved three amino acid sequence, the aspartic acid, phenylalanine, glycine (DFG) motif. This motif has two conformations, DFG out and DFG in, and plays a vital role in ligand binding which will be discussed further in section 3.1.3.

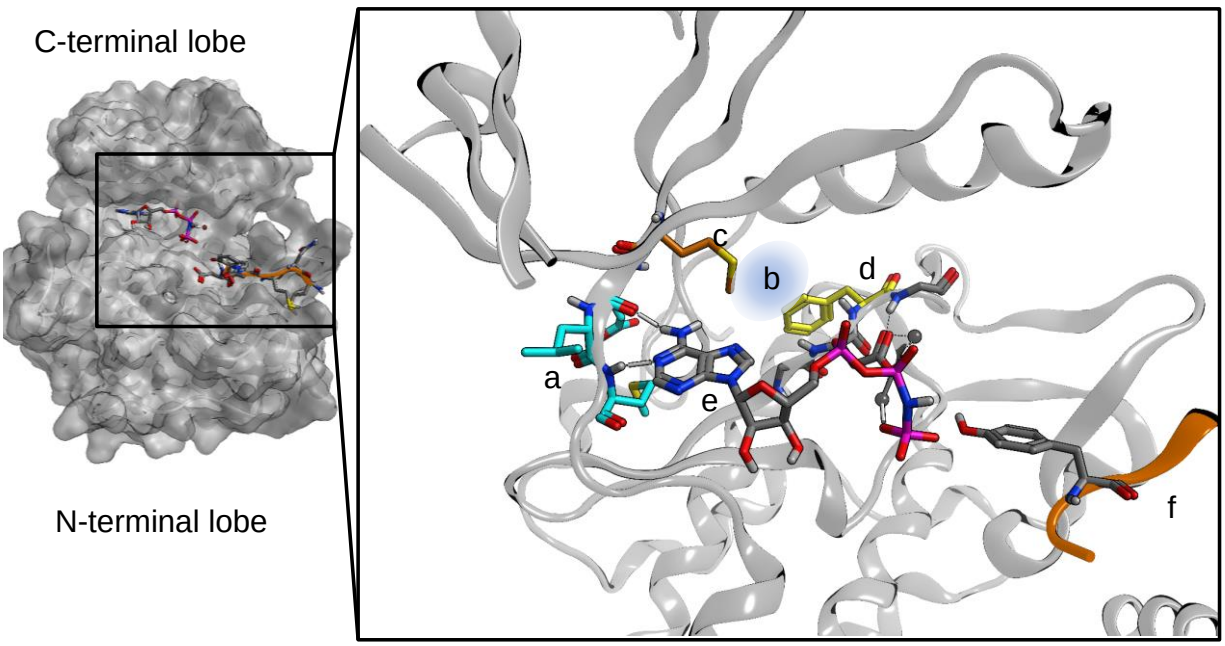

Figure 10. Left) Crystal structure of a tyrosine kinase complexed with an ATP analog and a peptide substrate with the C-terminal and N-terminal lobes annotated. Right) The catalytic site showing the hinge region (a), the hydrophobic backpocket (b), the gatekeeper residue (c), the DFG-region (d), an ATP-analog (e), and part of the substrate peptide (f). (PDB: 1ir3).

3.1.3 Kinases as drug targets

Because of their central role in controlling cell proliferation and apoptosis, deregulation of protein kinases have been linked to several disease states, most notably cancer[123-125]. As a consequence, the interest in developing inhibitors for kinases has been and still is substantial. While more than 20 ATP-competitive kinase inhibitors have been approved for clinical use[126], these are targeted to a relatively small portion of the kinome. Inhibitors of protein kinases are generally categorized by their mode of binding. Type I inhibitors are the most common. These target the active form of the protein kinase and bind to the ATP-binding site, typically by hydrogen bonding to the hinge region in a similar manner as ATP. Many of the type I inhibitors also protrude into a hydrophobic pocket located "behind" the ATP-binding site not utilized by ATP. The size and accessibility of this pocket is in part defined by the size and type of the so called gatekeeper residue located adjacent to the ATP-binding site. Since the gatekeeper residue varies between different kinases (although some residues are more prevalent than

others[126]), this pocket can be exploited to achieve kinase selectivity. Clinically approved examples of type I inhibitors include dasatinib[127] and vemurafenib[128] (Figure 11).

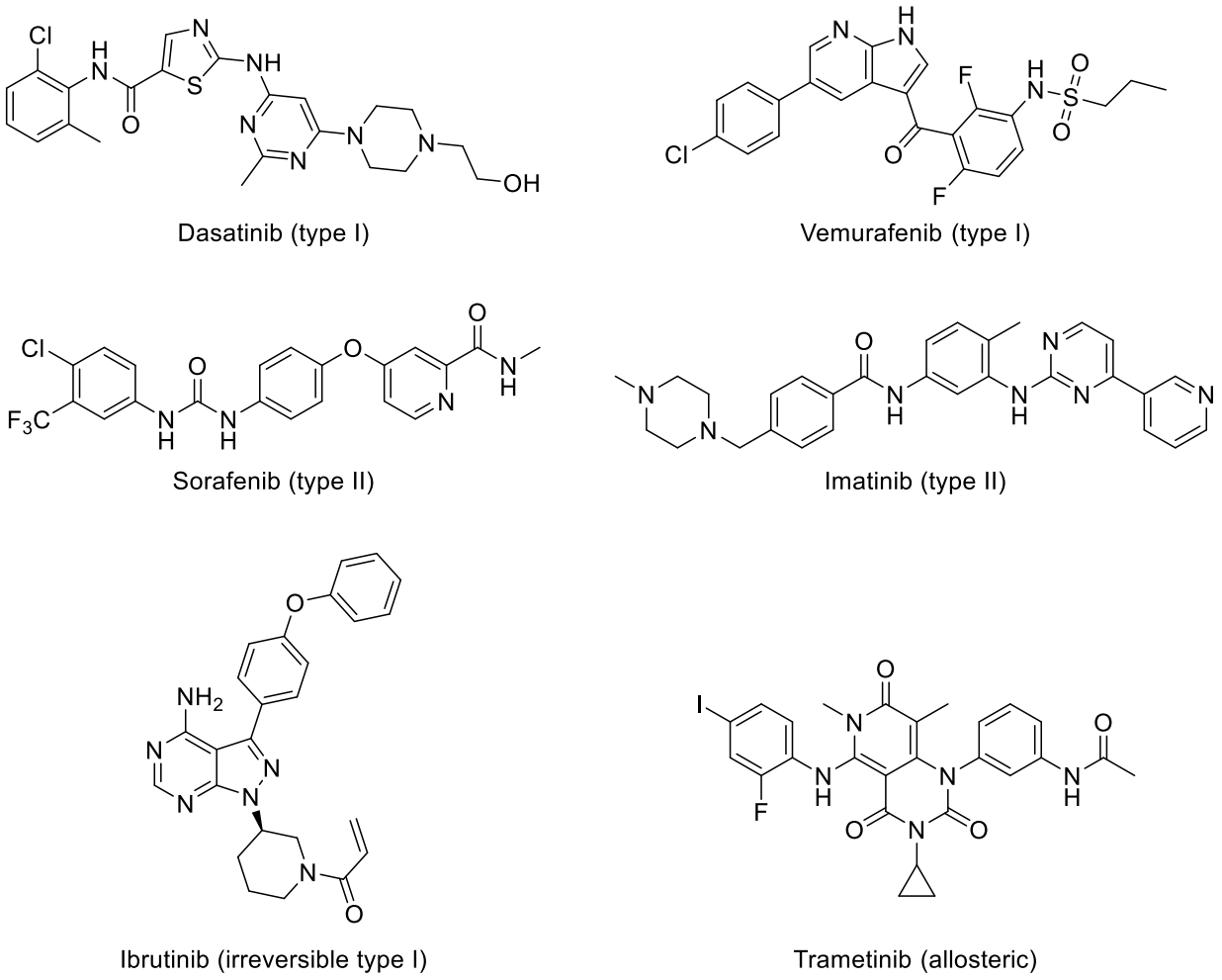

Figure 11. Examples of protein kinase inhibitors with binding mode and kinase target annotated.

The other major group, the type II inhibitors, binds to the inactive conformation of the enzyme, often referred to as the DFG out conformation[129]. This originates from observations in several kinases that the DFG region is flipped in the inactive form. This flip causes the phenylalanine (F) of the DFG region to point "out", opening up an additional hydrophobic pocket. Examples of type II inhibitors include sorafenib[130] and imatinib[131] (Figure 11), the latter being the first kinase inhibitor approved for treating cancer. There are also examples of inhibitors that bind to alternative, allosteric sites, outside the ATP-binding region, so called allosteric inhibitors[132]. An example of allosteric inhibitors are the Mitogen-Activated Protein

(MAP) Kinase/Extracellular Signal-Regulated Kinase (ERK) Kinase (MEK) 1 and 2 inhibitors that bind to a hydrophobic pocket close to the ATP-binding site and form a hydrogen bond to the γ-phosphate of ATP[126]. One example is trametinib[133] (Figure 11). These three types of inhibitors all bind reversibly to their target. The fourth group consists of the covalent inhibitors. These can be type I or II inhibitors modified with an electrophilic group positioned to make a covalent bond with an amino acid residue in the active site, often a cysteine. In the case of ibrutinib[134] (Figure 11), a Michael acceptor has been attached to a type I inhibitor.

3.1.4 Receptor Tyrosine Kinases and RET

Of the kinase subfamilies comprising the 500+ protein kinases of the human kinome[118], 58 have been identified as receptor tyrosine kinases (RTKs)[135]. RTKs play a central role in relaying signals from the outside to the inside of cells, thereby regulating cellular processes such as cell differentiation, migration and cell survival[123,135]. Structurally, RTKs are anchored to the cell membrane and consist of a transmembrane domain connecting an extracellular ligand binding domain with an intracellular tyrosine kinase domain[135]. Binding of a growth factor to the extracellular domain induces di- or oligomerization (exceptions include the insulin receptor which exists as a covalently linked dimer[135]) which in turn activates the intracellular kinase domain, either by inferring a conformational change or by (trans)phosphorylation[119].

REarranged during Transfection (RET) is a kinase belonging to the RTK subfamily. Binding of glial cell line-derived neurotrophic factors (GDNF) to GDNF family receptor (GFR)-α receptors located on the outside of the cell causes recruitment and dimerization of RET, resulting in activation of the kinase domain[136]. RET is involved in the development of the central and peripheral nervous systems. Additionally, dysregulation of RET has been found in thyroid cancers, including papillary thyroid carcinomas and multiple endocrine neoplasia type 2 (MEN 2)[136-138]. RET is therefore interesting to study for at least two reasons. Increased knowledge of how RET functions can give insight into neuronal development and also reveal information useful for understanding the role of RET in certain cancer cell lines. Since the action/activity of enzymes involved in developmental processes is inherently time dependent, temporal control of enzyme inhibition would be a valuable tool to study these processes. As discussed in Section 2.3.2, an inhibitor equipped with a photolabile protecting group can

provide both spatial and temporal control of inhibitor release. Despite the potential utility of caged protein kinase inhibitors, only a few examples have been reported[139,140].

Our group has previously developed a small molecule inhibitor of RET (**1**, Figure 12), with *in vitro* activity in the low nanomolar range, inhibitory effect on GDNF-induced RET phosphorylation of extracellular signal-regulated kinase (ERK)1/2, and high selectivity for RET[141]. In this study, we wanted to deactivate **1** with a photolabile protecting group and study the effects of *in situ* release of **1** in both biochemical and cell assays. In addition, we wanted to use the caged inhibitor to study the role of RET on motoneuron development in zebrafish embryos.

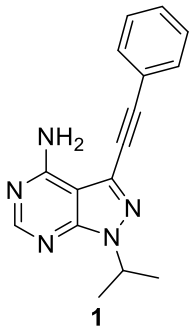

1

Figure 12. Structure of **1**.

3.2 Results and discussion

Of the different photolabile protecting groups mentioned in Chapter 2.3.2, we chose to initiate our investigations with the 6-nitroveratroyloxycarbonyl (NVOC) protecting group. Apart from being the most widely studied caging compound, there were three main reasons for our choice; 1) NVOC has previously been used in 6N protection of purines[142], structurally similar to **1**, providing a starting point for the synthesis; 2) NVOC can be removed at wavelengths >350 nm, i.e. wavelengths sufficiently low in energy to avoid extensive cell damage and; 3) NVOC-caged retinoic acid has been used to study the effect of retinoic acid on the development of zebrafish embryos[143], providing precedence of use in our model organism.

Compound **1** is a type I kinase inhibitor, hypothesized to bind by hydrogen bonding of N^5 and 4N‡ to the hinge region of RET. The phenethynyl moiety is proposed to protrude into the hydrophobic pocket of RET. Our hypothesis was that attaching the protecting group to a substituent that contributes to key interactions in the ATP binding site would lower the binding afffinity, achieving a clear difference between protected and free **1**. Docking **1** into the ATP-binding site of RET complexed with an inhibitor structurally related to **1** supports that the 4N functionality of **1** interacts with the hinge region of RET through a hydrogen bond to the amide oxygen of E805 (Figure 13a). The position is relatively deeply buried in the active site and a bulky group here should infer substantial steric hindrance. Superposition of caged **1** with **1** docked into the RET crystal structure clearly show steric clash between the hinge region and the caging group (Figure 13b).

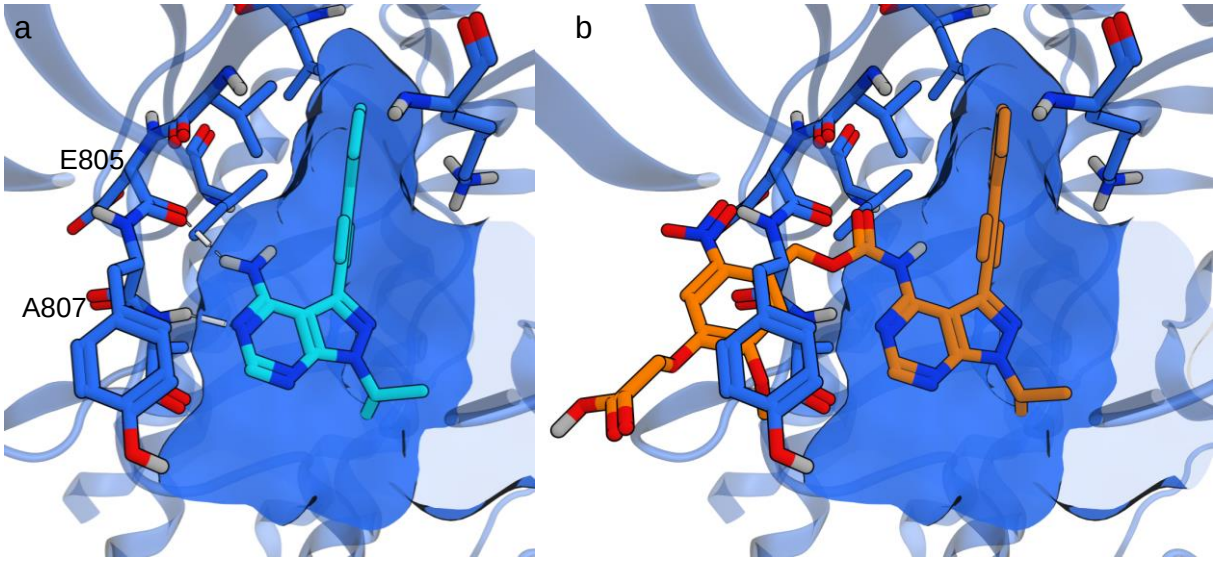

Figure 13. a) Model of **1** (turqoise) docked in the ATP-binding site of RET (blue, PDB: 2IVV) and b) caged **1** (orange) superimposed with **1** showing steric clash of the cage and the binding site. Hydrogen bonds between E805, A807 and **1** are represented as white lines.

3.2.1 Synthesis

Synthesis of **1** was performed following published procedures starting from commercially available 4-amino-1*H*-pyrazolo[3,4-*d*]pyrimidine (**2**) (Scheme 14).

‡ The N^5 and 4N substituents of pyrazolopyrimidines are homologous to the N^1 and 6N of purines, respectively.

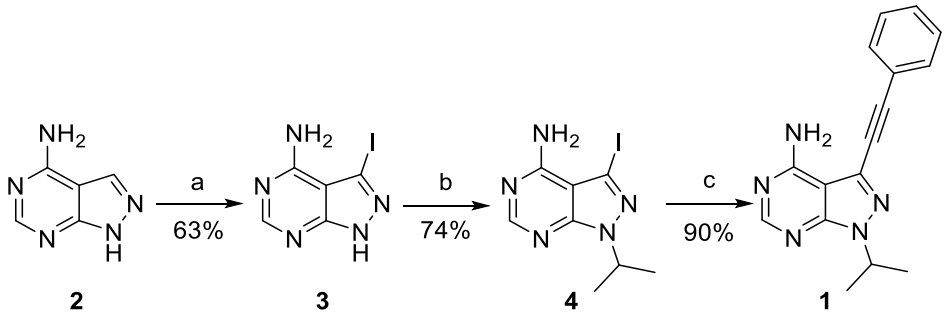

Scheme 14. Synthesis of **1**. a) NIS (1.1 equiv.) in DMF, 80 ºC, 5 h 30 min. b) *i*PrCl (1.1 equiv), K_2CO_3 (1.8 equiv.) in DMF, 200 ºC, 5 min, then *i*PrCl (0.5 equiv), 200 ºC, 5 min. c) $Pd(PPh_3)_4$ (5 mol%), CuI (9 mol%), Amberlite IRA-67 (4 equiv.), phenylacetylene (3.0 equiv.) in THF, 60 ºC, 18 h.

Since the acyl chloride of NVOC is commercially available, it is a natural starting point for the carbamate formation. However, reacting **1** with 6-nitroveratrylchloroformate (NVOC-Cl) (**5**) directly resulted in bisprotected **1** as the main product. Following a procedure for NVOC protection of ATP, 6-nitroveratryloxycarbonyltetrazolide[142] was preformed *in situ* by reacting NVOC-Cl (**5**) with tetrazole in the presence of base. Subsequent addition of **1** gave **6** in 42% yield (Scheme 15).

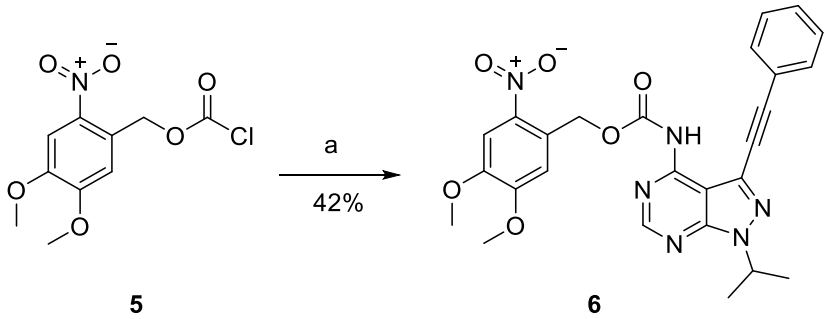

Scheme 15. Synthesis of **6**. a)(i) Tetrazole (0.45 M in MeCN), Et_3N (1.2 equiv.), 0 ºC to r.t. in THF. (ii) **1** (0.8 equiv.), 70 ºC, 48 h.

One of the criteria that needs to be fulfilled for a tool compound to be useful in biological experiments is that it is soluble in aqueous media, generally a buffer system. Although **1** is soluble in aqueous media, the protecting group adds considerable lipophilicity and **6** was found to have insufficient solubility for biochemical experiments.

Our next strategy was to introduce a hydrophilic group to increase aqueous solubility while keeping the structural modifications to a minimum. Introduction of a hydroxyl function in the

position of the isopropyl substituent of **1** was expected to have a small effect on binding affinity since this group is located in the sugar binding part of the ATP-binding pocket (see Figure 10). The new pyrazolopyrimidine substructure was synthesized by alkylation of 4-amino-3-iodo-1*H*-pyrazolo[3,4-*d*]pyrimidine (**3**) with (2-bromoethoxy)-tert-butyldimethylsilane under anhydrous basic conditions to give **7** in 74% yield (Scheme 16). $Pd(PPh_3)_4$-catalyzed Sonogashira coupling gave **8** in 95% yield. The 4N carbamate formation was performed as for **6** providing **9** in 65% yield. The NVOC protected hydroxyl-**1** was finally isolated after cleaving the silyl protecting group using tetrabutylammonium fluoride (TBAF) in THF (35% yield). The low yield in the last step was not optimized due to the low solubility of **10** in aqueous media.

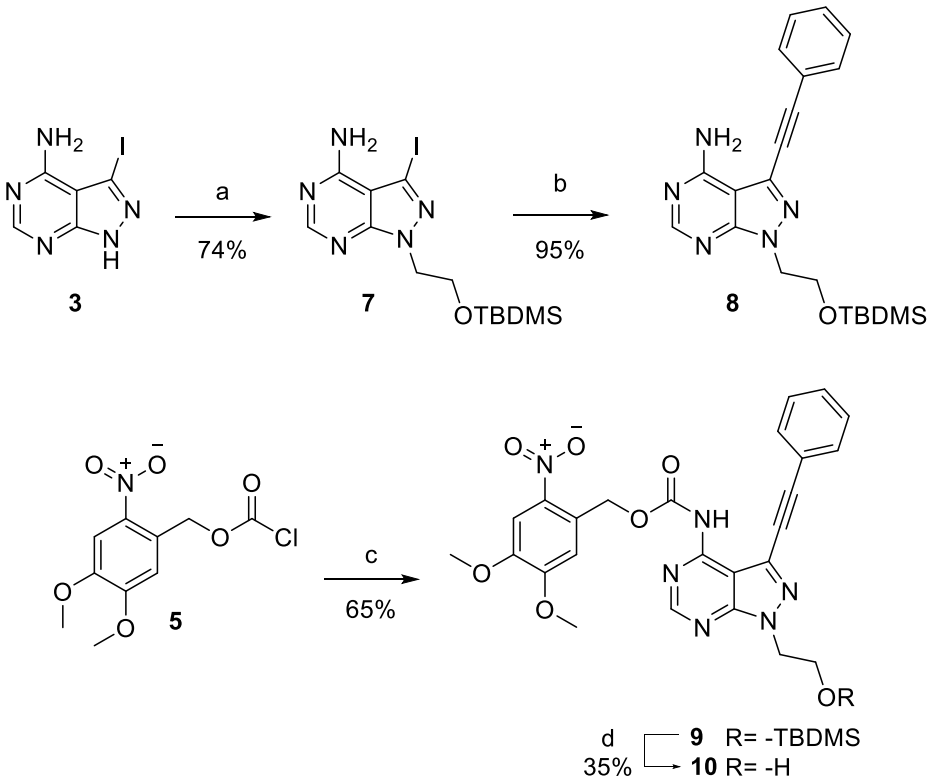

Scheme 16. Synthesis of **10**. a) (2-Br-ethoxy)-OTBDMS (1.2 equiv.), Cs_2CO_3 (1.2 equiv.) in DMF, r.t., 48 h. b) $Pd(PPh_3)_4$ (2.4 mol%), CuI (18 mol%), Amberlite IRA-67 (4 equiv.), phenylacetylene (2.9 equiv.) in THF, 60 ºC, 4 h. c) (i) tetrazole (0.45 M in MeCN), Et_3N (1.0 equiv.), 0 ºC to r.t. in THF, 1 h. (ii) **8** (0.5 equiv.), 70 ºC, 4 h. d) TBAF (2.1 equiv.) in THF, r.t., 3 h.

At this point, the increased lipophilicity caused by the introduction of NVOC shifted our attention to modifying the protecting group. One strategy for increasing the hydrophilicity of NVOC was to introduce a carboxylic acid on the protecting group. Nitrobenzyl protecting

groups bearing a carboxylic acid functionality have been reported[144] as a handle for attaching the PG to a solid support[145,146] and as a prodrug strategy[109]. We hypothesized that attaching a carboxylic acid to one of the methoxy substituents would have a minimal effect on the quantum yield of deprotection while increasing the hydrophilicity of the caged compound. The new protecting group 4-ethyloxycarbonylmethoxy-5-methoxy-2-nitro-benzyl alcohol **11** was synthesized from vanillin (Scheme 17). The alkylation, nitration and reduction were carried out without intermittent purifications. The short reaction time (10 min) and low temperature in the aldehyde reduction was necessary to avoid reduction of the ethyl ester. Running the reaction in ethanol at room temperature for 3 h resulted in a 3:1 mixture of diol and alcohol. Purification by column chromatography provided intermediate **11** in 14% yield over three steps. The relatively low yield was not optimized due to the affordable starting materials and the ability of postponing column chromatography to the last step.

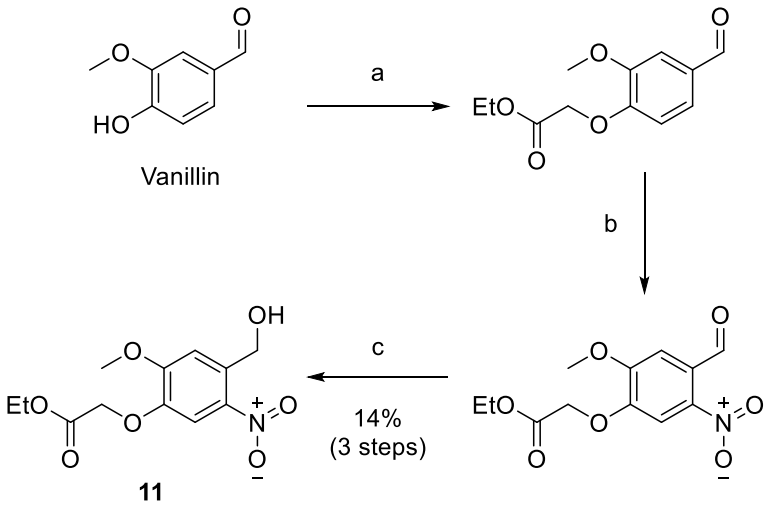

Scheme 17. Synthesis of carboxylate NVOC protecting group (**11**). a) K_2CO_3 (2.4 equiv.), KI (0.2 equiv.), ethyl bromoacetate (1.2 equiv.) in MeCN, 18 h. b) HNO_3 in HOAc, 0 ºC to r.t., 18 h. c) $NaBH_4$ (1 equiv.) in THF:EtOH 1.2:1, 0 ºC, 10 min.

Since the benzyl alcohol of **11** is not activated, a new approach for the carbamate formation was necessary. Using a protocol developed for *t*Boc-protection of primary anilines[147], **1** was heated at 105 °C with carbonyldiimidazole (CDI) in DMF followed by addition of **11** which resulted in **12** (50% yield, Scheme 18). Hydrolysis of the ethyl ester with LiOH in water and

dioxane (1:1) resulted in **13** (80% yield). As expected, this compound was soluble in aqueous buffer (1 vol% DMSO, up to 100 μM).

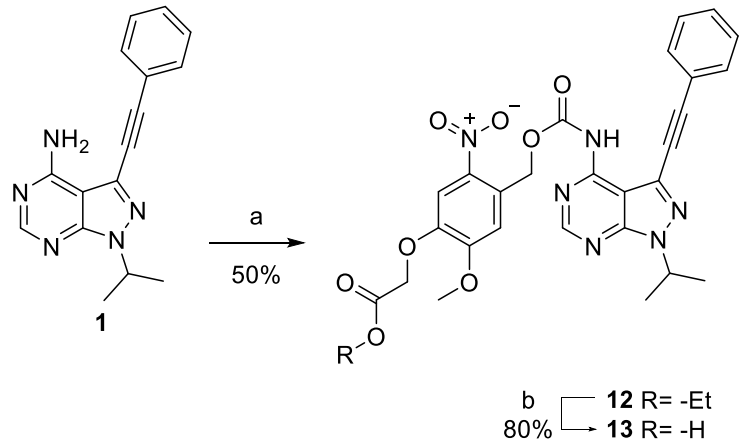

Scheme 18. Synthesis of **13**. a) (i) CDI (2.9 equiv.) in DMF, 105 °C, 2 h. (ii) **11** (2.9 equiv.), r.t., 19 h. b) LiOH (2.3 equiv.), r.t., 20 min.

Next, the photoinduced cleavage of the protecting group was investigated. **13** was irradiated with 365 nm light. The reaction kinetics was deduced by monitoring the deprotection using HPLC and the decaging followed first order kinetics with respect to disappearance of **13** as well as liberation of **1** (see Appendix 1, Figure A1).

3.2.2 Biochemical and Cell Assays

As a first evaluation of the photocontrollable inhibition of RET with **13**, an *in vitro* assay with purified RET kinase was used. The readout of the assay is luminescence originating from phosphorylation of a luciferase enzyme by ATP which in turn has been formed by ADP production during substrate phosphorylation by RET. The luminescence is therefore directly linked to RET activity. Two preparations of compound **13**, RET kinase and substrate were made, one of the preparations was exposed to light (365 nm, 15 min), while the other was kept in the dark. Next, ATP was added and the plates were incubated at room temperature for 30 min. Measuring the kinase activity revealed that the IC_{50}-value of the compound kept in the dark was 12 times higher than the light irradiated compound (6.8 μM to 590 nM, Figure 14).

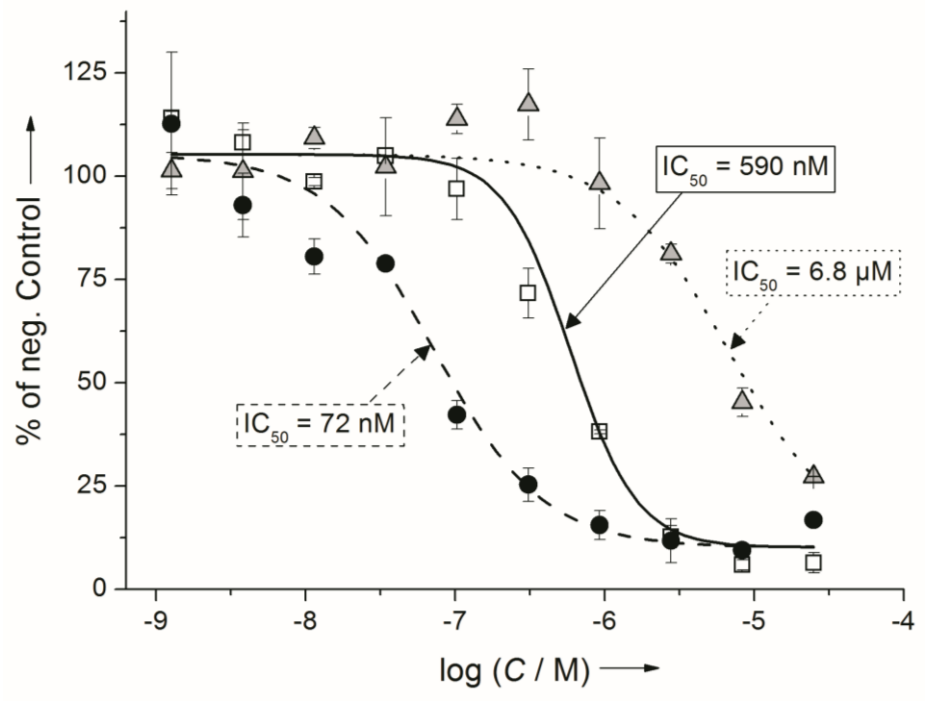

Figure 14. *In vitro* RET assay. The ATP depletion induced by RET-activity was monitored by luminescence intensity. The activity readout following incubation with **1** (circles), **13** (triangles) and light-exposed **13** (15 min 365 nm, squares) was referenced to a negative control incubation (without compound added). IC_{50}-values of 72 nM, 6.8 µM, and 590 nM for **1** (dashed line), **13** (dotted line), and irradiated **13** (solid line), respectively. Data is represented as mean ± standard deviation of duplicate samples.

These results show that the inhibitory activity of **13** can be controlled by light. The inhibitory activity that is observed for **13** without irradiation could result from weak binding of **13** to RET. Given the expected binding mode of **1** and the size of the protecting group, this is somewhat unlikely but cannot be excluded completely. There is also the possibility that the effect is a result of small amounts of contamination of free **1** (<0.5% by HPLC). For reference, the IC_{50} of **1** was determined to 72 nM. Since deprotection was not complete within the applied 15 min of irradiation, the higher IC_{50} measured for the decaged compound compared to free **1** (72 nM) was expected (Appendix 1, Figure A1). Tolerance to the UV-light used is essential for any light controlled biochemical or biological experiments. RET activity was therefore measured excluding the inhibitor with and without 365 nm irradiation. No changes in kinase activity could be detected after up to 15 min of light exposure (Appendix 1, Figure A2), validating the use of the applied light dose.

The photoactivation of **13** was then evaluated in a commercial whole cell assay with cells expressing RET[148,149]. Compound **13** was incubated with the cells for 3 h at 37 °C. Then, one of the preparations was irradiated with light (365 nm, 15 min), while the other was kept in the dark. Neurturin, a growth factor that activates RET was added and the cell plates were incubated for 3 h at 22 °C. Measurements of RET activity after addition of detection reagent revealed a clear difference in kinase activity between the irradiated and non-irradiated preparations. Irradiated **13** showed an IC_{50} of 8.7 μM (Figure 15) while non-irradiated **13** displayed partial inhibition at concentrations higher than 1 μM. However, no IC_{50} value could be obtained for non-irradiated **13**. As expected from the cell free assay, incubation with free **1** resulted in a lower IC_{50} (470 nM) than for irradiated caged **1**. The observed negative (lower than positive controls without growth factor) activities in the cell assay (Figure 15) have been reported for comparable assays and is likely an effect of growth factor independent RET-activity[148]. To confirm that irradiation did not cause any side effects, cells without inhibitor were irradiated for 15 min and no significant decrease in kinase activity could be observed (Appendix 1, Figure A2).

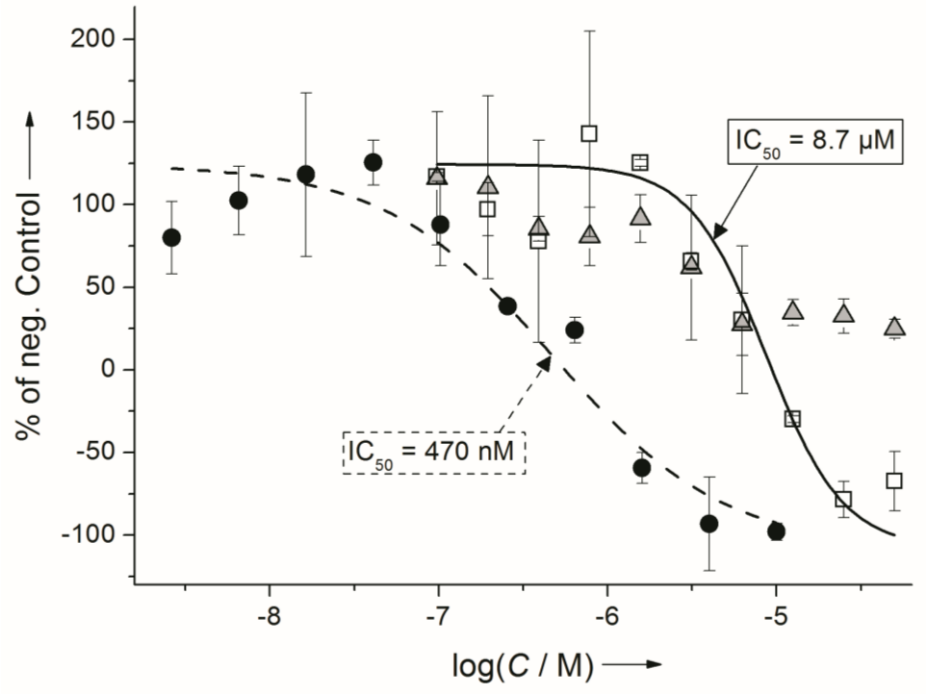

Figure 15. Dose-response curves from live-cell RET assay. The activity readout following incubation with **1** (circles), **13** (triangles) and light-exposed **13** (15 min 365 nm, squares) was referenced to a negative control incubation (without compound). IC_{50}-values were 470 nM for **1** (dashed line) and 8.7 μM for irradiated **13** (solid line). We were unable to extract meaningful IC_{50}-data with non-irradiated **13** included in the fit. Data is represented as mean ± standard deviation of duplicate samples.

3.2.3 Effects of inhibitor release on motoneuron development

The gene coding for Ret§ has been found to be expressed in motoneurons in both humans[150] and in zebrafish [151-153]. Although this expression suggests that Ret has a role in motoneuron development, this has not previously been shown for zebrafish. We wanted to test if photocontrolled inhibition of Ret could be performed *in vivo* as well as to gain additional information of the role of Ret in zebrafish motoneuron development.

A transgenic zebrafish line (tg(*olig2:dsRed*) was used for these studies. These fish have ventral spinal cord precursor cells that express the gene for a fluorescent protein that allows detection of motoneurons and oligodendrocytes (developed from these cells) using confocal microscopy.

A solution of **13** (final concentration of 50 μM) was added to Zebrafish embryos 3 hours post fertilization (hpf). Since the precursors of the axons start developing at 18 hpf[154], and Ret activity was assumed to be important for this process, irradiation was performed at 14 hpf. At 14 hpf, the embryos were washed with fresh medium and irradiated for 15 min (365 nm). The embryos were then allowed to develop until 2 days post fertilization when they were analyzed by confocal imaging. Control experiments were performed with non-irradiated embryos exposed to **13** and irradiated embryos in 1 vol% DMSO without compound. These embryos did not show any phenotypic anomalies and displayed normal motoneuron development (Figure 16a and b).

§ Ret refers to the protein in zebrafish while RET refers to the human ortholog.

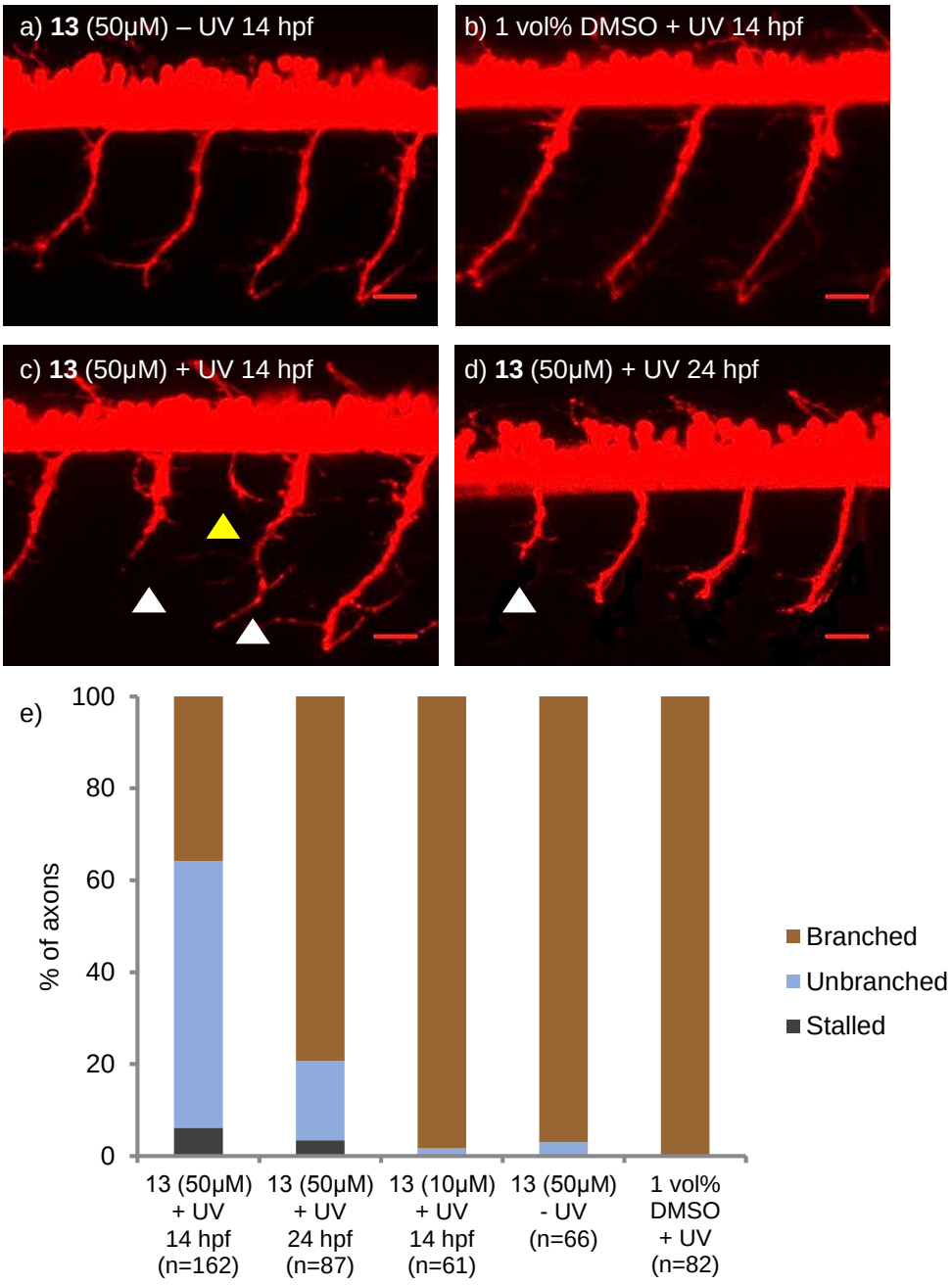

Figure 16. Confocal images of tg(*olig2:dsRed*) zebrafish fish showing motoneuron axons after treatment with **13**. Triangles mark stalling (white) and erroneous (yellow) axons. Scale bar: 20 µm. a) 50 µM **13** without irradiation, b) 1vol% DMSO with irradiation, c) 50 µM **13** irradiated at 14 hpf, d) 50 µM **13** irradiated at 24 hpf and e) quantification of axonal phenotypes in the different treatments. n = number of axonal processes quantified.

Embryos incubated with **13** and irradiated for 15 min at 14 hpf displayed motoneurons with shortened and malformed axons compared with the controls (Figure 16c). This phenotype was

also observed when embryos were treated with free **1** (10 and 50 μM), indicating that the effect of irradiated **13** was a result of released inhibitor (Appendix 1, Figure A3). Apart from altered axonal extensions, these embryos developed normally and formed motoneurons, indicating that the effect of Ret inhibition was specific to motoneuron extension. These results show that **13** can be absorbed by the embryo and that incubation with **13** without irradiation (at 50 μM) or irradiation without **13** (15 min at 365 nm) does not affect motoneuron development of embryos. Embryos exposed to **13** were also irradiated at 24 hpf (Figure 16d). This resulted in similar but less severe effects compared with irradiation at 14 hpf. These results show the time dependence of Ret-activity during development.

3.3 Conclusion

In this project, a water soluble caged RET kinase inhibitor was developed. The caged compound was shown to inhibit RET *in vitro*, both in a biochemical and in a cell assay with a clear difference between irradiation and no irradiation. The inhibitor can also be released in zebrafish embryos and it was shown that decaging by irradiation with light resulted in inhibition of motoneuron development *in vivo*. The time of release was shown to be essential for the inhibition process, highlighting the significance of a photocontrolled approach. The non-irradiated compound does not affect axonal extension at the concentrations used. The caged inhibitor in combination with two-photon excitation techniques could offer possibility of spatial control of the inhibition of RET, adding one more dimension of RET activity to be explored.

4. 8-(Triazolyl)purines as potential aminoacyl adenylate mimics (Paper II)

4.1 Introduction

Adenylate forming enzymes catalyze the functionalization of a range of biomolecules and play an important role in several biological processes[155]. Aminoacyl transfer RNA (aa-tRNA) synthetases are members of the adenylate forming enzymes and catalyze the coupling of amino acids to their cognate tRNAs, a key step in protein synthesis. Because of their role in protein synthesis, aa-tRNAs have been identified as targets for antiinfectives[156]. In this project, we have synthesized a series of 8-(triazolyl)purines designed as aminoacyl-adenosine monophosphate (aa-AMP) mimics intended as aa-tRNA synthetase inhibitors.

4.1.1 aa-tRNA synthetases and their inhibitors

The aa-tRNA synthetases are divided into two classes (I and II), consisting of 10 enzymes each[157]. The classes are further subdivided in three subclasses (a-c), depending of the structural features of the proteins[158]. The general reaction catalyzed by the aa-tRNA synthetases proceeds by first forming an aa-AMP by reaction between a carboxylate and ATP, a reaction driven by pyrophosphate release[158]. A nucleophilic attack by an adenosine on the 3' end of tRNA gives aa-tRNA and releases AMP. The aa-tRNA is then used in protein synthesis (Scheme 19).

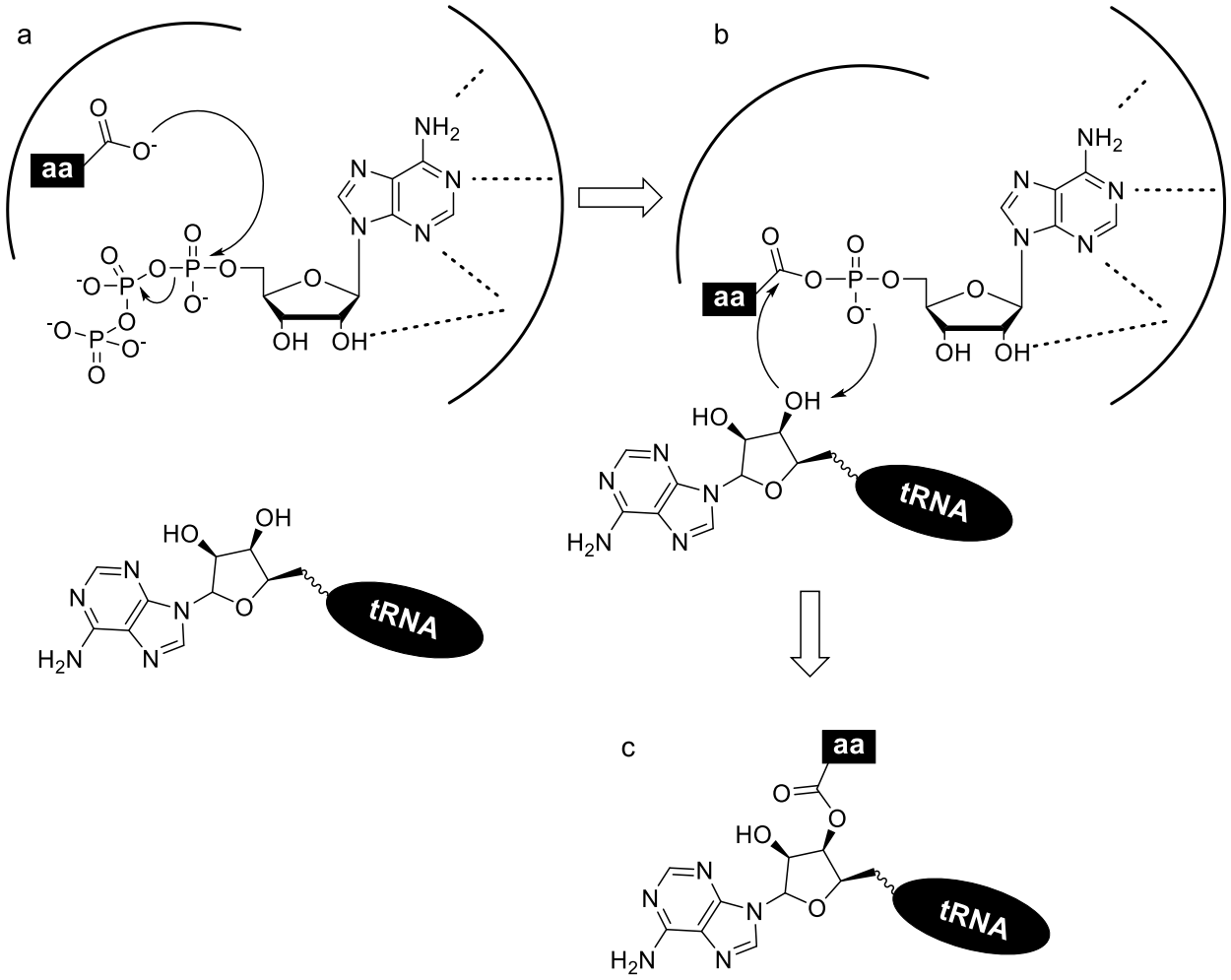

Scheme 19. Enzymatic adenylation mechanism. Reaction between a carboxylate and ATP forms an aa-AMP (a) and nucleophilic attack by an adenosine on tRNA (b) gives aa-tRNA (c) and releases AMP.

aa-tRNA synthetases have been linked to a wide range of disorders, including neuronal, autoimmune and cancer related diseases[159]. Due the essential role of aa-tRNA in protein synthesis, inhibitors with selectivity for bacterial or fungal over human aa-tRNA synthetases are interesting drug candidates[156,158]. Figure 17 provides examples of four different types of aa-tRNA synthetase inhibitors. Pseudomonic acid (mupirocin) is a natural product Ile-tRNA synthetase inhibitor being used as a topical antifungal agent[160]. The benzoxaboroles, represented by AN2690 are Leu-tRNA inhibitors, also developed as antifungal agents[161]. These compounds have been shown to bind to and lock Leu-tRNA in the editing site of Leu-tRNA synthetase[162]. Another type of compounds investigated as aa-tRNA synthetase inhibitors are mimics of the aa-AMP reaction intermediate, exemplified by the sulfamoyl-adenosines[163]. Quinolones have also been investigated as aa-tRNA synthetase inhibitors[164].

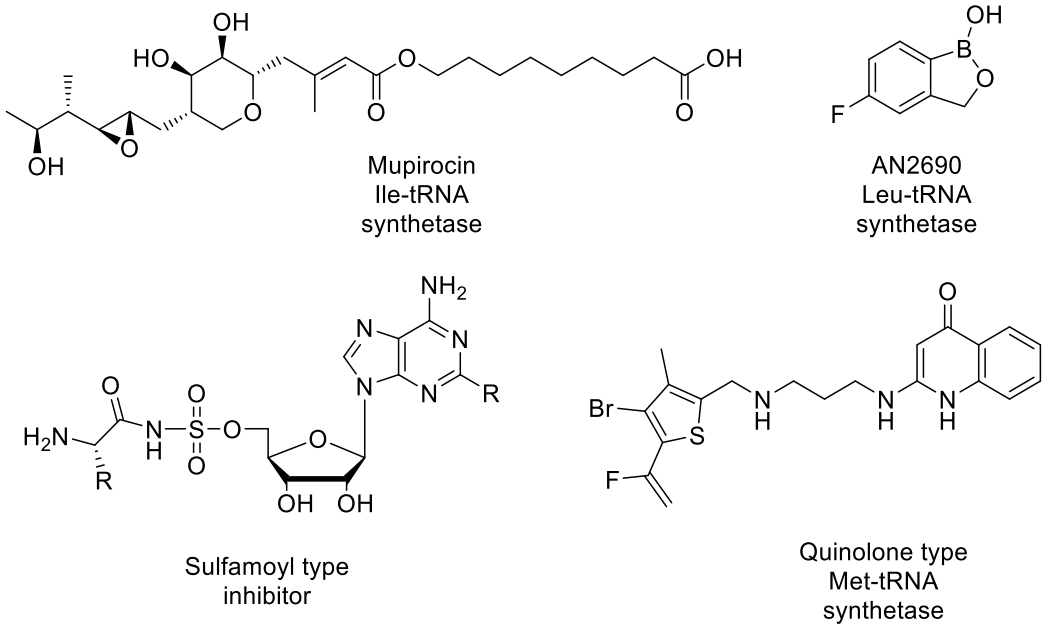

Figure 17. Examples of aa-tRNA synthetase inhibitors and their target when applicable.

4.2 Results and discussion

The design of a series of 8-(triazolyl)purines as aa-AMP mimics was based on the structure of the sulfamoyl adenosine derivative shown in Figure 17. Our hypothesis was that the triazole could act as a linker between the amino acid and the purine ring system while maintaining their relative positions in space (Scheme 20).

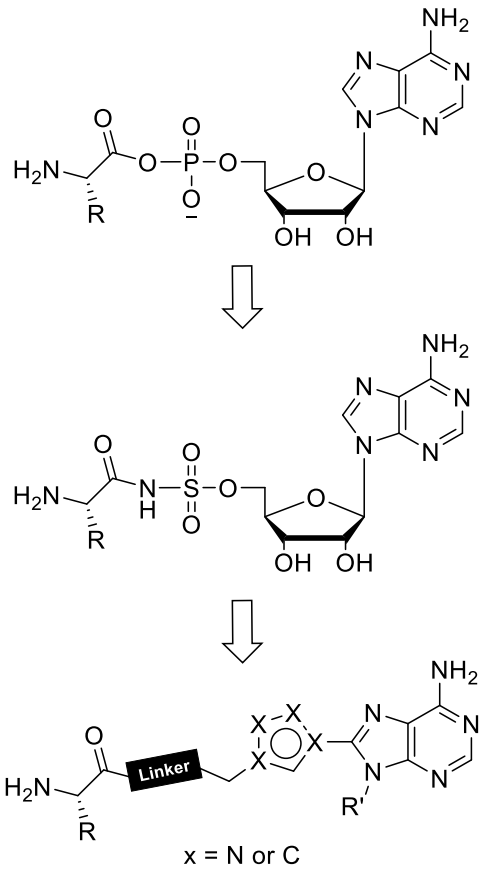

Scheme 20. Design strategy of 8-(triazolyl)purines as aa-AMP mimics.

As these 8-(triazolyl)purines are structurally similar to adenosine analogs previously synthesized in our group[165] as fluorescent base analogs, we hypothesized that this scaffold could be utilized for small molecule fluorescent probes.

4.2.1 Synthesis

Our initial strategy incorporated a 4-(purinyl)triazole and an imide linker between the aminoacyl and the triazole (Figure 18).

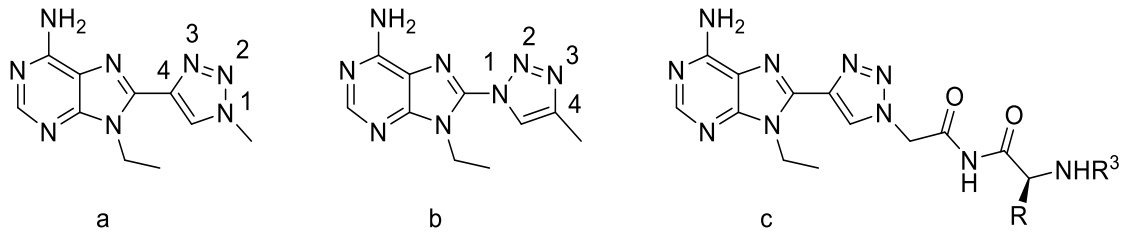

Figure 18. a) 4-(purinyl)triazole, b) 1-(purinyl)triazole and c) imide linked 4-(purinyl)triazole.

Starting from commercially available adenine (**14**), alkylation with ethyl iodide under anhydrous basic conditions provided 9-ethyladenine (**15**) in 66% yield (Scheme 21).

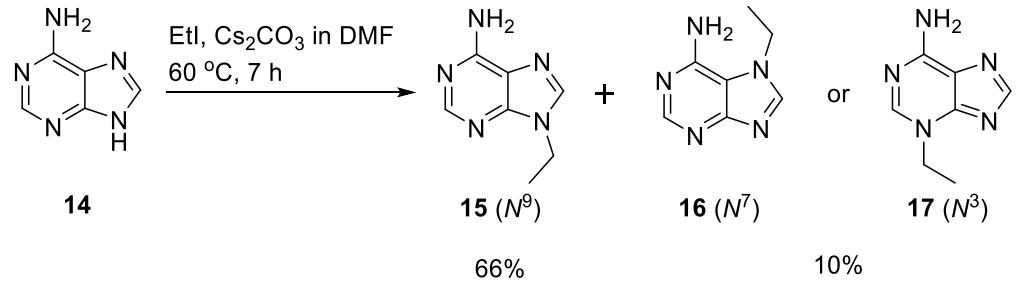

Scheme 21. Alkylation of adenine (**14**). EtI (1.2 equiv.), Cs_2CO_3 (1.2 equiv.) in DMF, 60 ºC, 7 h.

There are theoretically five nucleophilic positions on adenine, although alkylation generally occurs at only two of these. Besides N^9-alkylation, we observed a minor isomer isolated in 10% yield. This isomer corresponded to the ^{1}H-NMR (DMSO-d_6) chemical shifts published for 7-ethyladenine[21] for which nuclear Overhauser effect spectroscopy (NOESY) was used to determine the structure. Other accounts[166] however, state that alkylation generally favors the N^9-position but that the minor isomer is the N^3-alkylated isomer despite the fact that the major NH-isomers observed in solution are N^7H and N^9H[5]. We analyzed the major and minor isomers using 1D and 2D-NMR spectroscopic methods in order to elucidate the structures of the regioismers obtained in our case. According to a recent NMR study of N^3- and N^9-alkylated purines, the ^{13}C signals for C-8 and C-2 switch places depending on the substitution pattern, C-8 being upfield of C-2 in N^9-alkylation and the reversed being observed for N^3-alkylation[167]. This would account for the initially confusing observation that the methylene protons seem to couple to the "same" C-H carbon (at 140.4 ppm in the major isomer and 143.0 ppm for the

minor isomer) in heteronuclear multiple bond coherence (HMBC) experiments for the major and minor product (Figure 19).

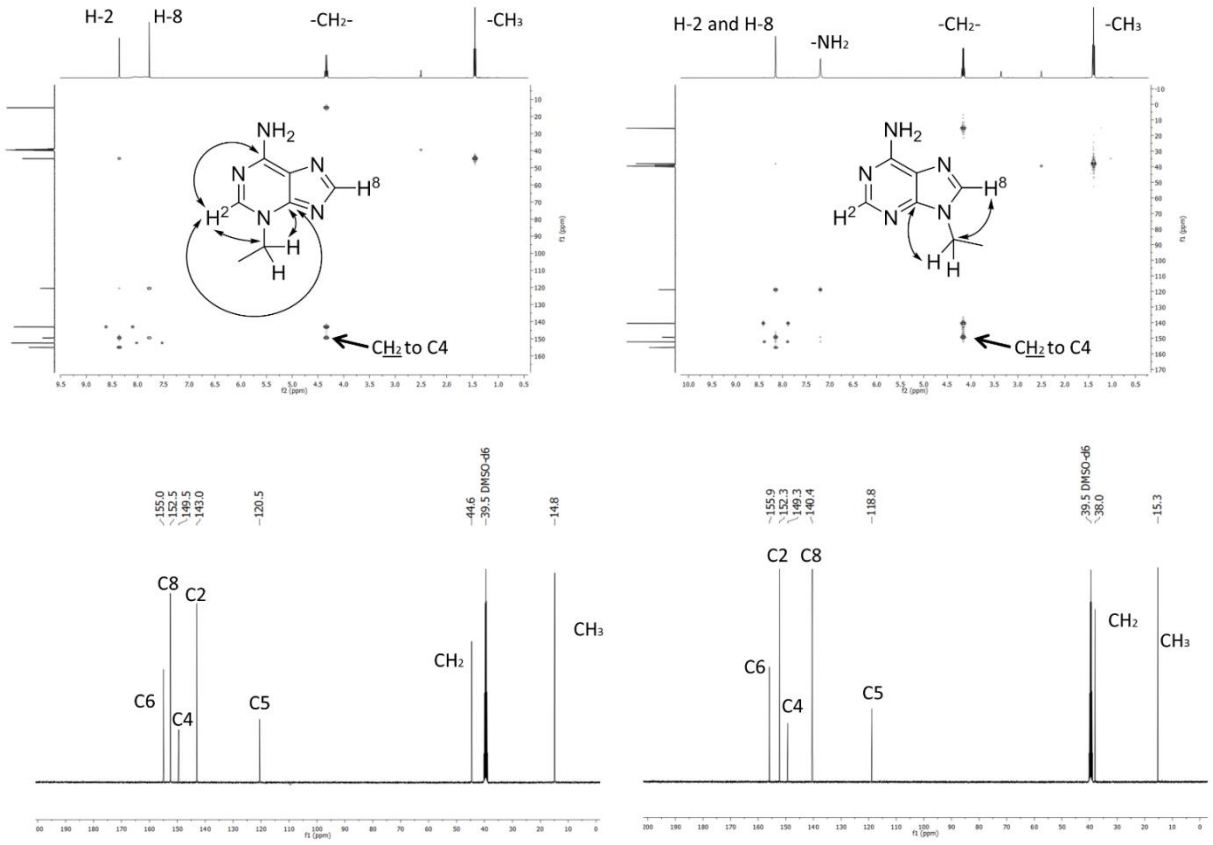

Figure 19. 1D and 2D NMR-elucidation of the two isomers obtained in the alkylation of adenine. Key ^{3}J C-H couplings are indicated by arrows. Assignment of ^{13}C signals follows the purine numbering (see Appendix 2 for additional ^{1}H- and ^{13}C-NMR spectra).

This is also likely to be the reason for the inconsistency in assignments mentioned above. However, the methylene protons have a ^{3}J ^{13}C-^{1}H coupling to C-4 in both isomers, an observation that clearly supports that the *N*3-ethylated compound is the minor isomer. In the minor isomer, there is also a ^{3}J ^{13}C-^{1}H coupling between H-2 (8.36 ppm) and the methylene carbon signal (154.9 ppm). H-2 is assigned by ^{3}J ^{13}C-^{1}H coupling to C-6 (155.0 ppm) and C-4 (149.5 ppm) and H-8 (7.78 ppm) has ^{3}J ^{13}C-^{1}H coupling to C-5 (120.5 ppm) and C-4. The upfield shift of C-5 has been observed by others, and so has the low intensity of C-4 and C-5, being bridging carbons (affecting T1-relaxation)[168]. It can also be noted that in *N*9-alkylated compounds, H-8 and H-2 have very similar chemical shifts while in *N*3-alkylated derivatives, H-8 shifts upfield and H-2 downfield[167]. The similar chemical shift for *N*9 corresponds with

our assignment of 9-ethyladenine. There is also a NOE coupling between the methylene protons and the downfield aromatic proton (H-2) in the byproduct, further supporting that the correct structure is an N^3-alkylated species. The pattern of the methylene carbon chemical shift in **15** being upfield of **17** also matches the literature[167]. The NMR spectral analysis supports the N^3-alkylated product as the minor isomer obtained in our study.

Returning to the synthesis of the 8-(triazolyl)purines, bromination of the alkylation product with Br_2 provided 8-bromo-9-ethyladenine (**18**) (Scheme 22).

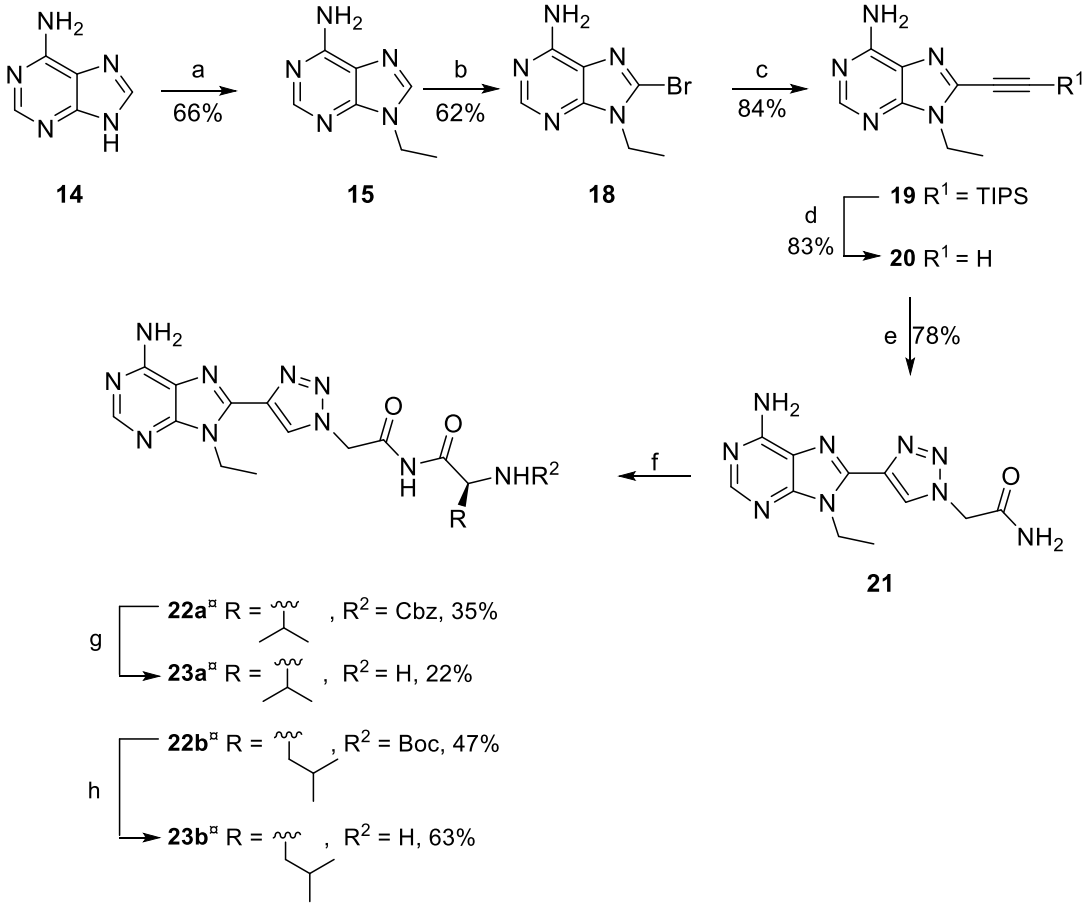

Scheme 22. Synthesis of the imide linked aminoacyl triazolylpurines. a) EtI (1.2 equiv.), Cs_2CO_3 (1.2 equiv.) in DMF, 60 °C, 7 h. b) Br_2 in HOAc buffer/THF/MeOH, 0 °C to r.t., 24 h. c) $Pd(PPh_3)_2Cl_2$ (5 mol%), CuI (20 mol%), amberlite IRA-67 (5 equiv), ethynyltriisopropylsilane (3.3 equiv) in THF, MW 120 °C, 30 min. d) PS-fluoride (2.4–3.6 equiv, 2-3mmol/g loading) in THF, r.t., N_2, 24 h. e) (i) NaN_3 (1.2 equiv), 2-bromoacetamide (1.1 equiv) in DMF, MW 80 °C, 20 min. (ii) **20** (1.0 equiv), sodium ascorbate (0.6 equiv), CuI (0.2 equiv), *N*,*N´*-dimethylenediamine (0.3 equiv), MW 80 °C, 2 h. f) NaH (2.0 equiv), R^2–amino acid-ONp (1.1 equiv.) in THF, 0 °C 15 min then at r.t., 3–5 h. g) H_2/Pd/C (10% CatCart, 30x4 mm, H-cube®, 21 °C, 25 min, MeOH, flow rate: 1 ml/min). h) 50% TFA in DCM, 1–1.5 h. ¤Unstable compounds.

Sonogashira coupling to introduce an ethynyl in the 8-position was initially attempted using TMS-acetylene which resulted in a mixture of protected and deprotected product as well as poor yields. Changing to acetylene with the more stable TIPS-acetylene gave the 8-alkynyl purine **19** in 84% yield and the terminal alkyne **20** was accessed after silyl deprotection with polymer supported fluoride (83% yield). The use of a polymer bound ammonium counter ion for fluoride facilitates the workup and purification of the reaction. A copper catalyzed alkyne azide cyclization (CuAAC) with 2-azidoacetamide provided **21** which was set up for the imide formation. As discussed in section 2.1.4, this reaction allows regioselective cyclization of a terminal alkyne and an azide to obtain 1,4-triazoles. Imide synthesis with *n*-BuLi as base and nitrophenyl activated ester[169] resulted in only traces of the target compound. Using NaH as base with either Cbz-L-valine 4-nitrophenyl ester or *t*Boc-L-leucine 4-nitrophenyl ester provided the imides **22a** and **22b** in 35% and 47% yield, respectively. Removal of the Cbz protecting group by hydrogenation (H-cube® with Pd/C 10 wt% catalyst cartridge) and subsequent purification by preparative HPLC provided **23a** in 22% yield. A byproduct (**24**) resulting from nucleophilic attack by methanol on the imide was observed by ^{1}H-NMR and LCMS (Scheme 23) and in part explains the poor yield. The same byproduct was observed when purification was attempted on silica with methanol in dichloromethane (DCM) as eluent. Deprotection of the *t*Boc protecting group of **22b** with TFA (50% in DCM) and subsequent purification by preparative HPLC provided **23b** in 63% yield. Unfortunately, these compounds were also unstable when stored at -10 ºC.

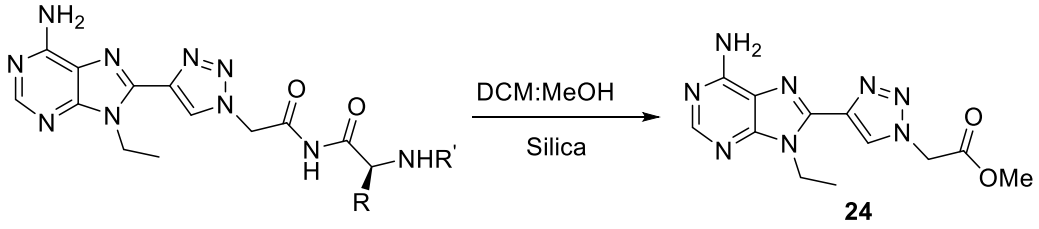

Scheme 23. Byproduct formed during purification with flash column chromatography using methanol in DCM as eluent.

Because of their instability, both in the presence of methanol and during storage, an alternative linker was needed. In the second strategy, the imide was replaced with an amide linker and the triazole was inverted (Figure 20).

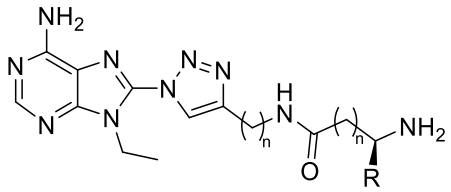

Figure 20. Amide linked 1-(purinyl)triazole type compound.

Inverting the triazole ring reduces the number of reaction steps and opened up to performing the CuAAC with easily accessible alkynyl amides and *in situ* formed 8-azidopurine[170]. Again, the synthesis started from 8-bromo-9-ethyladenine (**18**). Propargylamides **25a-c** and β-alkynylamides **25d-e** were synthesized by amide coupling of *N*-protected amino acids with propargylamine and 4-butynylamine with either HOBt and EDC or DCC (**25a** and **b**, 55% and 72% yield, respectively), or HATU and Et_3N (**25c**-**e**) in 66-88% yield. 8-Azido-9-ethyladenine was obtained by heating **18** and sodium azide at 90 °C for 22 h in DMF with the exclusion of light. Formation of the heteroarylazide was confirmed by LCMS and without isolation of the formed azide intermediate, CuI, sodium ascorbate (NaAsc), *N*,*N*´-dimethylethylenediamine (DMEDA) and Cbz-valine-propargylamide were added to the reaction mixture and heated at 90 °C for 24 h. Existing protocols for similar azidopurine forming reactions using DMSO failed to provide satisfactory conversions in our hands[171, 172]. The reaction resulted in the isolation of a compound which corresponded to the debenzoylated product **26a** by ^{1}H-NMR while the HRMS data did not correspond to the expected *m*/*z* (Table 1).

Table 1. Synthesis of compounds **26a-h**.

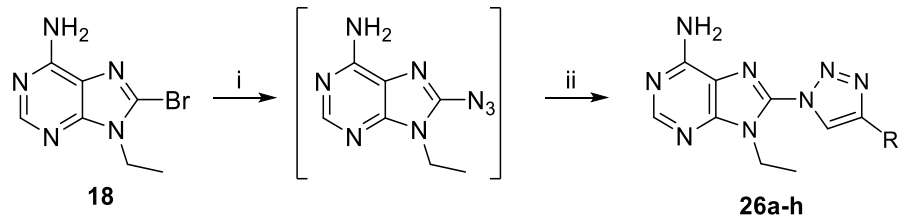

Entry	alkyne	Alkyne	Compound	R	Yield, (%)
1	**25a**	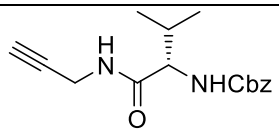	**26a**	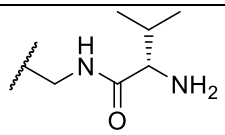	—*
2	**25b**	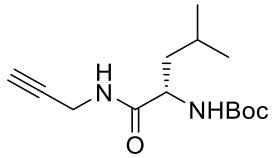	**26b**	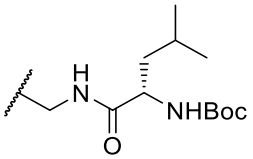	40
3	**25c**	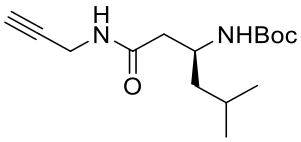	**26c**	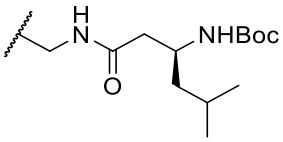	40
4	**25d**	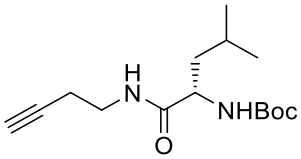	**26d**	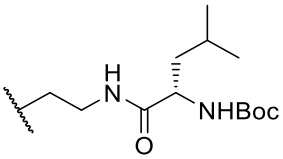	45
5	**25e**	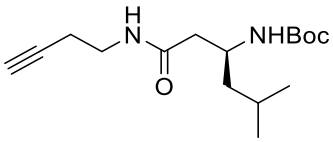	**26e**	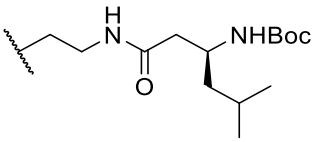	38
6	**25f**	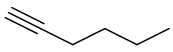	**26f**	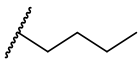	48
7	**25g**	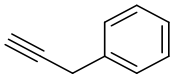	**26g**	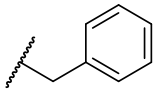	50
8	**25h**	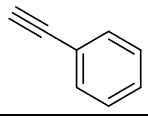	**26h**	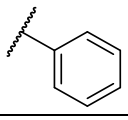	50

Compounds **26b**-**e** were purified by preparative HPLC while compounds **26f**-**h** were purified by flash chromatography on silica. (i) NaN_3 (1.8 equiv) in DMF, 90 °C, 22 h. (ii) alkyne (1.4 equiv), sodium ascorbate (0.4 equiv), CuI (20 mol%), DMEDA (0.3 equiv), r.t., 24 h, in the dark. *No product isolated.

Cyclization with Cbz-Leu-propargylamide under these reaction conditions also failed to provide the expected product in practical yields. To avoid deprotection during the cyclization, the protecting group was changed to *t*Boc and the reaction was carried out at room temperature overnight. Under these conditions, triazoles **26b**-**e** were isolated in 38-45% yield after purification by preparative HPLC. The target compounds were accessed by *t*Boc deprotection by TFA in DCM (Table 2). In order to better compare the potentially fluorescent properties of these "inverted" 1-(purinyl)triazoles with 4-(purinyl)triazoles previously published in the group, **26f**-**h** were synthesized. The *in situ* formed azido-purine was reacted with alkynes **25f**-**h** using the same reaction conditions as for **26b**-**e** providing **26f**-**h** in 48-50% yield (Table 1).

Table 2. Deprotection of **26b-e**.

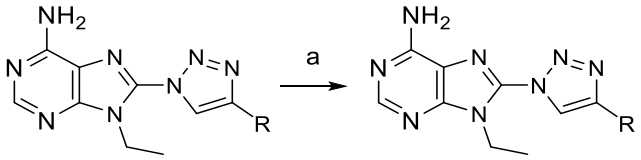

Entry	R	Compound		Yield, %
1	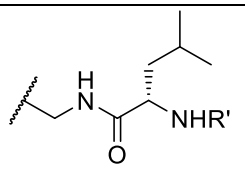	**26b** R^1=*t*Boc	**27b** R^1=H	94
2	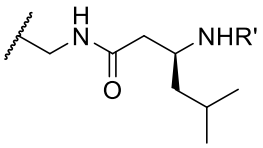	**26c** R^1=*t*Boc	**27c** R^1=H	99
3	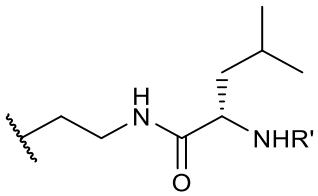	**26d** R^1=*t*Boc	**27d** R^1=H	99
4	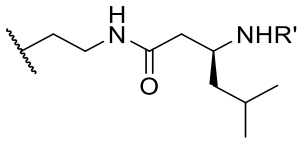	**26e** R^1=*t*Boc	**27e** R^1=H	71

Reaction conditions: a) 50% TFA in DCM, r.t., 1h.

The moderate yields (38-50%) for these cyclizations can at least partially be explained by reduction of 8-azido-9-ethyladenine to the corresponding amine. The *m/z* corresponding to the 8-amino byproduct was observed by LCMS and reduction of aromatic azides by excess NaN_3 in the presence of copper has been reported[173]. This issue is difficult to avoid since using less than 1.8 equiv. of NaN_3 resulted in low conversion of 8-bromo- to 8-azidopurine. This is also supported by the fact that an excess of NaN_3 is generally used in the synthesis of 8-azido purines[171,172,174].

4.2.2 Absorption/Emission properties of 1-(purinyl)triazoles

To determine the fluorescent properties of the synthesized compounds, absorption and emission spectra were collected and quantum yields were calculated for five of the compounds (Table 3).

Table 3. Absorption and emission properties of compounds **26f, 26g, 26h, 27b** and **27d** in MeOH.

Compound	Abs_{max} (nm)	Em_{max} (nm)	Φ_F [%]
26f	282	401	0.60
26g	283	404	0.57
26h	282, 291	401	0.21
27b	283	408	0.55
27d	284	409	0.64

The investigated compounds had similar absorption maxima at approximately 283 nm and emission maxima between 401-409 nm. The quantum yields were below 1% for this series. This is a dramatic difference compared with the previously reported 4-(purinyl)triazoles[165]. Comparing for example the benzyl substituted triazoles, the 1-purinyl compound (**26g**) had a quantum yield of 0.6% while the 4-purinyl analog had a quantum yield of 64%[165]. These results reveal a strong correlation between the position of the substituents of the triazole and quantum yield. Additionally, purines with a triazolyl substituent in the C2-postion was recently published

and quantum yields up to 53% were reported[175], further supporting a substantial influence of the purine substitution pattern on the quantum yield.

4.3 Conclusion

Two 4-(purinyl)triazoles and eight 1-(purinyl)triazoles were synthesized. The imide functionalized 4-(purinyl)triazoles proved impractical due to low stability. While the 1-(purinyl)triazoles were fluorescent, their quantum yields were very low and in stark contrast to similar 4-(purinyl)triazoles. These results can serve as guidance for the design of triazole bearing fluorescent probes in the future. Although not suitable as fluorescent probes, these compounds could be tested as Leu-tRNA synthetase inhibitors.

5. 8-(Triazolyl)purines as α-helix mimetics (Paper III and IV)

5.1 Introduction

Physical interactions between proteins constitute an important mechanism for cell function and are found in numerous cellular processes[176], possibly all of them. Their high prevalence and involvement in for example cell signaling has attracted attention to protein-protein interactions (PPIs) as potential drug targets. However, the features of PPIs make them challenging targets for small molecule inhibitors. One protein complex that has been identified as a target for treatment of cancer is that of p53/MDM2. This chapter will describe the development of 8-(triazolyl)purines as potential α-helix mimetics and p53/MDM2 inhibitors.

5.1.1 Features of protein-protein interactions

Besides multiprotein complexes, for example formed by activated protein kinases such as RET[177] discussed in Chapter 3, there are dimeric complexes which can be divided into homocomplexes, which are often stable complexes of two identical proteins and heterocomplexes, made up of proteins that can often exist independently as well as in complexed form[178]. In this context, the focus will be on PPIs between heterodimeric complexes since these are the ones most often targeted by small molecules. Although proteins interact with a large surface area compared with well defined substrate binding pockets[178], common features between interfaces have been identified. The contribution to the binding free energy (ΔG) is not evenly distributed over the amino acid residues at the interface. Amino acid residues with a disproportionately large contribution to ΔG have been identified. Such residues are referred to as hotspot residues and are defined by a large change in binding energy (ΔΔG >2 kcal/mol) when removed in an alanine scan[176]. These residues are clustered in hot regions[179], often near the center of the interface[176]. Moreover, the hot regions are generally

surrounded by residues that contribute less to binding but are believed to exclude water from the hotspot and thereby contribute to binding[176,180]. In the literature related to design of inhibitors of PPIs, the term hotspot is used interchangeably for single residues and for what is described as hot regions above[181]. One of the different methods used to affect PPIs focuses on mimicking secondary structures found at the interaction interface[182].

5.1.2 α-Helices

The α-helix is the most common secondary structure found in proteins[181], it commonly occurs on the surface of proteins[183] and has been found to be prevalent at protein interfaces[184]. An α-helix is a polypeptide chain twisted in a corkscrew fashion with about 3.6 amino acid residues/turn[185], rising 1.5 Å/residue[183]. The helix is stabilized by hydrogen bonding between the carbonyl oxygen of the backbone of amino acid *i* and the carboxamide proton on the backbone of amino acid *i*+4 (Figure 21). The amino acid side chains protrude out from the faces of the helix and residues at *i*, *i*+4 and *i*+7 positions protrude in the same direction (on the same face of the helix)[185]. The topography of the side chains have implications for the design of α-helix mimics discussed in the next section.

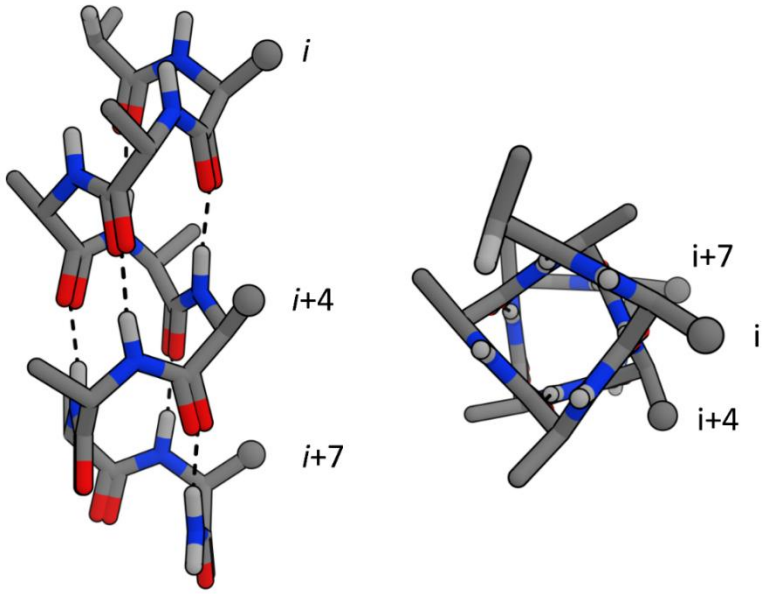

Figure 21. Model of an Ala α-helix (sideview left and topview right). Side chains on one face of the helix are illustrated as spheres. Hydrogen bonds are shown as dashed lines.

5.1.3 α-Helix mimetics and other inhibitors

Synthetic α-helix mimetics can be divided into three classes based on design strategy. The first class (type I inhibitors) consists of small peptide fragments, chemically modified to stabilize an α-helical structure[186]. This class is outside the scope of this work and will not be discussed further. The other two classes are both nonpeptidic and great efforts have been focused on developing nonpeptidic mimetics of the α-helical structure. The first class of the nonpeptidic mimetics aim at replacing the peptidic backbone with a scaffold that is able to place substituents in the same space as the side chains of selected residues of the helix being mimicked. These have been referred to as type III inhibitors[181], and this nomenclature will be used hereafter. Although multifaced α-helix mimetics have been published[187,188], most of the efforts has been directed towards scaffolds mimicking substituent positions on one face which will be the focus below. The first nonpeptidic α-helix mimic were the terphenyls from Hamilton's lab[189] (Figure 22). These have been followed by for example the terephtalamides[190], benzyolureas[191], and pyridazine centered compounds[192] (Figure 22). Another noteworthy example is the approach to mimic all secondary structures from Burgess laboratory[193]. α-Helix mimetics based on a pyrrolopyrimidine scaffold[194], structurally related to purines, have been reported and will be discussed further in Section 5.2.1.

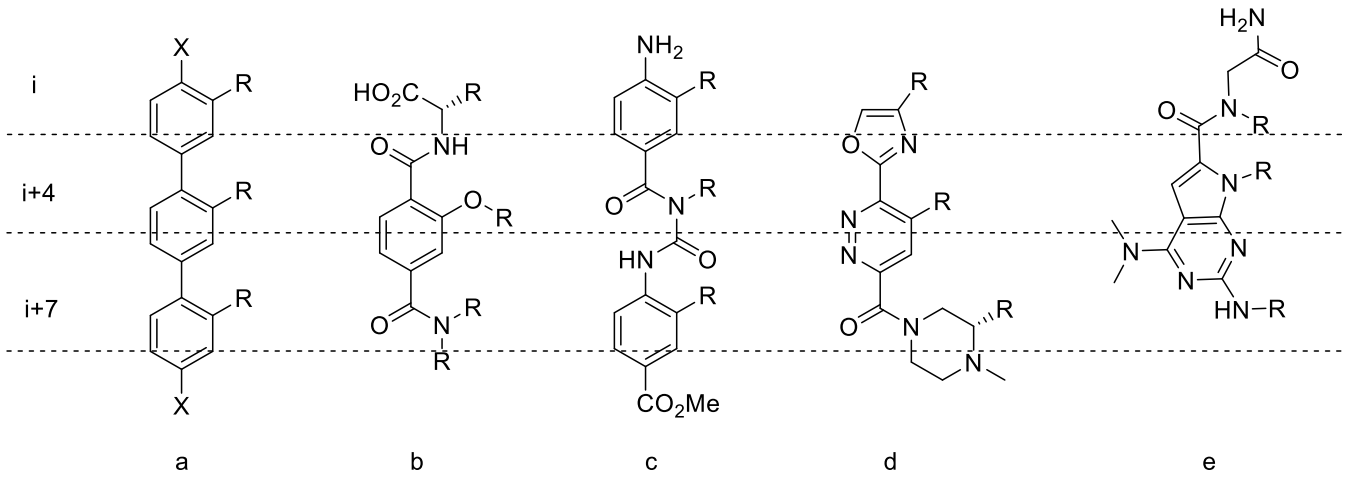

Figure 22. Examples of α-helix mimetics. a) terphenyls, b) terephtalamides, c) benzyolureas, d) pyridazine derivatives and e) pyrrolopyrimidines. *i*, *i*+4 and *i*+7 substituents are marked with dashed lines.

The third class (type II inhibitors)[181] comprises scaffolds that can place substituents in the correct spatial arrangement but that are structurally remote from an α-helix. Several noteworthy examples will be presented in section 5.1.4 in the context of p53/murine double minute 2 (MDM2) inhibitors.

5.1.4 The p53/MDM2 complex

p53 is a transcription factor that regulates the cell cycle, DNA repair and apoptosis as a response to DNA damage[195]. Inactivation of p53 is commonly occurring in cancer cells. Mutation in TP53, the gene coding for p53, is common as part of the apoptosis-avoiding mechanisms of cancers[196]. With or without mutation in the TP53 gene, p53 activity is controlled by a complex network of positive and negative feedbacks[197], an important part of which is played by MDM2, a protein that binds to p53, resulting in ubiquitination and subsequent degradation[195,196]. It has has been demonstrated that inhibition of MDM2 in cancer cells without TP53 mutation could reactivate p53 and initiate apoptosis[198]. The PPI interface of p53/MDM2 is well characterized[199]. A hotspot consisting of a short α-helix of p53 binding to a largely hydrophobic crevice on the MDM2 surface has been identified. The amino acid

side chains protruding from the α-helix face towards the MDM2 crevice are leucine (Leu), tryptophan (Trp) and phenylalanine (Phe) (Figure 23).

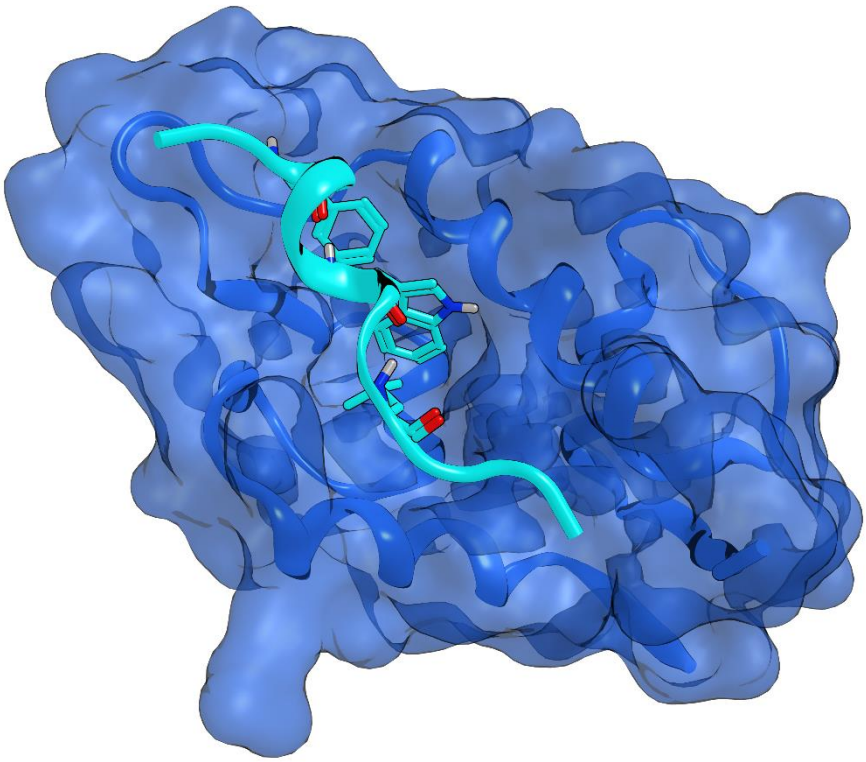

Figure 23. X-ray crystal image of p53-peptide (turquoise) bound to MDM2 (blue). The hotspot residues Phe, Trp and Leu of the p53 helix are visible. (PDB: 1YCR).

Several efforts have been made to develop compounds that mimic the p53 hotspot α-helix as inhibitors of MDM2[200]. The nutlins (Figure 24) were the first small molecule inhibitors of p53/MDM2[198] identified by HTS, and the contribution of the substituents of this compound class has been thoroughly studied[201]. Another successful and more recent example are the piperidinones[202] (AMG232 in Figure 24)[203] and related morpholinone compounds[204]. AMG232 is one of seven p53/MDM2 inhibitors currently in clinical trials[205]. A number of inhibitors based on indolyls[206,207], structurally related spiro compounds[208] and benzodiazepinediones[209] have also been reported.

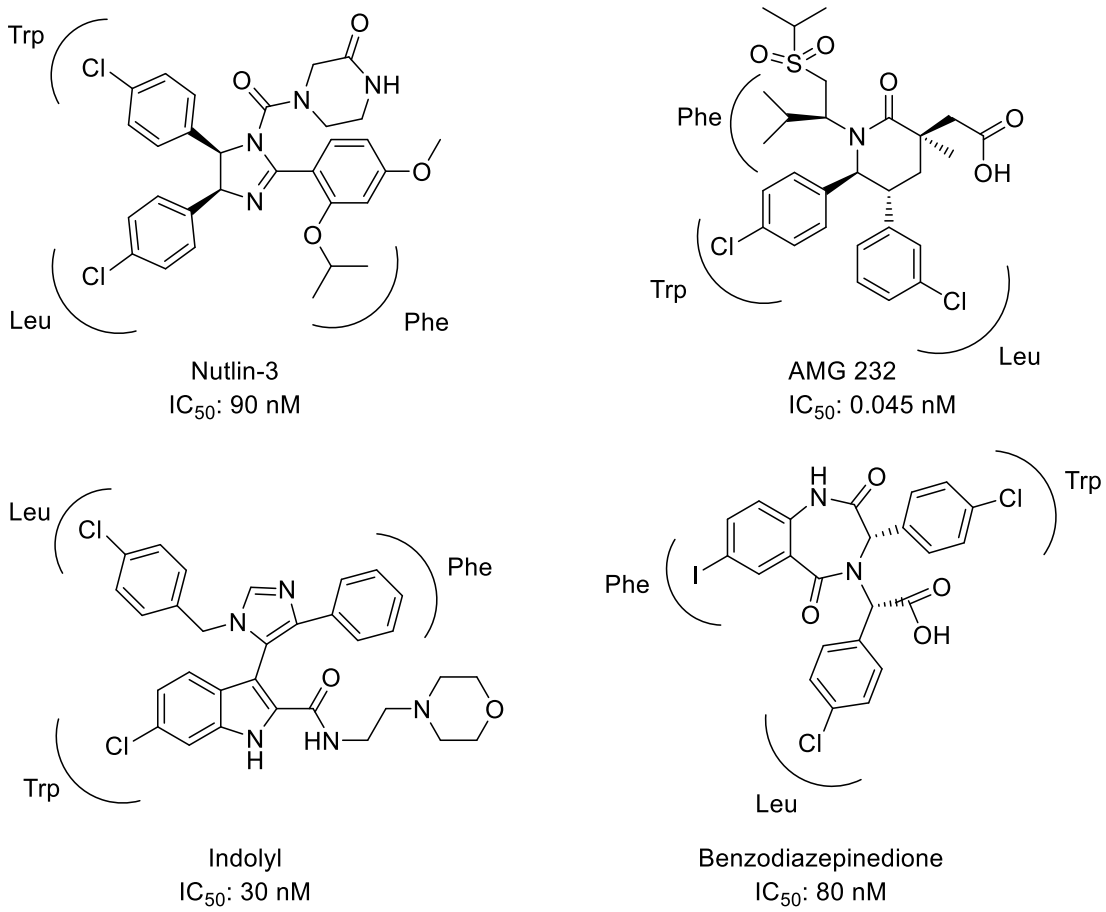

Figure 24. Examples from different compound classes of p53/MDM2 inhibitors. The binding sites for the LeuTrpPhe residues of p53 are represented by curved lines.

5.2 Results and discussion

5.2.1 Design, part 1

As mentioned above, pyrrolopyrimidine α-helix mimetics with low micromolar inhibitory activity against MDM2 and MDMX was reported in 2010[194]. These compounds have an amide in what would be equivalent to the 8-position of purines. Since triazoles are known amide bioisosters[210,211], we decided to investigate if the 8-(triazolyl)purine scaffold substituted in the 2-, 6- and 9-positions could be used as α-helix mimetics. In addition, since several 8-(triazolyl)purines have shown to be fluorescent[165], this could potentially be used for example for intracellular localization. Comparison of low energy conformations of 8-(triazolyl)purines, obtained by a conformational search using Macromodel in Maestro[212], with an idealized α-helix

indicate that the spatial arrangement of the substituents on the triazole, 2N and N^9-position coincides in space with the *i*, *i*+4 and *i*+7 on one face of the helix (Figure 25).

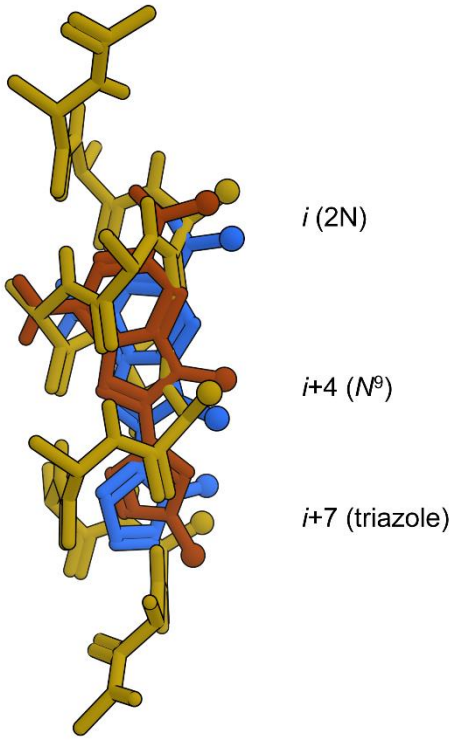

Figure 25. Superposition of low energy conformations of 8-(1,4-triazolyl)purine (brown) and 8-(1,5-triazolyl)purine (blue) with an Ala α-helix (yellow). Positions of the residues indicated with spheres are given to the right followed by the substituent positions on the triazole (in parenthesis).

5.2.2 Synthesis, part 1

The route to the triazole in the 8-position was planned to proceed analogously with the synthesis of the aa-AMP mimics (Chapter 4). In this project, we wanted access to both the 1,4- and 1,5-regioisomers of the triazole as this allows for variation of the spatial arrangement of substituents at a later stage in the synthesis. Substituents in the 6-position can be introduced by S_NAr provided that the position is preactivated. The N^9-position should be possible to selectively alkylate as discussed in Chapter 1. If the starting material is a 2-aminopurine, the 2N-position should also be possible to functionalize by reductive amination or alternatively by

the Mitsunobu reaction. 2-Amino-6-chloropurine (**28**) is commercially available and would serve as a suitable starting point for the synthesis.

Initial attempts to obtain compounds substituted on *N*9 and on the 2-amino group through alkylation with an alkyl halide under basic conditions on *N*9 and subsequent reductive amination of the 2-amino group were unsuccessful due to low reactitvity in the reductive amination. While it is possible to alkylate the 2-amino group with alkyl halide and base, this procedure is not practical since it leads to a mixture of mono- and dialkylated compounds.

An alternative method for alkylation of nucleophilic functionalities is the Mitsunobu reaction[29, 213] which uses a primary or secondary alcohol as the electrophile in the presence of dialkyldiazodicarboxylate and a trialkyl- or triarylphosphine. This methodology has been used to sequentially substitute 2-amino substituted purines in the *N*9 and 2N positions[32, 214]. The 2-amino position needs to be activated by *t*Boc protection and the difference in acidity together with the steric bulk of the *t*Boc group provide regioselectivity between 2N and *N*9. This methodology was used to obtain three 2N, *N*9-substituted purines (**30a**-**c**) in high yields from 2-amino-6-chloropurine (**28**) (Scheme 24).

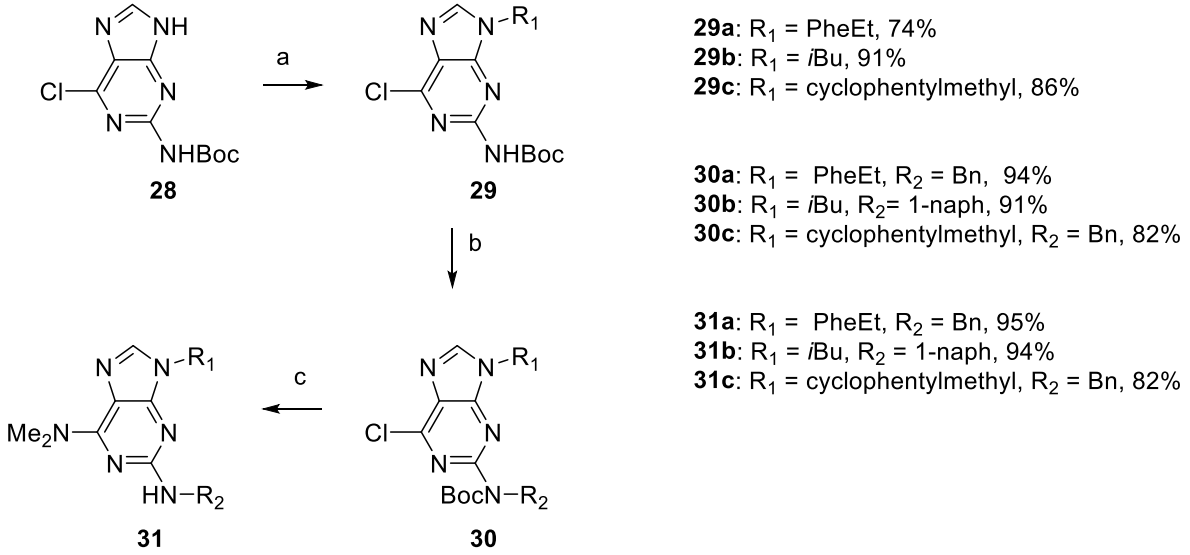

Scheme 24. Synthesis of **31a**-**c** a) R_1OH, DIAD, Ph_3P in THF, r.t. b) R_2OH, ADDP, *n*Bu_3P in THF, r.t. c) DMF, MW, 180 °C.

Heating **30a**-**c** in a microwave reactor at 180 ºC in DMF[215] introduced a dimethylamino group in the 6-position by S_NAr and simultaneously thermally removed the *t*Boc-protecting group in

high yields (**31a**-**c**, 82-95%). To set the stage for the Sonogashira coupling, the next step was bromination in the 8-position, an expectedly simple reaction that led to a detour described below.

5.2.3 8-Bromination of 2,6,9-trisubstituted purines (Paper III)

In both bromination of 9-ethyladenine (Chapter 2) and iodination of pyrazolopyrimidine (Chapter 1), commonly used reagents (Br_2 and *N*-iodosuccinimide (NIS), respectively) resulted in the expected products in fair yields. However, when bromination was attempted on the 2,6,9-trisubstituted substrates, poor results were obtained with common bromination reagents such as *N*-bromosuccinimide (NBS) in acetonitrile[84] and bromine in NaOAc/HOAc buffer in THF/MeOH[170] which was used to brominate 9-ethyladenine. Pyridinium tribromide ($PyrBr_3$), a brominating agent that has been shown to brominate other aryl compounds[216,217] as well as alkenes[218] and the α-position of ketones[219,220], was tested on purine **31d** (Scheme 25) which provided the 8-brominated derivative (**32a**) in excellent yield (93%).

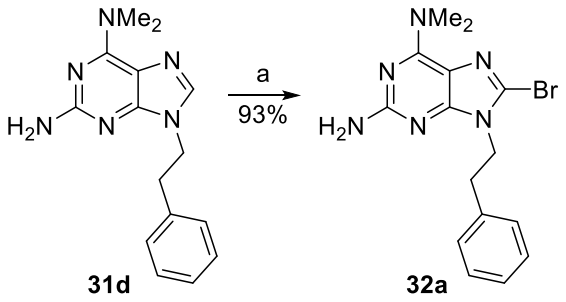

Scheme 25. 8-Bromination using $PyrBr_3$. a) $PyrBr_3$ in DCM, r.t., 5 h.

Workup and purification of the reaction mixture proved more convenient than with bromine. Furthermore, while elemental bromine is a high viscosity, low vapour pressure and pungent liquid, $PyrBr_3$ is a crystalline solid that can be weighed out. The high yield of our initial reaction together with the features of $PyrBr_3$ just mentioned encouraged us to explore the possibility of using $PyrBr_3$ as a more general alternative in purine bromination. We tested $PyrBr_3$ in the bromination of a range of purines with varying substituent pattern in 2-, 6- and 9-position (Table 4). Our initial reaction was run in DCM which was also chosen as a starting point for

the substrate screen. However, several of the purines tested had poor solubility in DCM and therefore DMF and acetonitrile were used in these cases. The general trend was that for the bromination to be successful, electron donating substituents were necessary in both the 2- and 6-position and high yields were obtained within 1-5 h when amino substituents were present in both positions.

Table 4. 8-Bromination of purines using $PyrBr_3$.

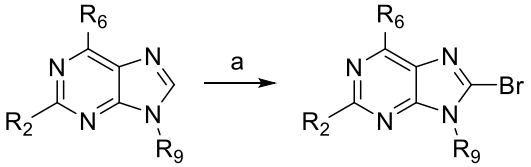

31 **32**

Entry	Starting material	R_6	R_2	R_9	Solvent	Time (h)	Product	Yield (%)[b]
1	**31e**	Cl	H	H	DCM	24	**32b**	nr[c]
2	**31f**	Cl	NH_2	H	DCM	o.n[a]	**32c**	ta[d]
3	**31g**	$N(Me)_2$	NH_2	H	DMF	6	**32d**	38
4	**31h**	$N(Me)_2$	NH_2	H	DCM	55	**32d**	46
5	**31i**	NH_2	H	Bn	DCM	48	**32e**	nr
6	**31j**	Cl	H	Bn	DCM	o.n	**32f**	nr
7	**31k**	OMe	H	Bn	DCM	o.n	**32g**	nr
8	**31l**	$N(Me)_2$	H	Bn	DCM	o.n	**32h**	ta
9	**31m**	$N(Me)_2$	NH_2	Bn	DCM	3	**32i**	90
10	**31n**	NHBn	NH_2	Bn	DCM	3	**32j**	87
11	**31o**	NH_2	NH_2	Bn	DMF	5	**32k**	27
12	**31p**	$N(Me)_2$	NH_2	Isobutyl	DCM	2.5	**32l**	80
13	**31q**	$N(Me)_2$	NHBn	Phenethyl	DCM	1	**32m**	91
14	**31r**	NHBn	NH*t*Boc	Bn	DCM	3	**32n**	36
15	**31m**	$N(Me)_2$	NH_2	Bn	DMF	3	**32i**	47
16	**31d**	$N(Me)_2$	NH_2	Phenethyl	DMF	3	**32a**	59
17	**31m**	$N(Me)_2$	NH_2	Bn	MeCN	o.n	**32i**	80
18	**31s**	OMe	NH_2	Bn	DCM	o.n	**32o**	37
19	**31t**	OMe	NH_2	Bn	DCM	o.n	**32o**	43[e]
20	**31u**	Cl	NH_2	Bn	DCM	16	**32p**	nr
21	**31m**	$N(Me)_2$	NH_2	Bn	DCM	4	**32i**	93[f]

[a] o.n=overnight
[b]Isolated yield.
[c]nr = no reaction i.e. only starting material could be observed by LCMS and/or TLC.
[d]ta= trace amounts i.e. only trace amounts of the product could be observed by LCMS.
[e]3 eqvivalents of $PyrBr_3$ was used.
[f]Polymer supported $PyrBr_3$ was used.

Switching for example to 6-chloro derivatives resulted in only trace amounts of product. For 2-amino-6-dimethylaminopurine, moderate yields were obtained both in DMF and DCM. In this case, the poor solubility of the 9-*H* derivatives was most likely the main reason for the poor yield. The strong correlation between yield and electron donating substituents indicates that the reaction is ionic and proceeds through an $E_{Ar}S$ mechanism. $PyrBr_3$ is in equilibrium with bromine and pyridinium bromide in solution (Scheme 26).

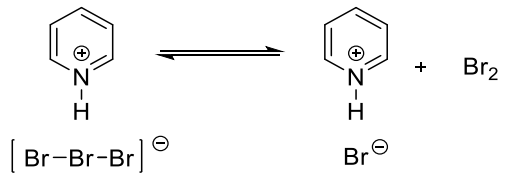

Scheme 26. Equlibrium between $PyrBr_3$ and bromine and pyridinium bromide.

Although both bromine and $PyrBr_3$ has been reported to act as brominating agents[221], the expected $E_{Ar}S$ mechanism suggests that bromine is the main brominating reagent in this case since electrophilic attack from an anion (tribromide) is not plausible.

5.2.4 Synthesis, part 1 (continued)

With the bromination protocol described in the previous section, **32m**,**q**,**r** were synthesized in high yields (84-93%), followed by Sonogashira coupling with TMS-acetylene catalyzed by $PdCl_2(PPh_3)_2$ and CuI (Scheme 27). Removal of the silyl protecting group without prior purification gave the terminal alkynes in 57-74% yield over two steps. As in paper II, polymer supported base in the Sonogashira coupling and fluoride in the deprotection were used to facilitate workup and purification.

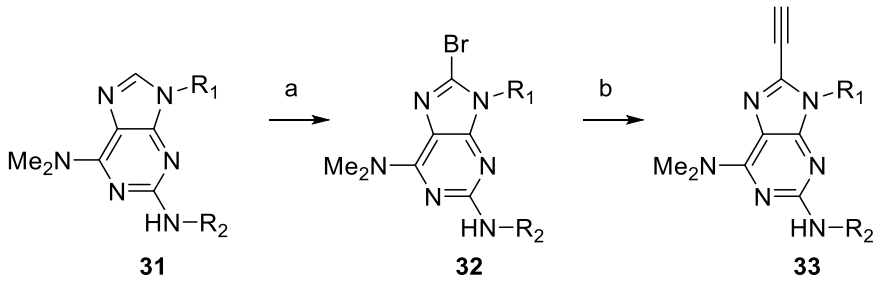

32m: R_1 = PheEt, R_2 = Bn, 93%
32q: R_1 = *i*Bu, R_2 = 1-naph, 84%
32r: R_1 = cyclophentylmethyl, R_2 = Bn, 90%

33a: R_1 = PheEt, R_2 = Bn, 73%
33b: R_1 = *i*Bu, R_2 = 1-naph, 74%
33c: R_1 = cyclophentylmethyl, R_2 = Bn, 57%

Scheme 27. Synthesis of **33a-c** a) $PyrBr_3$ in DCM, r.t. b) (i) $PdCl_2(PPh_3)_2$, CuI, Amberlite IRA-67, TMS-acetylene in THF, MW, 110 °C. (ii) PS-F in THF, r.t.

Cyclization with alkyl and benzyl azide in the presence of CuI, sodium ascorbate and DMEDA at room temperature overnight afforded 1,4-triazoles **34a-c** (55-82% yield) (Scheme 28). To avoid isolation of low molecular weight, potentially explosive alkyl azides, isobutyl azide was formed *in situ* from isobutyl bromide and sodium azide in DMF and used without purification in the cyclization reaction. Cyclization with benzylazide[222] catalyzed by $Cp^*RuCl(PPh_3)_2$ provided the 1,5-triazole **35a** in 22% yield.

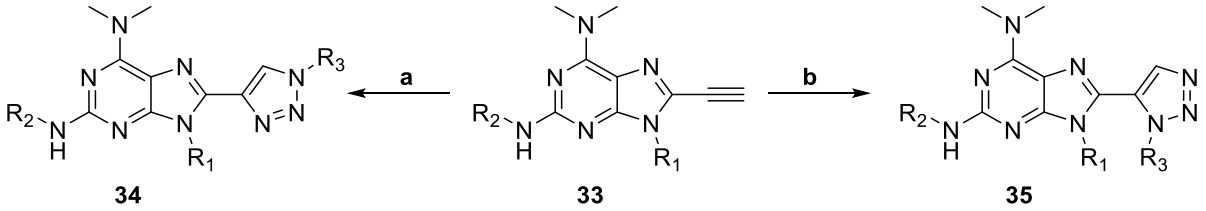

34a: R_1 = *i*Bu, R_2= 1-naphtyl, R_3 = Bn, 55%
34b: R_1 = phenethyl, R_2= Bn, R_3 = *i*Bu, 80%
34c: R_1 = cyclophentylmethyl, R_2 = Bn, R_3 = Bn, 82%

35a: R_1 = *i*Bu, R_2 = 1-naph, R_3 = Bn, 22%
35b: R_1 = phenethyl, R_2= Bn, R_3 = *i*Bu, 4%

Scheme 28. Synthesis of **34a-c** and **35a-b.** a) R_3=Bn, BnN_3 (1.6 equiv.), CuI (18 mol%), NaAsc (40 mol%), DMEDA (46 mol%) in DMF, r.t. R_3=*i*Bu, (i) *i*BuBr (2.1 equiv.) NaN_3 (2.1 equiv.) in DMF, 100 °C, 30 min. (ii), CuI (20 mol%), NaAsc (27 mol%), DMEDA (27 mol%), r.t., 22 h. b) R_3=Bn, BnN_3 (1.8 equiv.), $Cp^*RuCl(PPh_3)_2$ (10 mol%) in DMF, MW, 110 °C, 1 h. R_3=*i*Bu, (i) *i*BuBr (2.0 equiv.) NaN_3 (2.0 equiv.) in DMF, 100 °C, 30 min. (ii) $Cp^*RuCl(PPh_3)_2$ (10 mol%), MW, 110 °C, 5 h.

Compound **35b** was isolated in trace amounts after extensive purification. The lower yield in the 1,5-cyclization can be partly attributed to difficulties in purification. In order to be useful, the reaction conditions for the 1,5-triazoles would clearly need to be optimized. However, the compounds were first evaluated as p53/MDM2 inhibitors in a biochemical assay.

5.2.5 Biochemical evaluation and redesign

Four of the compounds (**34a**-**c** and **35a**) were tested in a fluorescence polarization (FP) assay that measures the displacement of a fluorescently tagged ligand (in this case a peptide segment from p53) by the investigated compound. In this assay, the system is irradiated with polarized light at a wavelength absorbed by the fluorophore. The polarization of the emitted light is affected by the molecular rotation of the fluorophore which in turn is dependent on if it is bound to the protein or not. In the presence of a ligand, the displacement of the fluorescently tagged compound is reflected in the polarization of the emitted light[223].

Unfortunately, none of the products showed any activity towards MDM2. During our work with these compounds, a number of highly active (low nanomolar) MDM2 inhibitors were published[202-204,208,224,225]. These compounds all belonged to the type II PPI-inhibitors discussed in section 5.1.3 and 5.1.4, with at least two features distinguishing them from the α-helix mimetic design used for compounds **34a**-**c** and **35a**-**b**. The compounds were generally smaller than typical α-helix mimetics and had a hydrophilic substituent attached to the "face" that would point out from the pocket towards the solvent. Crystal structures of a number of these compounds cocrystallized with MDM2 were also published[202,226]. After analysis of the crystal structures[227] and published compounds, as well as docking of 8-(triazolyl)purines in the p53-helix binding site of the MDM2/inhibitor crystal complexes, we decided to redesign our compounds according to the type II inhibitors. The new series of compounds had smaller substituents on the triazole and the 2N substituent (the Phe and Leu pockets). Since the tryptophan pocket of MDM2 is the deepest of the hydrophobic pockets, a large hydrophobic group was kept in this position. The dimethylamino group in the 6-position was exchanged for substituents that could possibly form hydrogen bonds with the hydrophilic amino acid residues on the edge of the hotspot region. An example of docking of an 8-(triazolyl)purine in MDM2 using Glide in the Schrödinger suite[228] is shown in Figure 26.

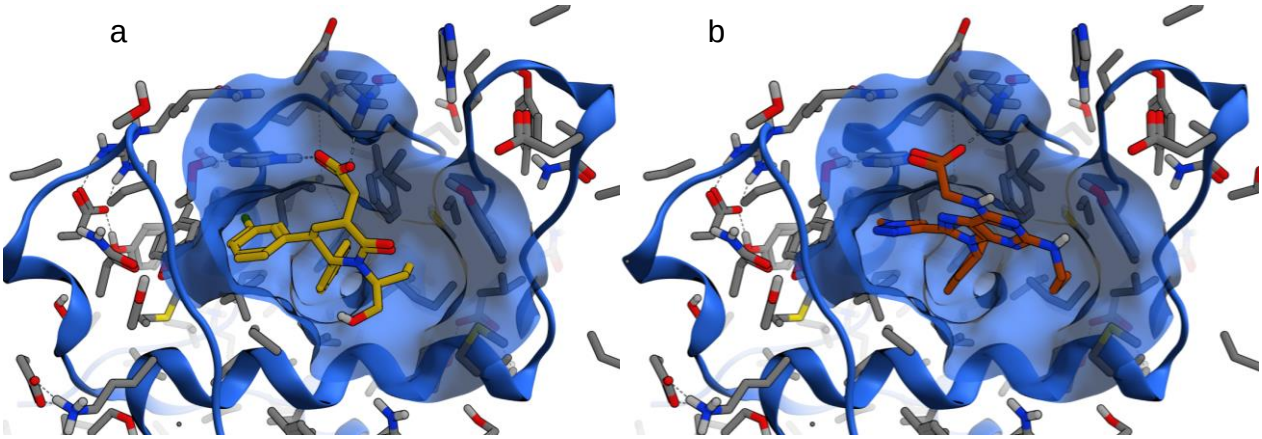

Figure 26. Docking of a 8-(triazolyl)purine derivative in MDM2. a) LeuTrpPhe-binding pocket of MDM2 (blue) with cocrystallized ligand (yellow) and b) with purine-compound (brown) docked into the binding site. (PDB: 4HBM).

5.2.6 Synthesis and biochemical evaluation, part 2

Introduction of the N^9- and 2N-substituents was achieved as described for the first set of compounds. When *p*-chlorobenzyl substituents were present, milder reaction conditions for the introduction of the dimethylamino group were used to avoid amination of the chlorobenzyl. Dimethylamine in ethanol (5.6 M) at 80 °C and subsequent removal of the *t*Boc-group with TFA in DCM provided **38c** in excellent yield (95% over two steps). S_NAr at the 6-position with thioglycol ethylester and glycine ethylester under basic conditions followed by *t*Boc removal (TFA in DCM) provided **38d**-**g** in 60-98% yields over two steps. To complement these substituents with a smaller hydrophilic functionality, a primary amine was introduced. Amination with NH_4OH (aq.) at 100 °C provided the aminated product. Subsequent bromination with $PyrBr_3$ with the *t*Boc group still in place failed to provide the product in accordance with the reactivity pattern observed in the bromination study (Section 5.2.3). The highest yields were obtained when the *t*Boc group was removed with TFA in DCM after workup of the amination. $PyrBr_3$ bromination was then performed on the crude product from the deprotection without prior purification. This procedure provided **39h** and **39i** in 51 and 73% yield over three steps, respectively. The Sonogashira reaction was performed as described above to provide terminal alkynes **40a**-**i** in 50-72% yields over two steps (Scheme 29).

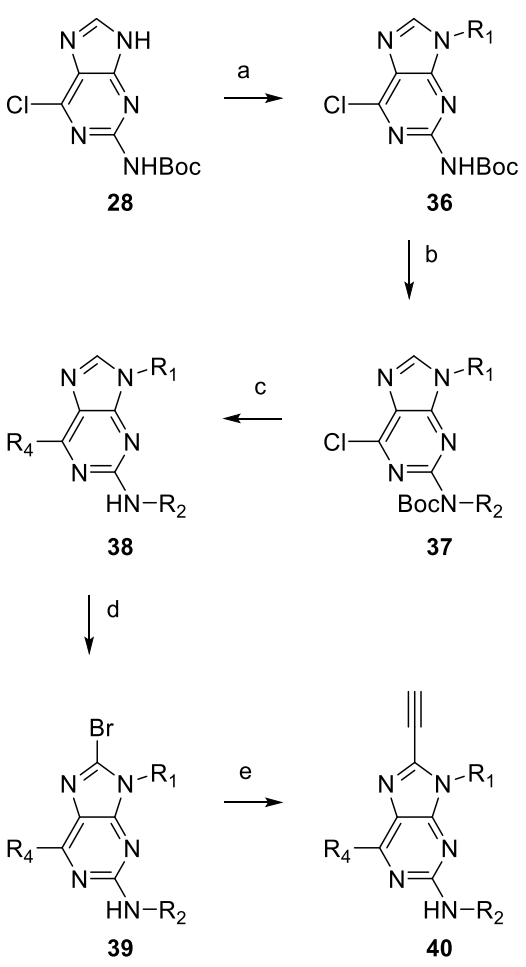

36: R_1 = 2-indanyl, 83%

37a: R_1 = 2-indanyl, R_2 = Bn, 94%
37b: R_1 = 2-indanyl, R_2 = *n*Pr, 75%
37c: R_1 = 2-indanyl, R_2 = p-ClBn, 91%
37d: R_1 = Bn, R_2 = Bn, 78%

38a: R_1 = 2-indanyl, R_2 = Bn, R_4 = NMe_2, 94%
38b: R_1 = 2-indanyl, R_2 = *n*Pr, R_4 = NMe_2, 87%
38c: R_1 = 2-indanyl, R_2 = p-ClBn, R_4 = NMe_2, 95%
38d: R_1 = 2-indanyl, R_2 = Bn, R_4 = $NHCH_2CO_2Et$, 91%
38e: R_1 = 2-indanyl, R_2 = *n*Pr, R_4 = $NHCH_2CO_2Et$, 98%
38f: R_1 = Bn, R_2 = Bn, R_4 = $NHCH_2CO_2Et$, 62%
38g: R_1 = Bn, R_2 = Bn, R_4 = SCH_2CO_2Et, 60%

39a: R_1 = 2-indanyl, R_2 = Bn, R_4 = NMe_2, 84%
39b: R_1 = 2-indanyl, R_2 = *n*Pr, R_4 = NMe_2, 83%
39c: R_1 = 2-indanyl, R_2 = p-ClBn, R_4 = NMe_2, 86%
39d: R_1 = 2-indanyl, R_2 = Bn, R_4 = $NHCH_2CO_2Et$, 73%
39e: R_1 = 2-indanyl, R_2 = *n*Pr, R_4 = $NHCH_2CO_2Et$, 96%
39f: R_1 = Bn, R_2 = Bn, R_4 = $NHCH_2CO_2Et$, 81%
39g: R_1 = Bn, R_2 = Bn, R_4 = SCH_2CO_2Et, 35%
39h: R_1 = Bn, R_2 = Bn, R_4 = NH_2, 51% (over 3 steps)
39i: R_1 = 2-indanyl, R_2 = *n*Pr, R_4 = NH_2, 73% (over 3 steps)

40a: R_1 = 2-indanyl, R_2 = Bn, R_4 = NMe_2, 70%
40b: R_1 = 2-indanyl, R_2 = *n*Pr, R_4 = NMe_2, 72%
40c: R_1 = 2-indanyl, R_2 = p-ClBn, R_4 = NMe_2, 69%
40d: R_1 = 2-indanyl, R_2 = Bn, R_4 = $NHCH_2CO_2Et$, 52%
40e: R_1 = 2-indanyl, R_2 = *n*Pr, R_4 = $NHCH_2CO_2Et$, 60%
40f: R_1 = Bn, R_2 = Bn, R_4 = $NHCH_2CO_2Et$, 69%
40g: R_1 = Bn, R_2 = Bn, R_4 = SCH_2CO_2Et, 50%
40h: R_1 = Bn, R_2 = Bn, R_4 = NH_2, 82%
40i: R_1 = 2-indanyl, R_2 = *n*Pr, R_4 = NH_2, 51%

Scheme 29. Synthesis of **40a-i**. a) R_1OH, DIAD, Ph_3P in THF, r.t. b) R_2OH, ADDP, nBu_3P in THF, r.t. c) R_4= NMe_2, DMF, MW, 180 °C. R_4 = $NHCH_2CO_2Et$, (i) $NH_2CH_2CO_2Et$, Et_3N in EtOH, 100 °C. (ii) 50% TFA in DCM, R_4 = SCH_2CO_2Et, (i) $SHCH_2CO_2Et$, NaH in toluene, 70 °C. (ii) 50% TFA in DCM. d) $PyBr_3$ in DCM, r.t. R_4 = NH_2, (i) NH_4OH (aq.) in dioxane, 100 °C. (ii) 50% TFA in DCM. (iii) $PyBr_3$ in DCM, r.t. e) (i) $PdCl_2(PPh_3)_2$, CuI, Amberlite IRA-67, TMS-acetylene in THF, MW, 110 °C. (ii) PS-F in THF, r.t.

Since the first set of compounds were expected to be too large and possibly too lipophilic, it was decided to introduce a methyl group on the triazole ring. When methylazide was used in the Cu-catalyzed cyclization, the highest yields were obtained when the *in situ* azide formation was run at room temperature followed by cyclization at 60 ºC (Scheme 30). Low yields were obtained when the reaction vial was flushed with nitrogen after azide formation which is assumed to be due to the volatility of methylazide. The 1,5-regioisomers were abandoned due to poor yields and cumbersome purification in these cyclizations.

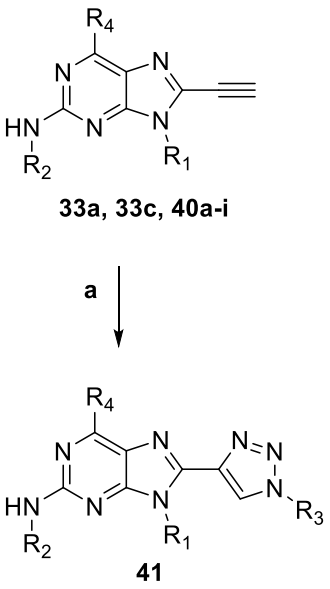

41a: R_1 = 2-indanyl, R_2 = Bn, R_4 = NMe_2, R_3 = Me, 83%
41b: R_1 = 2-indanyl, R_2 = *n*Pr, R_4 = NMe_2, R_3 = Me, 52%
41c: R_1 = 2-indanyl, R_2 = p-ClBn, R_4 = NMe_2, R_3 = Me, 87%
41d: R_1 = 2-indanyl, R_2 = Bn, R_4 = $NHCH_2CO_2Et$, R_3 = Me, 85%
41e: R_1 = 2-indanyl, R_2 = *n*Pr, R_4 = $NHCH_2CO_2Et$, R_3 = Bn, 74%
41f: R_1 = 2-indanyl, R_2 = *n*Pr, R_4 = $NHCH_2CO_2Et$, R_3 = Me, 87%
41g: R_1 = Bn, R_2 = Bn, R_4 = $NHCH_2CO_2Et$, R_3 = Bn, 46%
41h: R_1 = Bn, R_2 = Bn, R_4 = SCH_2CO_2Et, R_3 = Bn, 40%
41i: R_1 = Bn, R_2 = Bn, R_4 = NH_2, R_3 = Me, 66%
41j: R_1 = 2-indanyl, R_2 = *n*Pr, R_4 = NH_2, R_3 = Me, 84%
41k: R_1 = phenethyl, R_2= Bn, R_4 = NMe_2, R_3 = Me, 53%
41l: R_1 = cyclophentylmethyl, R_2 = Bn, R_4 = NMe_2, R_3 = Me, 68%

Scheme 30. Synthesis of **41a**-**l**. a) R_3=Bn, (i) BnBr (1-2 equiv.), NaN_3 (2 equiv.) in DMF, 100 °C, 30 min. (ii) CuI (20 mol%), NaAsc (30-50 mol%), DMEDA (20-30 mol%) in DMF, r.t. R_3=Me, (i) MeI (2 equiv.) NaN_3 (2 equiv.) in DMF, r.t., 3 h. (ii) CuI (20 mol%), NaAsc (30 mol%), DMEDA (20-30 mol%), 60 °C, 3 h.

The new series (**41a**-**l**) was also tested in a FP-assay. Two compounds, **41f** and **41j** (Figure 27), showed micromolar inhibitory effect in this initial assay. Compound **41f** was tested in two independent runs and the results showed high variability (18 ± 15 μM).

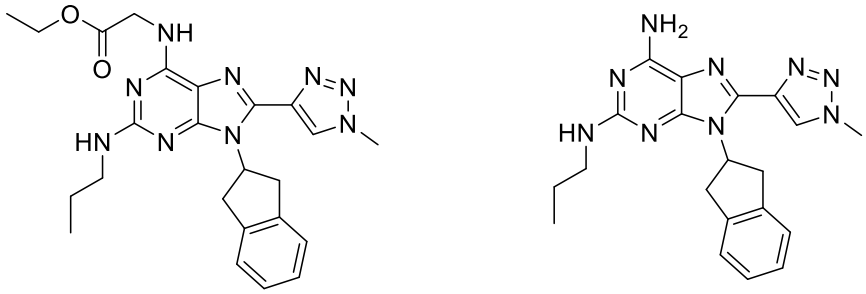

41f
IC_{50}: 18 (± 15) μM (FP)

41j
IC_{50}: 56 μM (FP)

Figure 27. Compounds with activity towards MDM2 in a FP-assay.

To confirm specific bnding to MDM2, **41f** was further tested in a surface plasmon resonance (SPR) assay. In this assay, MDM2 is immobilized on a functionalized gold surface. Polarized light is emitted through a prism and reflects on the surface. A dip in intensity of the reflected

light is caused by plasmon resonance. The angle of the reflected light is affected by the environment near the surface and will therefore be different if ligand is bound to MDM2 or not. This method allows direct detection of binding[229]. Compound **41f** showed nonspecific background binding in this assay and binding could not be confirmed with this method. The nonspecific binding could be explained by binding of **41f** to neutravidin on the surface of the chip used to immobilize MDM2, although additional experiments are required to confirm this. One way to avoid this issue in future tests is to use an alternative immobilization mechanism for MDM2 or to treat the plate with a neutravidin binder after immobilization of MDM2, to saturate superfluous neutravidin sites. The low potency for the type II compounds can possibly be explained by that while the methyl group on the triazole seem to fit into one of the hydrophobic sites of MDM2, it might bury the more polar triazole as well.

5.2.7 Evaluation of fluorescene properties

A discussed earlier, intrinsically fluorescent inhibitors could be used for example for localization of the compounds in cells. Since these 8-(triazolyl)purines are structurally related to fluorescent base analogs[165], we wanted to determine the absorption/emission properties of these newly synthesized purine derivatives. The absorption and emission maxima as well as quantum yield was determined for 19 different 2,6,8,9-tetrasubstituted purines. The results are summarized in Table 5 and a selection of absorption and emission spectra are shown in Figure 28.

Table 5. Absorption and fluorescent properties of 8-(triazolyl)purine derivatives.

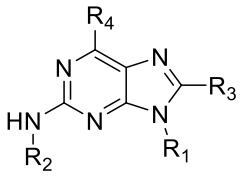

Entry	Cmpd	R_1	R_2	R_3	R_4	$\lambda_{abs,max}$ (nm)	$\lambda_{em,max}$ (nm)	Φ (%)
1	**41a**	2-indanyl	Bn	1,4-Me	NMe_2	310	376	2
2	**41k**	phenethyl	Bn	1,4-Me	NMe_2	315	376	2
3	**34c**	Cyclopentyl-methyl	Bn	1,4-Bn	NMe_2	317	377	2
4	**41b**	2-indanyl	*n*Pr	1,4-Me	NMe_2	311	378	1
5	**41d**	2-indanyl	Bn	1,4-Me	$NHCH_2CO_2Et$	311	377	8
6	**41l**	Cyclopentyl-methyl	Bn	1,4-Me	NMe_2	316	376	2
7	**41i**	Bn	Bn	1,4-Me	NH_2	314	375	7
8	**41j**	2-indanyl	*n*Pr	1,4-Me	NH_2	311	377	4
9	**41g**	Bn	Bn	1,4-Bn	$NHCH_2CO_2Et$	318	381	10
10	**41e**	2-indanyl	*n*Pr	1,4-Bn	$NHCH_2CO_2Et$	316	382	4
11	**41f**	2-indanyl	*n*Pr	1,4-Me	$NHCH_2CO_2Et$	313	380	5
12	**34a**	*i*Bu	1-naphtyl	1,4-Bn	NMe_2	318	378	2
13	**34b**	phenethyl	Bn	1,4-*i*Bu	NMe_2	316	378	5
14	**35a**	*i*Bu	1-naphtyl	1,5-Bn	NMe_2	322	437	37
15	**35b**	phenethyl	Bn	1,5-*i*Bu	NMe_2	320	422	51
16	**41h**	Bn	Bn	1,4-Bn	SCH_2CO_2Et	340	398	2
17	**31q**	phenethyl	Bn		NMe_2	292	351	<1
18	**32m**	phenethyl	Bn		NMe_2	294	412	<1
19	**33a**	phenethyl	Bn		NMe_2	319	391	<1

The 1,4-triazolyl compounds (entry 1-13 and 16) all had absorption maxima between 310-322 nm, with the exception of **41h** (entry 16), bearing a sulphur substituent in the 6-position. The absorption maximum of **41h** is redshifted to 340 nm. The substitution pattern on the triazole and in the N^9 and 2N positions seem to have little effect on the quantum yield. This can be expected since none of the substituents in these positions affect the conjugation of the heterocyclic core. Compounds with a 6-dimethylamino substituent all had low quantum yields

between 1-5% (entry 1-4, 6, 12, 13). Changing from tertiary to primary (entry 7, 8) or secondary amines (entry 5 and 9-11) gave slightly higher quantum yields (4-10%).

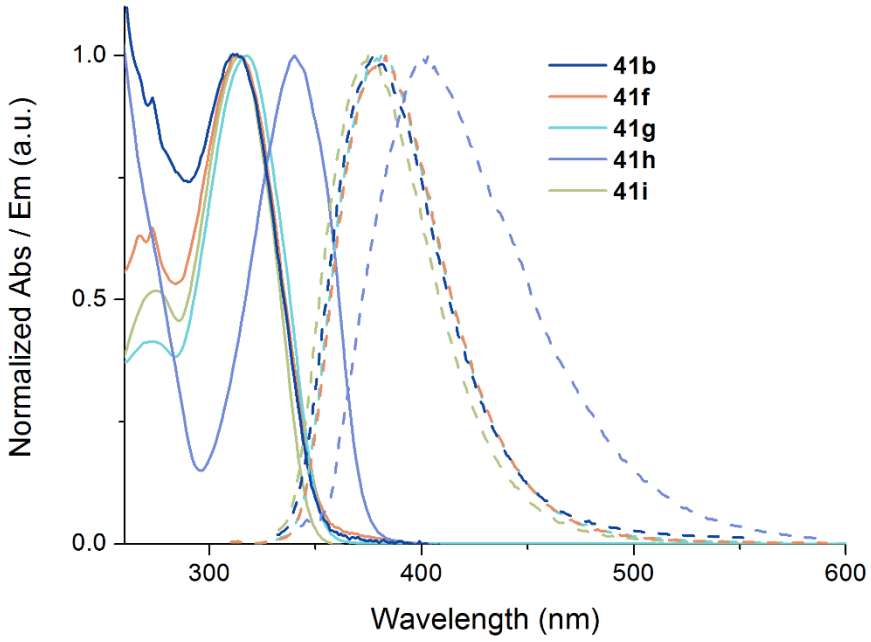

Figure 28. Normalized absorption (solid lines) and emission (dashed lines) spectra of five of the measured compounds.

Interestingly, changing the regioisomerism of the triazole form 1,4 (entry 13) to 1,5 (entry 15) resulted in a 10 fold increase of the quantum yield from 5% and 51% accompanied by an increase in Stokes shift from 62 to 102 nm. One explanation to this difference could be that the 1,5-isomer has hindered rotation around the triazole-purine bond. This would minimize rotational relaxation, a mechanism that is known to lower the quantum yield[95]. This explanation could perhaps also be extended to explain the difference between tertiary and secondary 6-amino substituents, assuming that an intramolecular hydrogen bond can form between the lone pair on N^7 and the hydrogen on the secondary amine. This would hinder rotation around the C-N bond and possibly lead to an increase in fluorescence. To investigate if the triazole is essential for fluorescence in these compounds, absorption and emission of **31a**, **q** and **m** bearing a proton, bromine and an alkyne in the 8-position was also measured. These compounds all displayed very weak fluorescent properties. These results show that the 8-triazole substituent is necessary to obtain measurable quantum yields on this set of compounds.

5.3 Conclusion

In conclusion, two series of 2,6,9-trisubstituted 8-(triazolyl)purines were synthesized. Two of the compounds of the second series, the smaller type II inhibitors, showed micromolar activity against MDM2, although their binding mode need to be evaluated further. The study of photophysical properties revealed a 10 fold difference between 1,4- and 1,5-regioisomers. Although the 1,5-triazoles tested in this study did not show activity as MDM2-inhibitors, the high quantum yield for the 1,5-isomer could have interesting implications for development of triazole containing fluorescent probes in other areas. In addition, we developed a convenient route for 8-bromination of electron rich purines using $PyrBr_3$ in equimolar amounts at room temperature.

6. Concluding remarks and future perspectives

This thesis describes the synthesis of purine and pyrazolopyrimidine derivatives for different biological applications. The ubiquitous presence of purines as constituents of our internal molecular machinery poses potential problems with selectivity which has to be taken into account. The question of selectivity is especially important when the goal is to study the phenotypic effects of modulating the activity of a certain enzyme in a biological system[230]. In addition to the importance of selectivity, the timing and spatial localization of the process might also be of importance. Using photoactivatable compounds as described in the first paper in this thesis gives the researcher control of when, and potentially also where, a compound is activated. We applied this technique to study a receptor tyrosine kinase and were able to demonstrate that the timing of irradiation was essential for the phenotypic response. In the future, this and possibly other caged kinase inhibitors could be used to study time dependent processes. It would also be possible to extend this methodology to space dependent events.

Bioactive compounds with intrinsic fluorescent properties have the added advantage that they can be followed visually in for example cells. Such compounds would not need conjugated labels, the use of which risks to perturb the system being studied. These possibilities aside, the difficulties in developing compounds with both fluorescent and bioactive properties is well illustrated in the last manuscript dealing with α-helix mimetics, which has been recognized as a difficult task in its own right. One possible application for fluorescent inhibitors would be as displacement probes in assays.

It is interesting to note that despite the effort invested in synthesizing purine derivatives, new methods are still being developed and the purine scaffold still poses a synthetic challenge. Substituent effects have a substantial impact on reactivity, as demonstrated by the dependence on substituent electronegativity in the bromination study in paper III. In the future, further development of the C-H activation reactions in the 8-position of purines[46-48] would be advantageous in that they avoid halogenation altogether.

Acknowledgements

Jag skulle vilja tacka följande personer som alla på något sätt bidragit till den här avhandlingen:

Först och främst min handledare, Morten Grøtli, för att ha gett mig möjligheten att arbeta med projektet, för aldrig sinande entusiasm och för att alltid vara öppen för idéer och diskussioner.

Min biträdande handledare, Kristina Luthman, för att alltid finnas där med goda råd och hjälp.

Mina medarbetare på de olika projekten, Itedale, Chris och Munefumi, och Jesper, Petronella och Joakim samt Kiplin Guy och Jaeki Min för fina samarbeten.

Mina hårt arbetande examensarbetare Jakob, Mattias och Jimmy, bra jobbat!

Mate Erdelyi för ovärderlig hjälp med NMR.

Ni som korrekturläst avhandlingen; Itedale, Mariell, Louise, Kristina och Morten.

Alla nuvarande och före detta gruppmedlemmar i läkemedelskemigruppen; Mariell, min kontors-, labb och prokjektkompis, tack! Peter D för hjälp att komma igång, både på labbet och vid datorn, och Tina, Itedale, Kristina, Christine, Markus, Maria, Carlos och alla andra för gott sällskap.

Matlaget Emma, Markus, Tobias, Jenny och Mariell för att ha förgyllt luncherna de senaste åren.

Alla andra på våning 8 för sällskap, kaffepauser och massor av hjälp under de här åren.

Familj och vänner för tålamod och stöd, tack!

Appendices

Appendix 1: Decaging of **13**

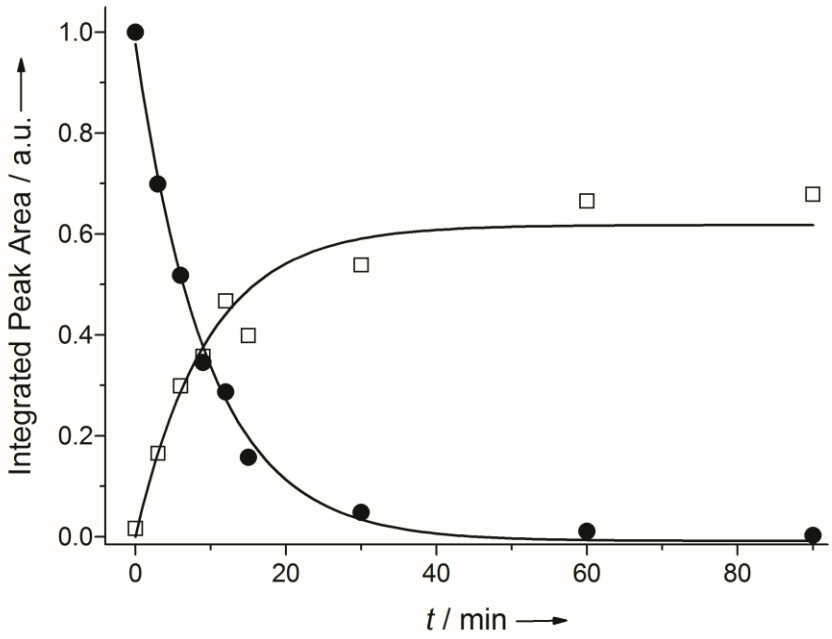

Figure A1. Light-induced decaging of **13**. A Tris buffer solution (1 vol% DMSO) of **13** (100 μM) was irradiated with light (365 nm, light flux: 700 μW/cm^2) and aliquots were drawn and analyzed using HPLC-UV. The integrated areas for the chromatogram peaks associated with **1** (hollow squares) and **13** (solid circles) were fitted globally (shared time constant) to a first order exponential (solid line), yielding a time constant of τ = 9.6 min for the decaging of **13**. It should be noted that the individually extracted time constants for the liberation of **1** and consumption of **13** (τ = 13.1 and 8.7 min, respectively) do not differ significantly from the globally fitted value.

UV tolerance of RET biochemical and Cell assays

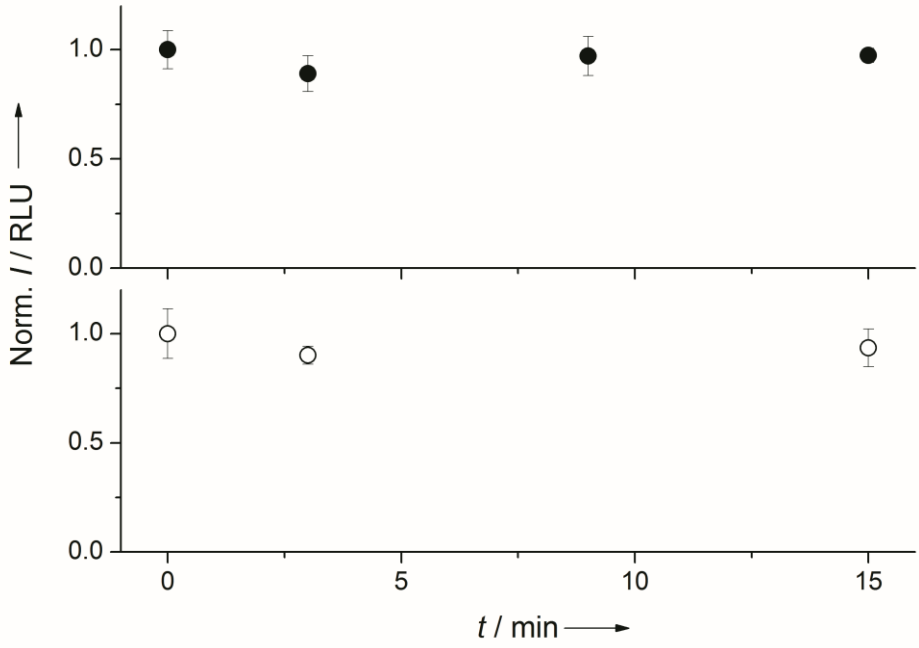

Figure A2. UV tolerance of RET incubation assays. Top panel: Cell-free assay; A reaction mixture comprising RET kinase (0.8 μg/mL) and substrate (40 μg/mL) without inhibitor was subjected to t = 0, 3, 9, or 15 min of 365 nm light. Thereafter, ATP was added (50 μM) and the RET kinase activity was assessed (solid circles). Bottom panel: Live-cell assay; Thawed and acclimatized cells (100 000 cells/mL) without inhibitor was subjected to t = 0, 3, or 15 min of 365 nm light. Thereafter, neurturin was added (at EC_{80}, determined to 15 ng/mL) and the RET kinase activity was assessed (hollow circles). Error bars are mean ± standard deviation of duplicate samples. It is clear that the applied UV-light has no apparent effect on the enzymatic activity in the cell-free or live-cell assay.

Additional control experiments of zebrafish spinal cord

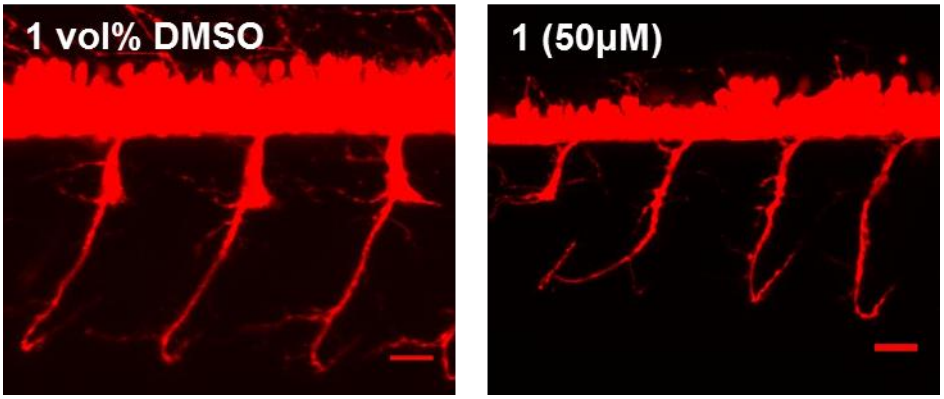

Figure A3. Maximal intensity projections of one hemisegment of the spinal cord in tg(*olig2:dsRed*) zebrafish at 2 dpf. Dechorinated embryos were treated at 6 hpf with 1 vol% DMSO or **1** (50 µM) during 90 min, and then washed. Scale bar: 20 µm.

Appendix 2: NMR spectra of adenine alkylation products

NMR spectra were recorded in DMSO-d_6 (24 mg sample in 0.75 ml) using a Varian 400/54 spectrometer at 400 MHz (^{1}H) and 100 MHz (^{13}C). The chemical shifts were referenced to the solvent peak (2.50 ppm for ^{1}H and 39.5 ppm for ^{13}C).

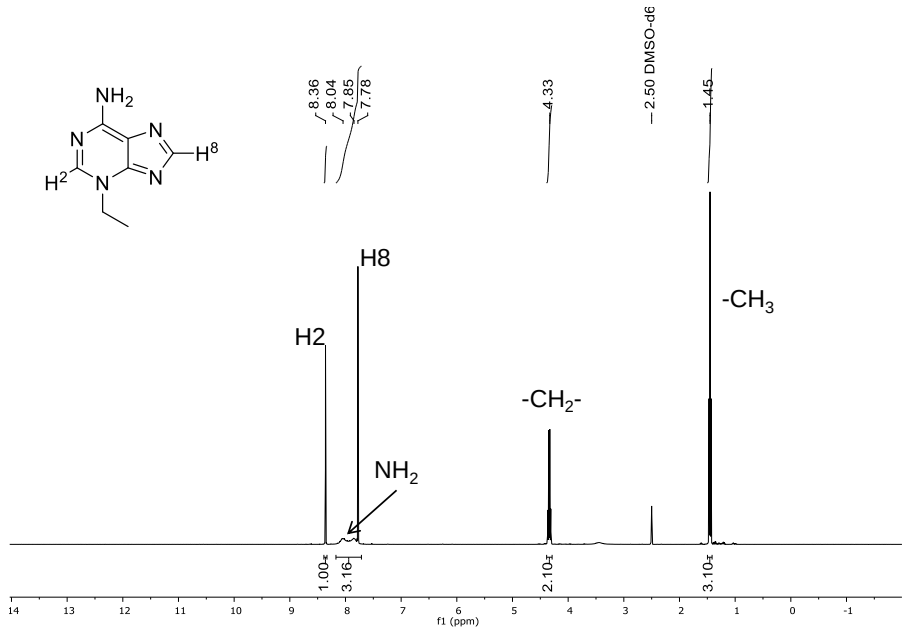

Figure A4. ^{1}H-NMR spectrum of 3-ethyladenine.

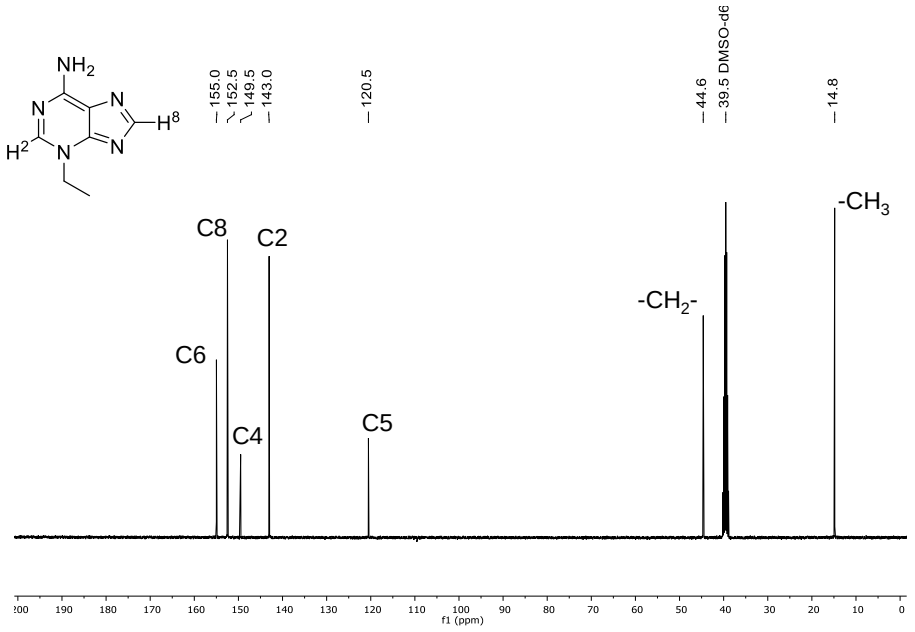

Figure A5. ^{13}C-NMR spectrum of 3-ethyladenine.

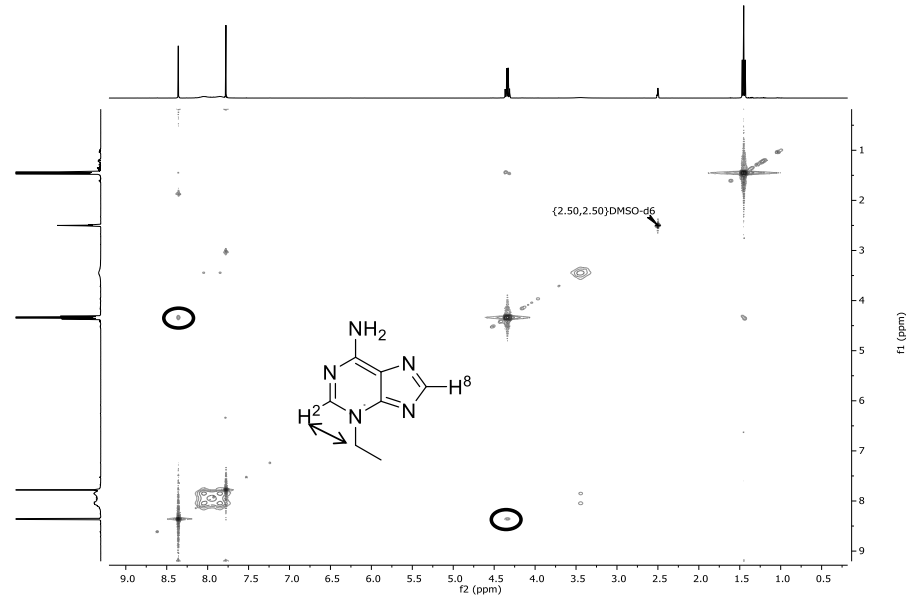

Figure A6. 2D-NOESY spectrum of 3-ethyladenine. The cross peaks corresponding to the NOE between the methylene protons and H^2 are circled.

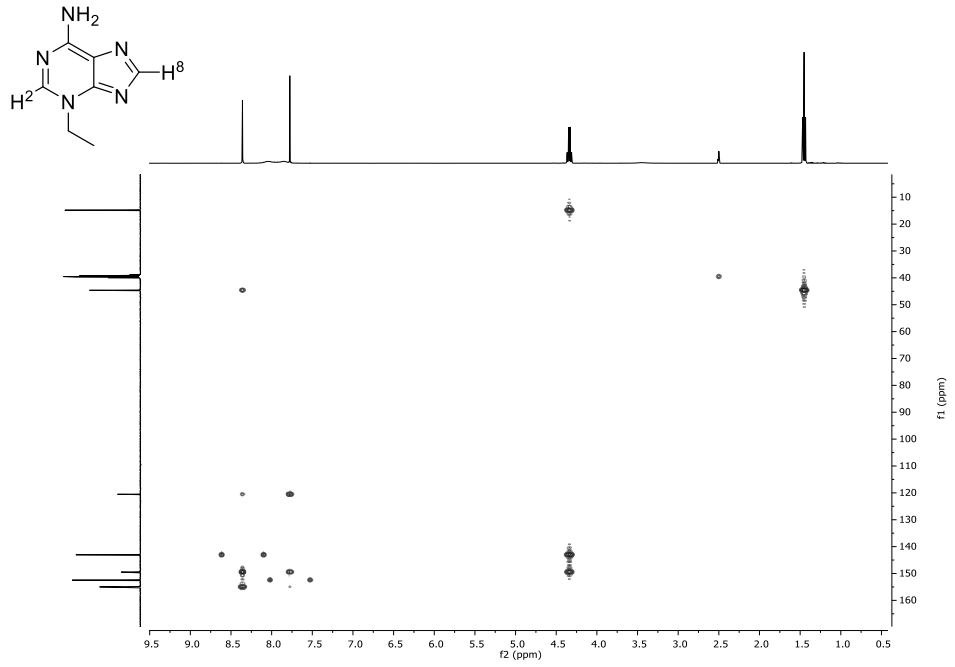

Figure A7. gHMBC spectrum of 3-ethyladenine.

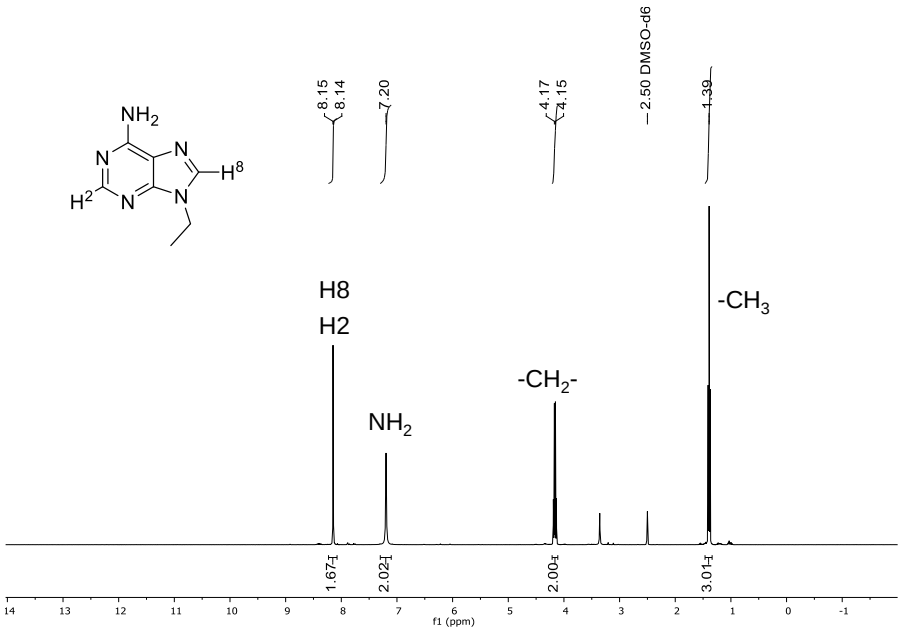

Figure A8. [1]H spectrum of 9-ethyladenine.

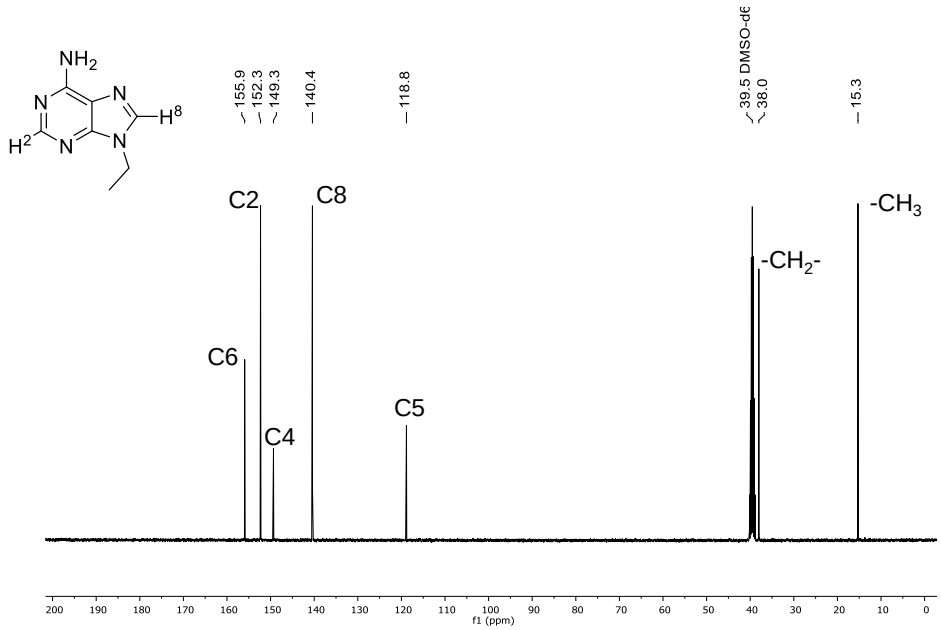

Figure A9. ^{13}C spectrum of 9-ethyladenine.

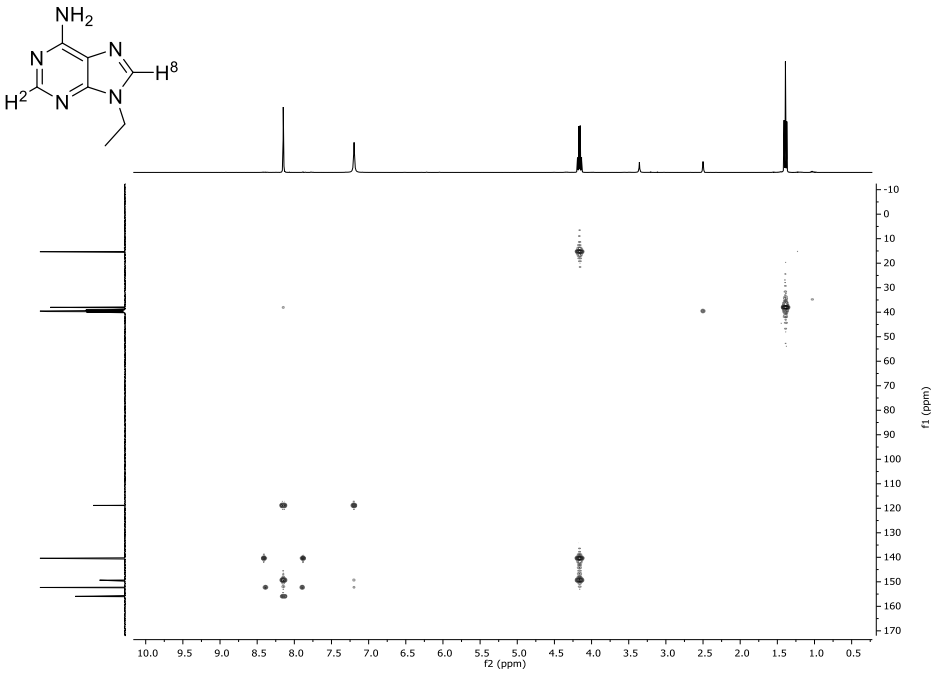

Figure A10. gHMBC spectrum of 9-ethyladenine.

References

1. E. Saxon, C. R. Bertozzi, *Cell Surface Engineering by a Modified Staudinger Reaction*, Science, **2000**, *287*, 2007-2010.
2. W. G. Lewis, L. G. Green, F. Grynszpan, Z. Radić, P. R. Carlier, P. Taylor, M. G. Finn, K. B. Sharpless, *Click Chemistry In Situ: Acetylcholinesterase as a Reaction Vessel for the Selective Assembly of a Femtomolar Inhibitor from an Array of Building Blocks*, Angew. Chem., Int. Ed., **2002**, *41*, 1053-1057.
3. A. C. Bishop, J. A. Ubersax, D. T. Petsch, D. P. Matheos, N. S. Gray, J. Blethrow, E. Shimizu, J. Z. Tsien, P. G. Schultz, M. D. Rose, J. L. Wood, D. O. Morgan, K. M. Shokat, *A chemical switch for inhibitor-sensitive alleles of any protein kinase*, Nature, **2000**, *407*, 395-401.
4. M. E. Welsch, S. A. Snyder, B. R. Stockwell, *Privileged scaffolds for library design and drug discovery*, Curr. Opin. Chem. Biol., **2010**, *14*, 347-361.
5. T. Bartl, Z. Zacharová, P. Sečkářová, E. Kolehmainen, R. Marek, *NMR Quantification of Tautomeric Populations in Biogenic Purine Bases*, Eur. J. Org. Chem., **2009**, *2009*, 1377-1383.
6. A. Broo, A. Holmén, *Ab initio MP2 and DFT calculations of geometry and solution tautomerism of purine and some purine derivatives*, Chem. Phys., **1996**, *211*, 147-161.
7. O. A. Stasyuk, H. Szatyłowicz, T. M. Krygowski, *Effect of the H-Bonding on Aromaticity of Purine Tautomers*, J. Org. Chem., **2012**, *77*, 4035-4045.
8. H. Kunz, *Emil Fischer—Unequalled Classicist, Master of Organic Chemistry Research, and Inspired Trailblazer of Biological Chemistry*, Angew. Chem., Int. Ed., **2002**, *41*, 4439-4451.
9. E. Fischer, *Ueber das Trichlorpurin*, Chem. Ber., **1897**, *30*, 2220-2225.
10. E. Fischer, *Ueber das Purin und seine Methylderivate*, Chem. Ber., **1898**, *31*, 2550-2574.
11. H. Rosemeyer, *The Chemodiversity of Purine as a Constituent of Natural Products*, Chem. Biodiversity, **2004**, *1*, 361-401.
12. T. Yosief, A. Rudi, Z. Stein, I. Goldberg, G. M. D. Gravalos, M. Schleyer, Y. Kashman, *Asmarines A-C; Three novel cytotoxic metabolites from the marine sponge Raspailia sp*, Tetrahedron Lett., **1998**, *39*, 3323-3326.
13. T. Yosief, A. Rudi, Y. Kashman, *Asmarines A-F, Novel Cytotoxic Compounds from the Marine Sponge Raspailia Species*, J. Nat. Prod., **2000**, *63*, 299-304.
14. A. E. Wright, G. P. Roth, J. K. Hoffman, D. B. Divlianska, D. Pechter, S. H. Sennett, E. A. Guzmán, P. Linley, P. J. McCarthy, T. P. Pitts, S. A. Pomponi, J. K. Reed, *Isolation, Synthesis, and*

Biological Activity of Aphrocallistin, an Adenine-Substituted Bromotyramine Metabolite from the Hexactinellida Sponge Aphrocallistes beatrix, J. Nat. Prod., **2009**, *72*, 1178-1183.

15. M. Legraverend, *Recent advances in the synthesis of purine derivatives and their precursors*, Tetrahedron, **2008**, *64*, 8585-8603.
16. J. Liu, Q. Dang, Z. Wei, F. Shi, X. Bai, *An Efficient and Regiospecific Strategy to N7-Substituted Purines and Its Application to a Library of Trisubstituted Purines*, J. Comb. Chem., **2006**, *8*, 410-416.
17. J. H. Lister, *The Purines Supplement 1*, John Wiley & Sons, Inc., **1996.**
18. B. Alhede, F. P. Clausen, J. Juhl-Christensen, K. K. McCluskey, H. F. Preikschat, *A simple and efficient synthesis of 9-substituted guanines. Cyclodesulfurization of 1-substituted 5-[(thiocarbamoyl)amino]imidazole-4-carboxamides under aqueous basic conditions*, J. Org. Chem., **1991**, *56*, 2139-2143.
19. T. Fujii, T. Saito, M. Kawanishi, *A general synthetic route to 3,9-dialkyladenines and their ring opening*, Tetrahedron Lett., **1978**, *19*, 5007-5010.
20. E. Camaioni, S. Costanzi, S. Vittori, R. Volpini, K.-N. Klotz, G. Cristalli, *New substituted 9-alkylpurines as adenosine receptor ligands*, Bioorg. Med. Chem., **1998**, *6*, 523-533.
21. C. Lambertucci, I. Antonini, M. Buccioni, D. D. Ben, D. D. Kachare, R. Volpini, K.-N. Klotz, G. Cristalli, *8-Bromo-9-alkyl adenine derivatives as tools for developing new adenosine A2A and A2B receptors ligands*, Bioorg. Med. Chem., **2009**, *17*, 2812-2822.
22. T. Borrmann, A. Abdelrahman, R. Volpini, C. Lambertucci, E. Alksnis, S. Gorzalka, M. Knospe, A. C. Schiedel, G. Cristalli, C. E. Müller, *Structure-Activity Relationships of Adenine and Deazaadenine Derivatives as Ligands for Adenine Receptors, a New Purinergic Receptor Family*, J. Med. Chem., **2009**, *52*, 5974-5989.
23. M. A. Biamonte, J. D. Shi, K. Hong, D. C. Hurst, L. Zhang, J. H. Fan, D. J. Busch, P. L. Karjian, A. A. Maldonado, J. L. Sensintaffar, Y. C. Yang, A. Kamal, R. E. Lough, K. Lundgren, F. J. Burrows, G. A. Timony, M. F. Boehm, S. R. Kasibhatla, *Orally active purine-based inhibitors of the heat shock protein 90*, J. Med. Chem., **2006**, *49*, 817-828.
24. M. Havelková, D. Dvořák, M. Hocek, *The Suzuki-Miyaura Cross-Coupling Reactions of 2-, 6- or 8-Halopurines with Boronic Acids Leading to 2-, 6- or 8-Aryl- and -Alkenylpurine Derivatives*, Synthesis, **2001**, *2001*, 1704-1710.
25. K. K. Ogilvie, S. L. Beaucage, M. F. Gillen, *Facile alkylation of purines, pyrimidines, nucleosides and nucleotides using tetrabutylammonium fluoride*, Tetrahedron Lett., **1978**, *19*, 1663-1666.
26. I. Shinkai, M. C. Vander Zwan, F. W. Hartner, R. A. Reamer, R. J. Tull, L. M. Weinstock, *Phase-transfer catalysis in the N-benzylation of adenine*, J. Heterocycl. Chem., **1981**, *18*, 197-198.
27. G. H. Hakimelahi, T. W. Ly, A. A. Moosavi-Movahedi, M. L. Jain, M. Zakerinia, H. Davari, H.-C. Mei, T. Sambaiah, A. A. Moshfegh, S. Hakimelahi, *Design, Synthesis, and Biological Evaluation of Novel Nucleoside and Nucleotide Analogues as Agents against DNA Viruses and/or Retroviruses*, J. Med. Chem., **2001**, *44*, 3710-3720.

28. V. Kotek, N. z. d. Chudíková, T. s. Tobrman, D. Dvořák, *Selective Synthesis of 7-Substituted Purines via 7,8-Dihydropurines*, Org. Lett., **2010**, *12*, 5724-5727.
29. K. C. K. Swamy, N. N. B. Kumar, E. Balaraman, K. V. P. P. Kumar, *Mitsunobu and Related Reactions: Advances and Applications*, Chem. Rev., **2009**, *109*, 2551-2651.
30. Y.-T. Chang, N. S. Gray, G. R. Rosania, D. P. Sutherlin, S. Kwon, T. C. Norman, R. Sarohia, M. Leost, L. Meijer, P. G. Schultz, *Synthesis and application of functionally diverse 2,6,9-trisubstituted purine libraries as CDK inhibitors*, Chem. Biol., **1999**, *6*, 361-375.
31. S. Fletcher, *Regioselective alkylation of the exocyclic nitrogen of adenine and adenosine by the Mitsunobu reaction*, Tetrahedron Lett., **2010**, *51*, 2948-2950.
32. S. Fletcher, V. M. Shahani, P. T. Gunning, *Facile and efficient access to 2,6,9-tri-substituted purines through sequential N9, N2 Mitsunobu reactions*, Tetrahedron Lett., **2009**, *50*, 4258-4261.
33. I. Čerňa, R. Pohl, B. Klepetářová, M. Hocek, *Synthesis of 6,8,9-Tri- and 2,6,8,9-Tetrasubstituted Purines by a Combination of the Suzuki Cross-coupling, N-Arylation, and Direct C–H Arylation Reactions*, J. Org. Chem., **2008**, *73*, 9048-9054.
34. A. F. Larsen, T. Ulven, *Direct N9-arylation of purines with aryl halides*, Chem. Comm., **2014**, *50*, 4997-4999.
35. S. Piguel, M. Legraverend, *Selective Amidation of 2,6-Dihalogenopurines: Application to the Synthesis of New 2,6,9-Trisubstituted Purines*, J. Org. Chem., **2007**, *72*, 7026-7029.
36. R. Xia, M.-S. Xie, H.-Y. Niu, G.-R. Qu, H.-M. Guo, *Radical Route for the Alkylation of Purine Nucleosides at C6 via Minisci Reaction*, Org. Lett., **2013**, *16*, 444-447.
37. H. Hayakawa, H. Tanaka, K. Sasaki, K. Haraguchi, T. Saitoh, F. Takai, T. Miyasaka, *A lithiation approach to cordycepin analogues variously substituted at the C-8 position*, J. Heterocycl. Chem., **1989**, *26*, 189-192.
38. N. J. Leonard, J. D. Bryant, *Regioselective electrophilic reactions on substituted purines. Predominant intermediacy of 6- or 8-purinyl carbanions*, J. Org. Chem., **1979**, *44*, 4612-4616.
39. R. Rayala, S. F. Wnuk, *Bromination at C-5 of pyrimidine and C-8 of purine nucleosides with 1,3-dibromo-5,5-dimethylhydantoin*, Tetrahedron Lett., **2012**, *53*, 3333-3336.
40. W. K. D. Brill, C. Riva-Toniolo, *The bromination of purines with a charge transfer complex between bromine and lutidine*, Tetrahedron Lett., **2001**, *42*, 6279-6282.
41. R. Volpini, S. Costanzi, C. Lambertucci, S. Vittori, C. Martini, M. Trincavelli, K.-N. Klotz, G. Cristalli, *2- and 8-alkynyl-9-ethyladenines: Synthesis and biological activity at human and rat adenosine receptors*, Purinerg. Signal., **2005**, *1*, 173-181.
42. L. A. Agrofoglio, I. Gillaizeau, Y. Saito, *Palladium-Assisted Routes to Nucleosides*, Chem. Rev., **2003**, *103*, 1875-1916.
43. A. A. Van Aerschot, P. Mamos, N. J. Weyns, S. Ikeda, E. De Clercq, P. A. Herdewijn, *Antiviral activity of C-alkylated purine nucleosides obtained by cross-coupling with tetraalkyltin reagents*, J. Med. Chem., **1993**, *36*, 2938-2942.

44. E. C. Western, J. R. Daft, E. M. Johnson, P. M. Gannett, K. H. Shaughnessy, *Efficient One-Step Suzuki Arylation of Unprotected Halonucleosides, Using Water-Soluble Palladium Catalysts*, J. Org. Chem., **2003**, *68*, 6767-6774.

45. A. Dierckx, P. Dinér, A. H. El-Sagheer, J. D. Kumar, T. Brown, M. Grøtli, L. M. Wilhelmsson, *Characterization of photophysical and base-mimicking properties of a novel fluorescent adenine analogue in DNA*, Nucleic Acids Res., **2011**, *39*, 4513-4524.

46. Z. Wang, K. Li, D. Zhao, J. Lan, J. You, *Palladium-Catalyzed Oxidative C-H/C-H Cross-Coupling of Indoles and Pyrroles with Heteroarenes*, Angew. Chem., Int. Ed., **2011**, *50*, 5365-5369.

47. F. Besselièvre, S. Piguel, *Copper as a Powerful Catalyst in the Direct Alkynylation of Azoles*, Angew. Chem., Int. Ed., **2009**, *48*, 9553-9556.

48. B. Pacheco Berciano, S. Lebrequier, F. o. Besselièvre, S. Piguel, *1,1-Dibromo-1-alkenes as Valuable Partners in the Copper-Catalyzed Direct Alkynylation of Azoles*, Org. Lett., **2010**, *12*, 4038-4041.

49. The following is an account of the early advances in Pd-catalyzed C-C coupling;C. C. C. Johansson Seechurn, M. O. Kitching, T. J. Colacot, V. Snieckus, Angew. Chem., Int. Ed. 2012, 51, 5062-5085.

50. J. Magano, J. R. Dunetz, *Large-Scale Applications of Transition Metal-Catalyzed Couplings for the Synthesis of Pharmaceuticals*, Chem. Rev., **2011**, *111*, 2177-2250.

51. K. C. Nicolaou, P. G. Bulger, D. Sarlah, *Palladium-Catalyzed Cross-Coupling Reactions in Total Synthesis*, Angew. Chem., Int. Ed., **2005**, *44*, 4442-4489.

52. http://www.nobelprize.org/nobel_prizes/chemistry/laureates/2010/

53. H. A. Dieck, F. R. Heck, *Palladium catalyzed synthesis of aryl, heterocyclic and vinylic acetylene derivatives*, J. Organomet. Chem., **1975**, *93*, 259-263.

54. K. Sonogashira, Y. Tohda, N. Hagihara, *A convenient synthesis of acetylenes: catalytic substitutions of acetylenic hydrogen with bromoalkenes, iodoarenes and bromopyridines*, Tetrahedron Lett., **1975**, *16*, 4467-4470.

55. R. Chinchilla, C. Nájera, *The Sonogashira Reaction: A Booming Methodology in Synthetic Organic Chemistry*, Chem. Rev., **2007**, *107*, 874-922.

56. M. Karak, L. C. A. Barbosa, G. C. Hargaden, *Recent mechanistic developments and next generation catalysts for the Sonogashira coupling reaction*, RSC Advances, **2014**, *4*, 53442-53466.

57. P. Bertus, F. Fecourt, C. Bauder, P. Pale, *Evidence for the in situ formation of copper acetylides during Pd/Cu catalyzed synthesis of enynes: a new synthesis of allenynols*, New J. Chem., **2004**, *28*, 12-14.

58. T. C. Berg, V. Bakken, L.-L. Gundersen, D. Petersen, *Cyclization and rearrangement products from coupling reactions between terminal o-alkynylphenols or o-ethynyl(hydroxymethyl)benzene and 6-halopurines*, Tetrahedron, **2006**, *62*, 6121-6131.

59. M. Hocek, I. Votruba, H. Dvořáková, *Synthesis of carba-analogues of myoseverin by regioselective cross-coupling reactions of 2,6-dichloro-9-isopropylpurine*, Tetrahedron, **2003**, *59*, 607-611.

60. P. Lang, G. Magnin, G. Mathis, A. Burger, J.-F. Biellmann, *Synthesis of 8-(ω-Hydroxyalkyl)-, 8-(ω-Hydroxyalk-1-enyl)-, and 8-(ω-Hydroxyalk-1-ynyl)adenines Using the tert-Butyldimethylsilyloxymethyl Group, a New and Versatile Protecting Group of Adenine*, J. Org. Chem., **2000**, *65*, 7825-7832.

61. G. O'Mahony, E. Ehrman, M. Grøtli, *Synthesis of adenosine-based fluorosides containing a novel heterocyclic ring system*, Tetrahedron Lett., **2005**, *46*, 6745-6748.

62. F. Seela, M. Zulauf, M. Sauer, M. Deimel, *7-Substituted 7-Deaza-2'-deoxyadenosines and 8-Aza-7-deaza-2'-deoxyadenosines: Fluorescence of DNA-Base Analogues Induced by the 7-Alkynyl Side Chain*, HeIv. Chim. Acta, **2000**, *83*, 910-927.

63. P. Kielkowski, H. Macíčková-Cahová, R. Pohl, M. Hocek, *Transient and Switchable (Triethylsilyl)ethynyl Protection of DNA against Cleavage by Restriction Endonucleases*, Angew. Chem., Int. Ed., **2011**, *50*, 8727-8730.

64. M. Meldal, C. W. Tornøe, *Cu-Catalyzed Azide-Alkyne Cycloaddition*, Chem. Rev., **2008**, *108*, 2952-3015.

65. V. V. Rostovtsev, L. G. Green, V. V. Fokin, K. B. Sharpless, *A Stepwise Huisgen Cycloaddition Process: Copper(I)-Catalyzed Regioselective "Ligation" of Azides and Terminal Alkynes*, Angew. Chem., Int. Ed., **2002**, *41*, 2596-2599.

66. C. W. Tornøe, C. Christensen, M. Meldal, *Peptidotriazoles on Solid Phase: [1,2,3]-Triazoles by Regiospecific Copper(I)-Catalyzed 1,3-Dipolar Cycloadditions of Terminal Alkynes to Azides*, J. Org. Chem., **2002**, *67*, 3057-3064.

67. P. Thirumurugan, D. Matosiuk, K. Jozwiak, *Click Chemistry for Drug Development and Diverse Chemical–Biology Applications*, Chem. Rev., **2013**, *113*, 4905-4979.

68. V. O. Rodionov, V. V. Fokin, M. G. Finn, *Mechanism of the Ligand-Free CuI-Catalyzed Azide–Alkyne Cycloaddition Reaction*, Angew. Chem., Int. Ed., **2005**, *44*, 2210-2215.

69. M. Ahlquist, V. V. Fokin, *Enhanced Reactivity of Dinuclear Copper(I) Acetylides in Dipolar Cycloadditions*, Organometallics, **2007**, *26*, 4389-4391.

70. L. Zhang, X. G. Chen, P. Xue, H. H. Y. Sun, I. D. Williams, K. B. Sharpless, V. V. Fokin, G. C. Jia, *Ruthenium-catalyzed cycloaddition of alkynes and organic azides*, J. Am. Chem. Soc., **2005**, *127*, 15998-15999.

71. B. C. Boren, S. Narayan, L. K. Rasmussen, L. Zhang, H. T. Zhao, Z. Y. Lin, G. C. Jia, V. V. Fokin, *Ruthenium-catalyzed azide-alkyne cycloaddition: Scope and mechanism*, J. Am. Chem. Soc., **2008**, *130*, 8923-8930.

72. S. W. Kwok, J. R. Fotsing, R. J. Fraser, V. O. Rodionov, V. V. Fokin, *Transition-Metal-Free Catalytic Synthesis of 1,5-Diaryl-1,2,3-triazoles*, Org. Lett., **2010**, *12*, 4217-4219.

73. J.-M. Kee, B. Villani, L. R. Carpenter, T. W. Muir, *Development of Stable Phosphohistidine Analogues*, J. Am. Chem. Soc., **2010**, *132*, 14327-14329.

74. J. Veselý, L. Havliček, M. Strnad, J. J. Blow, A. Donella-Deana, L. Pinna, D. S. Letham, J.-y. Kato, L. Detivaud, S. Leclerc, L. Meijer, *Inhibition of Cyclin-Dependent Kinases by Purine Analogues*, Eur. J. Biochem., **1994**, *224*, 771-786.

75. L. Meijer, E. Raymond, *Roscovitine and Other Purines as Kinase Inhibitors. From Starfish Oocytes to Clinical Trials*, Acc. Chem. Res., **2003**, *36*, 417-425.

76. N. S. Gray, L. Wodicka, A.-M. W. H. Thunnissen, T. C. Norman, S. Kwon, F. H. Espinoza, D. O. Morgan, G. Barnes, S. LeClerc, L. Meijer, S.-H. Kim, D. J. Lockhart, P. G. Schultz, *Exploiting Chemical Libraries, Structure, and Genomics in the Search for Kinase Inhibitors*, Science, **1998**, *281*, 533-538.

77. L. P. Jordheim, D. Durantel, F. Zoulim, C. Dumontet, *Advances in the development of nucleoside and nucleotide analogues for cancer and viral diseases*, Nat. Rev. Drug. Discov., **2013**, *12*, 447-464.

78. E. Vitaku, D. T. Smith, J. T. Njardarson, *Analysis of the Structural Diversity, Substitution Patterns, and Frequency of Nitrogen Heterocycles among U.S. FDA Approved Pharmaceuticals*, J. Med. Chem., **2014**.

79. G. B. Elion, *Acyclovir: Discovery, mechanism of action, and selectivity*, J. Med. Virol., **1993**, *41*, 2-6.

80. G. B. Elion, *The Quest for a Cure*, Annu. Rev. Pharmacol., **1993**, *33*, 1-25.

81. R. Foster, D. Faulds, *Abacavir*, Drugs, **1998**, *55*, 729-736.

82. R. K. Robins, *Potential Purine Antagonists. I. Synthesis of Some 4,6-Substituted Pyrazolo [3,4-d] pyrimidines1*, J. Am. Chem. Soc., **1956**, *78*, 784-790.

83. P. L. Southwick, B. Dhawan, *Preparation of 4,6-diaminopyrazolo[3,4-d] pyrimidines with variations in substitution at the 1- and 3-positions*, J. Heterocycl. Chem., **1975**, *12*, 1199-1205.

84. T. Y. H. Wu, P. G. Schultz, S. Ding, *One-Pot Two-Step Microwave-Assisted Reaction in Constructing 4,5-Disubstituted Pyrazolopyrimidines*, Org. Lett., **2003**, *5*, 3587-3590.

85. N. Todorovic, E. Awuah, T. Shakya, G. D. Wright, A. Capretta, *Microwave-assisted synthesis of N1- and C3-substituted pyrazolo[3,4-d]pyrimidine libraries*, Tetrahedron Lett., **2011**, *52*, 5761-5763.

86. M. Klein, M. Morillas, A. Vendrell, L. Brive, M. Gebbia, I. M. Wallace, G. Giaever, C. Nislow, F. Posas, M. Grøtli, *Design, Synthesis and Characterization of a Highly Effective Inhibitor for Analog-Sensitive (as) Kinases*, PLoS ONE, **2011**, *6*, e20789.

87. H. Rosemeyer, M. Zulauf, N. Ramzaeva, G. Becher, E. Feiling, K. Mühlegger, I. Münster, A. Lohmann, F. Seela, *Stereoelectronic Effects of Modified Purines on the Sugar Conformation of Nucleosides and Fluorescence Properties*, Nucleos. Nucleot., **1997**, *16*, 821-828.

88. M. Chauhan, R. Kumar, *Medicinal attributes of pyrazolo[3,4-d]pyrimidines: A review*, Bioorg. Med. Chem., **2013**, *21*, 5657-5668.

89. S. Schenone, M. Radi, F. Musumeci, C. Brullo, M. Botta, *Biologically Driven Synthesis of Pyrazolo[3,4-d]pyrimidines As Protein Kinase Inhibitors: An Old Scaffold As a New Tool for Medicinal Chemistry and Chemical Biology Studies*, Chem. Rev., **2014**, *114*, 7189-7238.

90. A. Jablonski, *Efficiency of Anti-Stokes Fluorescence in Dyes*, Nature, **1933**, 131.

91. J. R. Lakowicz, *Principles of Fluorescence Spectroscopy*, Springer, 233 Spring Street, New York, NY 10013, USA, **2006**.

92. J. Li, J.-J. Zhu, *Quantum dots for fluorescent biosensing and bio-imaging applications*, Analyst, **2013**, *138*, 2506-2515.

93. Y. Wang, R. Hu, G. Lin, I. Roy, K.-T. Yong, *Functionalized Quantum Dots for Biosensing and Bioimaging and Concerns on Toxicity*, ACS Applied Materials & Interfaces, **2013**, *5*, 2786-2799.

94. J. Zhang, R. E. Campbell, A. Y. Ting, R. Y. Tsien, *Creating new fluorescent probes for cell biology*, Nat. Rev. Mol. Cell. Biol., **2002**, *3*, 906-918.

95. L. D. Lavis, R. T. Raines, *Bright Building Blocks for Chemical Biology*, ACS Chem. Biol., **2014**, *9*, 855-866.

96. L. D. Lavis, R. T. Raines, *Bright Ideas for Chemical Biology*, ACS Chem. Biol., **2008**, *3*, 142-155.

97. A. Nadler, C. Schultz, *The Power of Fluorogenic Probes*, Angew. Chem., Int. Ed., **2013**, *52*, 2408-2410.

98. A. Loudet, K. Burgess, *BODIPY Dyes and Their Derivatives: Syntheses and Spectroscopic Properties*, Chem. Rev., **2007**, *107*, 4891-4932.

99. A. Chatterjee, J. Guo, H. S. Lee, P. G. Schultz, *A Genetically Encoded Fluorescent Probe in Mammalian Cells*, J. Am. Chem. Soc., **2013**, *135*, 12540-12543.

100. R. W. Sinkeldam, N. J. Greco, Y. Tor, *Fluorescent Analogs of Biomolecular Building Blocks: Design, Properties, and Applications*, Chem. Rev., **2010**, *110*, 2579-2619.

101. L. M. Wilhelmsson, *Fluorescent nucleic acid base analogues*, Q. Rev. Biophys., **2010**, *43*, 159-183.

102. D. C. Ward, E. Reich, L. Stryer, *Fluorescence Studies of Nucleotides and Polynucleotides: I. FORMYCIN, 2-AMINOPURINE RIBOSIDE, 2,6-DIAMINOPURINE RIBOSIDE, AND THEIR DERIVATIVES*, J. Biol. Chem., **1969**, *244*, 1228-1237.

103. A. Dierckx, F.-A. Miannay, N. Ben Gaied, S. Preus, M. Björck, T. Brown, L. M. Wilhelmsson, *Quadracyclic Adenine: A Non-Perturbing Fluorescent Adenine Analogue*, Chem. Eur. J., **2012**, *18*, 5987-5997.

104. J. Son, J.-J. Lee, J.-S. Lee, A. Schüller, Y.-T. Chang, *Isozyme-Specific Fluorescent Inhibitor of Glutathione S-Transferase Omega 1*, ACS Chem. Biol., **2010**, *5*, 449-453.

105. D. Kim, H. Jun, H. Lee, S.-S. Hong, S. Hong, *Development of New Fluorescent Xanthines as Kinase Inhibitors*, Org. Lett., **2010**, *12*, 1212-1215.

106. G. M. Chinigo, M. Paige, S. Grindrod, E. Hamel, S. Dakshanamurthy, M. Chruszcz, W. Minor, M. L. Brown, *Asymmetric Synthesis of 2,3-Dihydro-2-arylquinazolin-4-ones: Methodology and Application to a Potent Fluorescent Tubulin Inhibitor with Anticancer Activity*, J. Med. Chem., **2008**, *51*, 4620-4631.

107. E. M. Callaway, R. Yuste, *Stimulating neurons with light*, Curr. Opin. Neurobiol., **2002**, *12*, 587-592.

108. J. P. Olson, M. R. Banghart, B. L. Sabatini, G. C. R. Ellis-Davies, *Spectral Evolution of a Photochemical Protecting Group for Orthogonal Two-Color Uncaging with Visible Light*, J. Am. Chem. Soc., **2013**, *135*, 15948-15954.

109. J. Ni, D. A. Auston, D. A. Freilich, S. Muralidharan, E. A. Sobie, J. P. Y. Kao, *Photochemical Gating of Intracellular Ca2+ Release Channels*, J. Am. Chem. Soc., **2007**, *129*, 5316-5317.

110. M. Mentel, V. Laketa, D. Subramanian, H. Gillandt, C. Schultz, *Photoactivatable and Cell-Membrane-Permeable Phosphatidylinositol 3,4,5-Trisphosphate*, Angew. Chem., Int. Ed., **2011**, *50*, 3811-3814.

111. C. Brieke, F. Rohrbach, A. Gottschalk, G. Mayer, A. Heckel, *Light-Controlled Tools*, Angew. Chem., Int. Ed., **2012**, *51*, 8446-8476.

112. J. H. Kaplan, B. Forbush, J. F. Hoffman, *Rapid photolytic release of adenosine 5'-triphosphate from a protected analog: utilization by the sodium:potassium pump of human red blood cell ghosts*, Biochemistry, **1978**, *17*, 1929-1935.

113. Y. V. Il'ichev, M. A. Schwörer, J. Wirz, *Photochemical Reaction Mechanisms of 2-Nitrobenzyl Compounds: Methyl Ethers and Caged ATP*, J. Am. Chem. Soc., **2004**, *126*, 4581-4595.

114. H. Gorner, *Effects of 4,5-dimethoxy groups on the time-resolved photoconversion of 2-nitrobenzyl alcohols and 2-nitrobenzaldehyde into nitroso derivatives*, Photoch. Photob. Sci., **2005**, *4*, 822-828.

115. K. Schaper, M. Etinski, T. Fleig, *Theoretical Investigation of the Excited States of 2-Nitrobenzyl and 4,5-Methylendioxy-2-nitrobenzyl Caging Groups*, Photochemistry and Photobiology, **2009**, *85*, 1075-1081.

116. J. Kohl-Landgraf, F. Buhr, D. Lefrancois, J.-M. Mewes, H. Schwalbe, A. Dreuw, J. Wachtveitl, *Mechanism of the Photoinduced Uncaging Reaction of Puromycin Protected by a 6-Nitroveratryloxycarbonyl Group*, J. Am. Chem. Soc., **2014**, *136*, 3430-3438.

117. J. A. Adams, *Kinetic and Catalytic Mechanisms of Protein Kinases*, Chem. Rev., **2001**, *101*, 2271-2290.

118. G. Manning, D. B. Whyte, R. Martinez, T. Hunter, S. Sudarsanam, *The Protein Kinase Complement of the Human Genome*, Science, **2002**, *298*, 1912-1934.

119. T. Hunter, *The Genesis of Tyrosine Phosphorylation*, Cold Spring Harbor Perspectives in Biology, **2014**, *6*.

120. S. K. Hanks, T. Hunter, *Protein kinases 6. The eukaryotic protein kinase superfamily: kinase (catalytic) domain structure and classification*, FASEB J., **1995**, *9*, 576-596.

121. S. K. Hanks, T. Hunter, in *The Protein Kinase FactsBook* (Ed.: G. H. Hanks), Academic Press, San Diego, **1995**, pp. 7-47.

122. M. Huse, J. Kuriyan, *The Conformational Plasticity of Protein Kinases*, Cell, **2002**, *109*, 275-282.

123. P. Blume-Jensen, T. Hunter, *Oncogenic kinase signalling*, Nature, **2001**, *411*, 355-365.

124. M. E. Gerritsen, D. J. Matthews, *Targeting Protein Kinases for Cancer Therapy*, John Wiley & Sons, Hoboken, NJ, USA, **2010**.

125. P. Cohen, *Protein kinases [mdash] the major drug targets of the twenty-first century?*, Nat. Rev. Drug. Discov., **2002**, *1*, 309-315.

126. Z. Zhao, H. Wu, L. Wang, Y. Liu, S. Knapp, Q. Liu, N. S. Gray, *Exploration of Type II Binding Mode: A Privileged Approach for Kinase Inhibitor Focused Drug Discovery?*, ACS Chem. Biol., **2014**, *9*, 1230-1241.

127. H. Kantarjian, E. Jabbour, J. Grimley, P. Kirkpatrick, *Dasatinib*, Nat. Rev. Drug. Discov., **2006**, *5*, 717-718.

128. G. Bollag, J. Tsai, J. Zhang, C. Zhang, P. Ibrahim, K. Nolop, P. Hirth, *Vemurafenib: the first drug approved for BRAF-mutant cancer*, Nat. Rev. Drug. Discov., **2012**, *11*, 873-886.

129. J. Zhang, P. L. Yang, N. S. Gray, *Targeting cancer with small molecule kinase inhibitors*, Nat. Rev. Cancer, **2009**, *9*, 28-39.

130. S. Wilhelm, C. Carter, M. Lynch, T. Lowinger, J. Dumas, R. A. Smith, B. Schwartz, R. Simantov, S. Kelley, *Discovery and development of sorafenib: a multikinase inhibitor for treating cancer*, Nat. Rev. Drug. Discov., **2006**, *5*, 835-844.

131. R. Capdeville, E. Buchdunger, J. Zimmermann, A. Matter, *Glivec (STI571, imatinib), a rationally developed, targeted anticancer drug*, Nat. Rev. Drug. Discov., **2002**, *1*, 493-502.

132. Z. Fang, C. Grütter, D. Rauh, *Strategies for the Selective Regulation of Kinases with Allosteric Modulators: Exploiting Exclusive Structural Features*, ACS Chem. Biol., **2012**, *8*, 58-70.

133. H. Abe, S. Kikuchi, K. Hayakawa, T. Iida, N. Nagahashi, K. Maeda, J. Sakamoto, N. Matsumoto, T. Miura, K. Matsumura, N. Seki, T. Inaba, H. Kawasaki, T. Yamaguchi, R. Kakefuda, T. Nanayama, H. Kurachi, Y. Hori, T. Yoshida, J. Kakegawa, Y. Watanabe, A. G. Gilmartin, M. C. Richter, K. G. Moss, S. G. Laquerre, *Discovery of a Highly Potent and Selective MEK Inhibitor: GSK1120212 (JTP-74057 DMSO Solvate)*, ACS Med. Chem. Lett., **2011**, *2*, 320-324.

134. L. A. Honigberg, A. M. Smith, M. Sirisawad, E. Verner, D. Loury, B. Chang, S. Li, Z. Pan, D. H. Thamm, R. A. Miller, J. J. Buggy, *The Bruton tyrosine kinase inhibitor PCI-32765 blocks B-cell activation and is efficacious in models of autoimmune disease and B-cell malignancy*, P. Natl. Acad. Sci. USA, **2010**, *107*, 13075-13080.

135. M. A. Lemmon, J. Schlessinger, *Cell Signaling by Receptor Tyrosine Kinases*, Cell, **2010**, *141*, 1117-1134.

136. I. Plaza-Menacho, L. Mologni, N. Q. McDonald, *Mechanisms of RET signaling in cancer: Current and future implications for targeted therapy*, Cell. Signal., **2014**, *26*, 1743-1752.

137. L. M. Mulligan, *RET revisited: expanding the oncogenic portfolio*, Nat. Rev. Cancer, **2014**, *14*, 173-186.

138. E. Arighi, M. G. Borrello, H. Sariola, *RET tyrosine kinase signaling in development and cancer*, Cytokine & Growth Factor Reviews, **2005**, *16*, 441-467.

139. A. R. Morckel, H. Lusic, L. Farzana, J. A. Yoder, A. Deiters, N. M. Nascone-Yoder, *A photoactivatable small-molecule inhibitor for light-controlled spatiotemporal regulation of Rho kinase in live embryos*, Development, **2012**, *139*, 437-442.

140. J. S. Wood, M. Koszelak, J. Liu, D. S. Lawrence, *A Caged Protein Kinase Inhibitor*, J. Am. Chem. Soc., **1998**, *120*, 7145-7146.

141. P. Dinér, J. P. Alao, J. Söderlund, P. Sunnerhagen, M. Grøtli, *Preparation of 3-Substituted-1-Isopropyl-1H-pyrazolo[3,4-d]pyrimidin-4-amines as RET Kinase Inhibitors*, J. Med. Chem., **2012**, *55*, 4872-4876.

142. K. Alvarez, J.-J. Vasseur, T. Beltran, J.-L. Imbach, *Photocleavable Protecting Groups as Nucleobase Protections Allowed the Solid-Phase Synthesis of Base-Sensitive SATE-Prooligonucleotides*, J. Org. Chem., **1999**, *64*, 6319-6328.

143. P. Neveu, I. Aujard, C. Benbrahim, T. Le Saux, J.-F. Allemand, S. Vriz, D. Bensimon, L. Jullien, *A Caged Retinoic Acid for One- and Two-Photon Excitation in Zebrafish Embryos*, Angew. Chem., Int. Ed., **2008**, *47*, 3744-3746.

144. T. Milburn, N. Matsubara, A. P. Billington, J. B. Udgaonkar, J. W. Walker, B. K. Carpenter, W. W. Webb, J. Marque, W. Denk, *Synthesis, photochemistry, and biological activity of a caged photolabile acetylcholine receptor ligand*, Biochemistry, **1989**, *28*, 49-55.

145. H. Venkatesan, M. M. Greenberg, *Improved Utility of Photolabile Solid Phase Synthesis Supports for the Synthesis of Oligonucleotides Containing 3'-Hydroxyl Termini*, J. Org. Chem., **1996**, *61*, 525-529.

146. D. L. McMinn, M. M. Greenberg, *Novel solid phase synthesis supports for the preparation of oligonucleotides containing 3'-alkyl amines*, Tetrahedron, **1996**, *52*, 3827-3840.

147. S. Pothukanuri, Z. Pianowski, N. Winssinger, *Expanding the Scope and Orthogonality of PNA Synthesis*, Eur. J. Org. Chem., **2008**, *2008*, 3141-3148.

148. P. Forsell, H. Almqvist, P. Hillertz, T. Åkerud, M. Otrocka, L. Eisele, K. Sun, H. Andersson, S. Trivedi, A. R. Wollberg, N. Dekker, D. Rottici, K. Sandberg, *The Use of TrkA-PathHunter Assay in High-Throughput Screening to Identify Compounds That Affect Nerve Growth Factor Signaling*, J. Biomol. Screen., **2013**, *18*, 659-669.

149. G. K. Smith, E. R. Wood, *Cell-based assays for kinase drug discovery*, Drug Discovery Today: Technol., **2010**, *7*, e13-e19.

150. T. Attié-Bitach, M. Abitbol, M. Gérard, A.-L. Delezoide, J. Augé, A. Pelet, J. Amiel, V. Pachnis, A. Munnich, S. Lyonnet, M. Vekemans, *Expression of the RET proto-oncogene in human Embryos*, American Journal of Medical Genetics, **1998**, *80*, 481-486.

151. B. W. Bisgrove, D. W. Raible, V. Walter, J. S. Eisen, D. J. Grunwald, *Expression of c-ret in the zebrafish embryo: Potential roles in motoneuronal development*, J. Neurobiol., **1997**, *33*, 749-768.

152. S. W. W. Camelia V Marcos-Gutiérrez, Nigel Holder, Vassilis Pachnis, *The zebrafish homologue of the ret receptor and its pattern of expression during embryogenesis*, Oncogene, **1997**, *14*, 879-889.

153. I. T. Shepherd, J. Pietsch, S. Elworthy, R. N. Kelsh, D. W. Raible, *Roles for GFRα1 receptors in zebrafish enteric nervous system development*, Development, **2004**, *131*, 241-249.
154. P. Myers, J. Eisen, M. Westerfield, *Development and axonal outgrowth of identified motoneurons in the zebrafish*, J. NeuroSci., **1986**, *6*, 2278-2289.
155. S. Schmelz, J. H. Naismith, *Adenylate-forming enzymes*, Curr. Opin. Struc. Biol., **2009**, *19*, 666-671.
156. P. Schimmel, J. Tao, J. Hill, *Aminoacyl tRNA synthetases as targets for new anti-infectives*, FASEB J., **1998**, *12*, 1599-1609.
157. P. Schimmel, *Development of tRNA synthetases and connection to genetic code and disease*, Protein Sci., **2008**, *17*, 1643-1652.
158. M. Ibba, D. Söll, *AMINOACYL-tRNA SYNTHESIS*, Annu. Rev. Biochem., **2000**, *69*, 617-650.
159. S. G. Park, P. Schimmel, S. Kim, *Aminoacyl tRNA synthetases and their connections to disease*, P. Natl. Acad. Sci. USA, **2008**, *105*, 11043-11049.
160. A. T. Fuller, G. Mellows, M. Woolford, G. T. Banks, K. D. Barrow, E. B. Chain, *Pseudomonic Acid: an Antibiotic produced by Pseudomonas fluorescens*, Nature, **1971**, *234*, 416-417.
161. P. Yao, P. L. Fox, *Aminoacyl-tRNA synthetases in medicine and disease, Vol. 5*, **2013**.
162. F. L. Rock, W. Mao, A. Yaremchuk, M. Tukalo, T. Crépin, H. Zhou, Y.-K. Zhang, V. Hernandez, T. Akama, S. J. Baker, J. J. Plattner, L. Shapiro, S. A. Martinis, S. J. Benkovic, S. Cusack, M. R. K. Alley, *An Antifungal Agent Inhibits an Aminoacyl-tRNA Synthetase by Trapping tRNA in the Editing Site*, Science, **2007**, *316*, 1759-1761.
163. G. H. M. Vondenhoff, A. Van Aerschot, *Aminoacyl-tRNA synthetase inhibitors as potential antibiotics*, Eur. J. Med. Chem., **2011**, *46*, 5227-5236.
164. I. A. Critchley, C. L. Young, K. C. Stone, U. A. Ochsner, J. Guiles, T. Tarasow, N. Janjic, *Antibacterial Activity of REP8839, a New Antibiotic for Topical Use*, Antimicrobial Agents and Chemotherapy, **2005**, *49*, 4247-4252.
165. C. Dyrager, K. Börjesson, P. Dinér, A. Elf, B. Albinsson, L. M. Wilhelmsson, M. Grøtli, *Synthesis and Photophysical Characterisation of Fluorescent 8-(1H-1,2,3-Triazol-4-yl)adenosine Derivatives*, Eur. J. Org. Chem., **2009**, *2009*, 1515-1521.
166. J. H. Lister, The Purines Supplement 1, John Wiley & Sons, Inc., 1996.
167. B. Rubio-Ruiz, A. Conejo-García, M. A. Gallo, A. Espinosa, A. Entrena, *1H and 13C NMR spectral assignments of pyridinium salts linked to a N-9 or N-3 adenine moiety*, Magn. Reson. Chem., **2012**, *50*, 466-469.
168. M. T. Chenon, R. J. Pugmire, D. M. Grant, R. P. Panzica, L. B. Townsend, *Carbon-13 magnetic resonance. XXVI. Quantitative determination of the tautomeric populations of certain purines*, J. Am. Chem. Soc., **1975**, *97*, 4636-4642.
169. D. Ke, C. Zhan, X. Li, A. D. Q. Li, J. Yao, *A Simple Synthesis of Imide-Dipeptides*, Synlett, **2009**, *2009*, 1506,1510.

170. P. Minetti, M. O. Tinti, P. Carminati, M. Castorina, M. A. Di Cesare, S. Di Serio, G. Gallo, O. Ghirardi, F. Giorgi, L. Giorgi, G. Piersanti, F. Bartoccini, G. Tarzia, *2-n-Butyl-9-methyl-8-[1,2,3]triazol-2-yl-9H-purin-6-ylamine and Analogues as A2A Adenosine Receptor Antagonists. Design, Synthesis, and Pharmacological Characterization*, J. Med. Chem., **2005**, *48*, 6887-6896.

171. L. R. Comstock, S. R. Rajski, *Efficient Synthesis of Azide-Bearing Cofactor Mimics*, J. Org. Chem., **2004**, *69*, 1425-1428.

172. E. Yousefi-Salakdeh, M. Murtola, A. Zetterberg, E. Yeheskiely, R. Strömberg, *Synthesis of 8-aminoadenosine 5'-(aminoalkyl phosphates), analogues of aminoacyl adenylates*, Bioorg. Med. Chem., **2006**, *14*, 2653-2659.

173. J. T. Markiewicz, O. Wiest, P. Helquist, *Synthesis of Primary Aryl Amines Through a Copper-Assisted Aromatic Substitution Reaction with Sodium Azide*, J. Org. Chem., **2010**, *75*, 4887-4890.

174. J. o. Neres, N. P. Labello, R. V. Somu, H. I. Boshoff, D. J. Wilson, J. Vannada, L. Chen, C. E. Barry, E. M. Bennett, C. C. Aldrich, *Inhibition of Siderophore Biosynthesis in Mycobacterium tuberculosis with Nucleoside Bisubstrate Analogues: Structure-Activity Relationships of the Nucleobase Domain of 5'-O-[N-(Salicyl)sulfamoyl]adenosine*, J. Med. Chem., **2008**, *51*, 5349-5370.

175. A. Kovaļovs, I. Novosjolova, Ē. Bizdēna, I. Bižāne, L. Skardziute, K. Kazlauskas, S. Jursenas, M. Turks, *1,2,3-Triazoles as leaving groups in purine chemistry: a three-step synthesis of N6-substituted-2-triazolyl-adenine nucleosides and photophysical properties thereof*, Tetrahedron Lett., **2013**, *54*, 850-853.

176. A. A. Bogan, K. S. Thorn, *Anatomy of hot spots in protein interfaces*, J. Mol. Biol., **1998**, *280*, 1-9.

177. C. F. Ibáñez, *Structure and Physiology of the RET Receptor Tyrosine Kinase*, Cold Spring Harbor Perspectives in Biology, **2013**, *5*.

178. S. Jones, J. M. Thornton, *Principles of protein-protein interactions*, P. Natl. Acad. Sci. USA, **1996**, *93*, 13-20.

179. O. Keskin, B. Ma, R. Nussinov, *Hot Regions in Protein–Protein Interactions: The Organization and Contribution of Structurally Conserved Hot Spot Residues*, J. Mol. Biol., **2005**, *345*, 1281-1294.

180. O. Keskin, A. Gursoy, B. Ma, R. Nussinov, *Principles of Protein–Protein Interactions: What are the Preferred Ways For Proteins To Interact?*, Chem. Rev., **2008**, *108*, 1225-1244.

181. V. Azzarito, K. Long, N. S. Murphy, A. J. Wilson, *Inhibition of [alpha]-helix-mediated protein-protein interactions using designed molecules*, Nat. Chem., **2013**, *5*, 161-173.

182. L.-G. Milroy, T. N. Grossmann, S. Hennig, L. Brunsveld, C. Ottmann, *Modulators of Protein–Protein Interactions*, Chem. Rev., **2014**, *114*, 4695-4748.

183. J. S. Richardson, in *Advances in Protein Chemistry, Vol. Volume 34* (Eds.: J. T. E. C.B. Anfinsen, M. R. Frederic), Academic Press, **1981**, pp. 167-339.

184. B. N. Bullock, A. L. Jochim, P. S. Arora, *Assessing Helical Protein Interfaces for Inhibitor Design*, J. Am. Chem. Soc., **2011**, *133*, 14220-14223.

185. H. Yin, G.-I. Lee, A. D. Hamilton, in *Drug Discovery Research*, John Wiley & Sons, Inc., **2006**, pp. 281-299.
186. L. K. Henchey, A. L. Jochim, P. S. Arora, *Contemporary strategies for the stabilization of peptides in the α-helical conformation*, Curr. Opin. Chem. Biol., **2008**, *12*, 692-697.
187. M. K. P. Jayatunga, S. Thompson, A. D. Hamilton, *α-Helix mimetics: Outwards and upwards*, Bioorg. Med. Chem. Lett., **2014**, *24*, 717-724.
188. S. Thompson, A. D. Hamilton, *Amphiphilic [small alpha]-helix mimetics based on a benzoylurea scaffold*, Org. Biomol. Chem., **2012**, *10*, 5780-5782.
189. B. P. Orner, J. T. Ernst, A. D. Hamilton, *Toward Proteomimetics: Terphenyl Derivatives as Structural and Functional Mimics of Extended Regions of an α-Helix*, J. Am. Chem. Soc., **2001**, *123*, 5382-5383.
190. H. Yin, G.-i. Lee, K. A. Sedey, J. M. Rodriguez, H.-G. Wang, S. M. Sebti, A. D. Hamilton, *Terephthalamide Derivatives as Mimetics of Helical Peptides: Disruption of the Bcl-xL/Bak Interaction*, J. Am. Chem. Soc., **2005**, *127*, 5463-5468.
191. J. M. Rodriguez, A. D. Hamilton, *Benzoylurea Oligomers: Synthetic Foldamers That Mimic Extended α Helices*, Angew. Chem., Int. Ed., **2007**, *46*, 8614-8617.
192. S. M. Biros, L. Moisan, E. Mann, A. Carella, D. Zhai, J. C. Reed, J. Rebek Jr, *Heterocyclic α-helix mimetics for targeting protein–protein interactions*, Bioorg. Med. Chem. Lett., **2007**, *17*, 4641-4645.
193. E. Ko, J. Liu, L. M. Perez, G. Lu, A. Schaefer, K. Burgess, *Universal Peptidomimetics*, J. Am. Chem. Soc., **2010**, *133*, 462-477.
194. J. H. Lee, Q. Zhang, S. Jo, S. C. Chai, M. Oh, W. Im, H. Lu, H.-S. Lim, *Novel Pyrrolopyrimidine-Based α-Helix Mimetics: Cell-Permeable Inhibitors of Protein−Protein Interactions*, J. Am. Chem. Soc., **2010**, *133*, 676-679.
195. D. Alarcon-Vargas, Z. e. Ronai, *p53–Mdm2—the affair that never ends*, Carcinogenesis, **2002**, *23*, 541-547.
196. K. H. Vousden, X. Lu, *Live or let die: the cell's response to p53*, Nat. Rev. Cancer, **2002**, *2*, 594-604.
197. S. L. Harris, A. J. Levine, *The p53 pathway: positive and negative feedback loops*, Oncogene, **2005**, *24*, 2899-2908.
198. L. T. Vassilev, B. T. Vu, B. Graves, D. Carvajal, F. Podlaski, Z. Filipovic, N. Kong, U. Kammlott, C. Lukacs, C. Klein, N. Fotouhi, E. A. Liu, *In Vivo Activation of the p53 Pathway by Small-Molecule Antagonists of MDM2*, Science, **2004**, *303*, 844-848.
199. P. H. Kussie, S. Gorina, V. Marechal, B. Elenbaas, J. Moreau, A. J. Levine, N. P. Pavletich, *Structure of the MDM2 Oncoprotein Bound to the p53 Tumor Suppressor Transactivation Domain*, Science, **1996**, *274*, 948-953.
200. K. K. Hoe, C. S. Verma, D. P. Lane, *Drugging the p53 pathway: understanding the route to clinical efficacy*, Nat. Rev. Drug. Discov., **2014**, *13*, 217-236.

201. D. C. Fry, C. Wartchow, B. Graves, C. Janson, C. Lukacs, U. Kammlott, C. Belunis, S. Palme, C. Klein, B. Vu, *Deconstruction of a Nutlin: Dissecting the Binding Determinants of a Potent Protein–Protein Interaction Inhibitor*, ACS Med. Chem. Lett., **2013**, *4*, 660-665.

202. Y. Rew, D. Sun, F. Gonzalez-Lopez De Turiso, M. D. Bartberger, H. P. Beck, J. Canon, A. Chen, D. Chow, J. Deignan, B. M. Fox, D. Gustin, X. Huang, M. Jiang, X. Jiao, L. Jin, F. Kayser, D. J. Kopecky, Y. Li, M.-C. Lo, A. M. Long, K. Michelsen, J. D. Oliner, T. Osgood, M. Ragains, A. Y. Saiki, S. Schneider, M. Toteva, P. Yakowec, X. Yan, Q. Ye, D. Yu, X. Zhao, J. Zhou, J. C. Medina, S. H. Olson, *Structure-Based Design of Novel Inhibitors of the MDM2–p53 Interaction*, J. Med. Chem., **2012**, *55*, 4936-4954.

203. D. Sun, Z. Li, Y. Rew, M. Gribble, M. D. Bartberger, H. P. Beck, J. Canon, A. Chen, X. Chen, D. Chow, J. Deignan, J. Duquette, J. Eksterowicz, B. Fisher, B. M. Fox, J. Fu, A. Z. Gonzalez, F. Gonzalez-Lopez De Turiso, J. B. Houze, X. Huang, M. Jiang, L. Jin, F. Kayser, J. Liu, M.-C. Lo, A. M. Long, B. Lucas, L. R. McGee, J. McIntosh, J. Mihalic, J. D. Oliner, T. Osgood, M. L. Peterson, P. Roveto, A. Y. Saiki, P. Shaffer, M. Toteva, Y. Wang, Y. C. Wang, S. Wortman, P. Yakowec, X. Yan, Q. Ye, D. Yu, M. Yu, X. Zhao, J. Zhou, J. Zhu, S. H. Olson, J. C. Medina, *Discovery of AMG 232, a Potent, Selective, and Orally Bioavailable MDM2–p53 Inhibitor in Clinical Development*, J. Med. Chem., **2014**, *57*, 1454-1472.

204. A. Z. Gonzalez, J. Eksterowicz, M. D. Bartberger, H. P. Beck, J. Canon, A. Chen, D. Chow, J. Duquette, B. M. Fox, J. Fu, X. Huang, J. B. Houze, L. Jin, Y. Li, Z. Li, Y. Ling, M.-C. Lo, A. M. Long, L. R. McGee, J. McIntosh, D. L. McMinn, J. D. Oliner, T. Osgood, Y. Rew, A. Y. Saiki, P. Shaffer, S. Wortman, P. Yakowec, X. Yan, Q. Ye, D. Yu, X. Zhao, J. Zhou, S. H. Olson, J. C. Medina, D. Sun, *Selective and Potent Morpholinone Inhibitors of the MDM2–p53 Protein–Protein Interaction*, J. Med. Chem., **2014**, *57*, 2472-2488.

205. Y. Zhao, A. Aguilar, D. Bernard, S. Wang, *Small-Molecule Inhibitors of the MDM2–p53 Protein–Protein Interaction (MDM2 Inhibitors) in Clinical Trials for Cancer Treatment*, J. Med. Chem., **2014**.

206. P. Furet, P. Chène, A. De Pover, T. S. Valat, J. H. Lisztwan, J. Kallen, K. Masuya, *The central valine concept provides an entry in a new class of non peptide inhibitors of the p53–MDM2 interaction*, Bioorg. Med. Chem. Lett., **2012**, *22*, 3498-3502.

207. M. Bista, S. Wolf, K. Khoury, K. Kowalska, Y. Huang, E. Wrona, M. Arciniega, Grzegorz M. Popowicz, Tad A. Holak, A. Dömling, *Transient Protein States in Designing Inhibitors of the MDM2-p53 Interaction*, Structure, **2013**, *21*, 2143-2151.

208. Z. Zhang, X.-J. Chu, J.-J. Liu, Q. Ding, J. Zhang, D. Bartkovitz, N. Jiang, P. Karnachi, S.-S. So, C. Tovar, Z. M. Filipovic, B. Higgins, K. Glenn, K. Packman, L. Vassilev, B. Graves, *Discovery of Potent and Orally Active p53-MDM2 Inhibitors RO5353 and RO2468 for Potential Clinical Development*, ACS Med. Chem. Lett., **2013**, *5*, 124-127.

209. B. L. Grasberger, T. Lu, C. Schubert, D. J. Parks, T. E. Carver, H. K. Koblish, M. D. Cummings, L. V. LaFrance, K. L. Milkiewicz, R. R. Calvo, D. Maguire, J. Lattanze, C. F. Franks, S. Zhao, K.

Ramachandren, G. R. Bylebyl, M. Zhang, C. L. Manthey, E. C. Petrella, M. W. Pantoliano, I. C. Deckman, J. C. Spurlino, A. C. Maroney, B. E. Tomczuk, C. J. Molloy, R. F. Bone, *Discovery and Cocrystal Structure of Benzodiazepinedione HDM2 Antagonists That Activate p53 in Cells*, J. Med. Chem., **2005**, *48*, 909-912.

210. W. S. Horne, M. K. Yadav, C. D. Stout, M. R. Ghadiri, *Heterocyclic Peptide Backbone Modifications in an α-Helical Coiled Coil*, J. Am. Chem. Soc., **2004**, *126*, 15366-15367.
211. D. S. Pedersen, A. Abell, *1,2,3-Triazoles in Peptidomimetic Chemistry*, Eur. J. Org. Chem., **2011**, *2011*, 2399-2411.
212. MacroModel, version 10.3, Schrödinger, LLC, New York, NY, 2014.
213. O. Mitsunobu, *The Use of Diethyl Azodicarboxylate and Triphenylphosphine in Synthesis and Transformation of Natural Products*, Synthesis, **1981**, *1981*, 1-28.
214. S. Fletcher, V. M. Shahani, A. J. Lough, P. T. Gunning, *Concise access to N9-mono-, N2-mono- and N2,N9-di-substituted guanines via efficient Mitsunobu reactions*, Tetrahedron, **2010**, *66*, 4621-4632.
215. L. Čechová, P. Jansa, M. Šála, M. Dračínský, A. Holý, Z. Janeba, *The optimized microwave-assisted decomposition of formamides and its synthetic utility in the amination reactions of purines*, Tetrahedron, **2011**, *67*, 866-871.
216. A. T. Gillmore, M. Badland, C. L. Crook, N. M. Castro, D. J. Critcher, S. J. Fussell, K. J. Jones, M. C. Jones, E. Kougoulos, J. S. Mathew, L. McMillan, J. E. Pearce, F. L. Rawlinson, A. E. Sherlock, R. Walton, *Multkilogram Scale-Up of a Reductive Alkylation Route to a Novel PARP Inhibitor*, Org. Process Res. Dev., **2012**, *16*, 1897-1904.
217. S. Suzuki, A. Nagata, M. Kuratsu, M. Kozaki, R. Tanaka, D. Shiomi, K. Sugisaki, K. Toyota, K. Sato, T. Takui, K. Okada, *Trinitroxide-Trioxytriphenylamine: Spin-State Conversion from Triradical Doublet to Diradical Cation Triplet by Oxidative Modulation of a π-Conjugated System*, Angew. Chem., Int. Ed., **2012**, *51*, 3193-3197.
218. T. Araki, T. Ozawa, H. Yokoe, M. Kanematsu, M. Yoshida, K. Shishido, *Diastereoselective Intramolecular Carbamoylketene/Alkene [2 + 2] Cycloaddition: Enantioselective Access to Pyrrolidinoindoline Alkaloids*, Org. Lett., **2012**, *15*, 200-203.
219. J. M. O'Brien, J. S. Kingsbury, *A Practical Synthesis of 3-Acyl Cyclobutanones by [2 + 2] Annulation. Mechanism and Utility of the Zn(II)-Catalyzed Condensation of α-Chloroenamines with Electron-Deficient Alkenes*, J. Org. Chem., **2011**, *76*, 1662-1672.
220. M. Fridén-Saxin, T. Seifert, M. R. Landergren, T. Suuronen, M. Lahtela-Kakkonen, E. M. Jarho, K. Luthman, *Synthesis and Evaluation of Substituted Chroman-4-one and Chromone Derivatives as Sirtuin 2-Selective Inhibitors*, J. Med. Chem., **2012**, *55*, 7104-7113.
221. W. P. Reeves, C. V. Lu, J. S. Russel, *Bromination of Aniline with Pyridinium Hydrobromide Perbromide: some Mechanistic Considerations*, Mendeleev Commun., **1994**, *4*, 223-224.

222. Y. Ju, D. Kumar, R. S. Varma, *Revisiting Nucleophilic Substitution Reactions: Microwave-Assisted Synthesis of Azides, Thiocyanates, and Sulfones in an Aqueous Medium*, J. Org. Chem., **2006**, *71*, 6697-6700.

223. N. J. Moerke, in *Current Protocols in Chemical Biology*, John Wiley & Sons, Inc., **2009**.

224. Y. Zhao, S. Yu, W. Sun, L. Liu, J. Lu, D. McEachern, S. Shargary, D. Bernard, X. Li, T. Zhao, P. Zou, D. Sun, S. Wang, *A Potent Small-Molecule Inhibitor of the MDM2–p53 Interaction (MI-888) Achieved Complete and Durable Tumor Regression in Mice*, J. Med. Chem., **2013**, *56*, 5553-5561.

225. F. Gonzalez-Lopez de Turiso, D. Sun, Y. Rew, M. D. Bartberger, H. P. Beck, J. Canon, A. Chen, D. Chow, T. L. Correll, X. Huang, L. D. Julian, F. Kayser, M.-C. Lo, A. M. Long, D. McMinn, J. D. Oliner, T. Osgood, J. P. Powers, A. Y. Saiki, S. Schneider, P. Shaffer, S.-H. Xiao, P. Yakowec, X. Yan, Q. Ye, D. Yu, X. Zhao, J. Zhou, J. C. Medina, S. H. Olson, *Rational Design and Binding Mode Duality of MDM2–p53 Inhibitors*, J. Med. Chem., **2013**, *56*, 4053-4070.

226. K. Michelsen, J. B. Jordan, J. Lewis, A. M. Long, E. Yang, Y. Rew, J. Zhou, P. Yakowec, P. D. Schnier, X. Huang, L. Poppe, *Ordering of the N-Terminus of Human MDM2 by Small Molecule Inhibitors*, J. Am. Chem. Soc., **2012**, *134*, 17059-17067.

227. PDB codes for the compared crystal structures: 4HBM, 4ERE, 4ERF, 1RV1, 1YCR, 3JZK, 1T4E.

228. Schrödinger, Glide version 5.8, (2012) LLC, New York.

229. A. J. T. Richard B. M. Schasfoort, *Handbook of Surface Plasmon Resonance*, RCS publishing, Cambridge, UK, **2008**.

230. P. Workman, I. Collins, *Probing the Probes: Fitness Factors For Small Molecule Tools*, Chem. Biol., **2010**, *17*, 561-577.